MULTIVARIATE ANALYSIS OF *CHLAMYDIA PNEUMONIAE*

LUNG INFECTION IN TWO INBRED MOUSE STRAINS

Except where reference is made to the work of others, the work described in this dissertation is my own or was done in collaboration with my advisory committee. This dissertation does not include proprietary or classified information.

_____

Chengming Wang

Certificate of Approval:

_____	_____
Sandra J. Ewald	Bernhard Kaltenboeck, Chair
Professor	Professor
Pathobiology	Pathobiology
_____	_____
Joseph J. Giambrone	Stuart B. Price
Professor	Associate Professor
Poultry Science	Pathobiology

_____

Stephen L. McFarland
Acting Dean
Graduate School

MULTIVARIATE ANALYSIS OF *CHLAMYDIA PNEUMONIAE* LUNG INFECTION IN TWO INBRED MOUSE STRAINS

Chengming Wang

A Dissertation

Submitted to

the Graduate Faculty of

Auburn University

in Partial Fulfillment of the

Requirements for the

Degree of

Doctor of Philosophy

Auburn, Alabama
December 16, 2005

MULTIVARIATE ANALYSIS OF *CHLAMYDIA PNEUMONIAE*

LUNG INFECTION IN TWO INBRED MOUSE STRAINS

Chengming Wang

_____

Signature of Author

_____

Date

VITA

Chengming Wang, son of Liangfa Wang and Keyun Hong, was born on December 20, 1967 in a little village of Shucheng County, Anhui province, P. R. of China. He obtained the degree of Doctor of Veterinary Medicine in 1989 from Anhui Science and Technology University. He then attended Nanjing Agricultural University and graduated in 1992 with a Master's degree in Infectious Diseases and Veterinary Preventive Medicine. He was a visiting scholar in Germany between 1997 and 1998, and in 2000 he started his graduate studies in the Department of Poultry Science at Auburn University and graduated in 2002 with the degree of Master of Science. In 2002 he commenced his Ph.D. graduate studies in the Program of Biomedical Sciences in the College of Veterinary Medicine at Auburn University.

DISSERTATION ABSTRACT

MULTIVARIATE ANALYSIS OF *CHLAMYDIA PNEUMONIAE*

LUNG INFECTION IN TWO INBRED MOUSE STRAINS

Chengming Wang

Doctor of Philosophy, December 16, 2005
(Master of Science, Auburn University, 2002)
(Master of Science, Nanjing Agricultural University, 1992)
(DVM, Anhui Science and Technology University, 1989)
168 Typed Pages

Directed by Dr. Bernhard Kaltenboeck

This investigation was aimed at dissecting the mechanisms of *C. pneumoniae* pathogenesis by multivariate analysis of challenge experiments in a mouse model of *C. pneumoniae* lung infection. To facilitate these analyses, a platform method for real-time, single-step, duplex reverse transcriptase quantitative PCR (RT-qPCR) for quantification of mRNA was established on the LightCycler® platform as the first part of this study. This method allows simultaneous reverse transcription and real-time PCR amplification of analyte genes and mRNA of reference genes in a single-tube reaction. Twenty-minute RT reactions at 55°C followed by 18 high-stringency step-down thermal cycles and 25 relaxed-stringency fluorescence acquisition cycles produced sensitive and accurate RT-PCR results.

C. pneumoniae is an agent of community-acquired respiratory infection, and is strongly associated with atherosclerotic coronary heart disease. In the second part of this study, a balanced multivariate experimental design investigated the major factors that influence disease (measured as lung weight increase), chlamydial lung burden, and transcript levels of 25 genes. The influence of the categorical factors i) host genetic background, ii) pre-challenge immunity against *C. pneumoniae*, iii) time after challenge infection, iv) dietary protein content, and v) dietary antioxidant content was investigated. The combined effects of the main factors mouse strain, immune status, and time after challenge inoculation resulted in opposite outcomes for lung disease and elimination of *C. pneumoniae*, while dietary protein and antioxidant content had little overall influence. A/J mice prioritized minimizing disease at the cost of low pathogen elimination while C57BL/6 mice prioritized elimination of *C. pneumoniae* at the cost of high disease. C57BL/6 mice had generally higher transcript levels than A/J for most cellular markers except for T cell maturation markers. Most cytokines, inflammatory modulators, and cellular markers were significantly lower in naïve than in immune mice and significantly higher on day-3 than on day-10 post inoculation. The high disease outcome in C57BL/6 mice correlated with lower GATA3 and higher arginase 2 transcripts than in A/J, while low *C. pneumoniae* load correlated with high Tim3 and arginase 2 transcripts.

A simple best-fit partial least square regression model using day-3 Tim3, GATA3, and arginase 2 transcript concentrations predicted 85% of the day-10 disease and 72% of the day-10 *C. pneumoniae* lung load. Thus, host-dependent levels of early Th1 and Th2 responses, and their balance, significantly correlated with late disease and pathogen load of *C. pneumoniae* lung infection.

ACKNOWLEDGMENTS

My doctoral studies and dissertation writing could not have been accomplished without encouragement, direction, advice and challenge from the following people.

First, I would like to thank my dissertation committee members: Drs. Sandra J. Ewald, Joseph J. Giambrone, Bernhard Kaltenboeck and Stuart B. Price. In all, they have instructed me in six courses, and each of them helped me with their unique expertise in different areas of my research. Many thanks go to my outside reader, Dr. Stephen Kempf, for his time and direction in preparing this dissertation.

Words cannot express my appreciation, respect and gratitude to my advisor, Dr. Kaltenboeck. Four years' study in his lab has been my most enjoyable and successful educational pursuits. I have been trained how to optimize protocols and design experiments, how to produce reliable results while avoiding possible pitfalls, how to analyze and interpret the data, and finally how to assemble all of the data into the manuscript form. I see my major professor as a great scientific advisor as well as a model of being an honest, objective and determined person from whom I have gained the knowledge and experience necessary to conduct this chlamydial research. From him, I have been learned to be a good student as well as a good person.

I would like to thank my colleagues in the Chlamydia Laboratory, Ms. Dongya Gao, Dr. Alexander Vaglenov, Dr. Teayoun Kim, Dr. Dan Li and Mr. Yihang Li, for their precious assistance and helpful discussions through my studies. I am indebted to Dr. Jin Huang and Mr. James Krehling for their true friendship and constant support. Special thanks go to my family, especially my dear wife, Chuanling Xu, and my loving son, Shouyi Wang for their love and support.

Style manual of journal used

Infection and Immunity

Computer software used

Microsoft Word 2000 for text and tables

STATISTICA 7.0 for statistical analysis

Adobe Illustrator CS and DeltaGraph 5.0 for figures

TABLE OF CONTENTS

LIST OF TABLES

LIST OF FIGURES

CHAPTER 2

CHAPTER 3

.

CHAPTER 1: LITERATURE REVIEW

BIOLOGY OF CHLAMYDIACEAE

Pathogen characteristics

Bacteria of the order *Chlamydiales* are obligate intracellular parasites of eukaryotic cells. They have a distinctive developmental cycle with two distinct morphological forms: the elementary body (EB) and the reticulate body (RB). The chlamydial EB is close to the limit of light microscopic visibility with approximately 0.3 μm in diameter and is round or occasionally pear-shaped, and contains electron-dense structures. It is the infectious stage of the chlamydial developmental cycle, and functions as a tough "spore-like" body whose purpose is to permit chlamydial survival in the non-supportive environment outside the host cell. The ultra-structure of the EB has been extensively studied (25, 82, 90, 91, 119, 128).

The RB is the chlamydial developmental stage during intracellular replication, and it is non-infectious. Typically, the RB has a diameter of approximately 1 μm. The RB is metabolically active, and the cytoplasm is rich in ribosomes, which are required for protein synthesis. As the RB begins to differentiate into an elementary body, sites of re-condensation of nucleic acid appear in its cytoplasm. In the maturing inclusion, chlamydial particles appear to be packed tightly in the inclusion membrane. Development of chlamydiae is highly dependent on nutrient supply and metabolic status

of host cells. Nutrient deficiencies such as low glucose levels lead to delayed development and to few, aberrant chlamydial organisms within the inclusions.

Microbiological culture

Classically, chlamydial agents have been propagated in the yolk sacs of chicken embryos (132). Cultivation in cell culture is now preferred, and the use of appropriate techniques is important for high-yield culture (79). Buffalo Green Monkey Kidney (BGMK) cells support chlamydial replication effectively, particularly when cultivated in Iscove's Modified Dulbecco's Medium. EBs are purified by sedimentation, separated from cellular nuclei by low-speed centrifugation, and separated from cell debris by step-gradient centrifugation in a 30% RenoCal-76 - 50% sucrose step-gradient. Extensive sonication increases yield and infectivity of chlamydial EBs (79).

Taxonomy of *Chlamydiales*

Based on phylogenetic trees using 16S and 23S rRNA sequence similarities of *Chlamydiales* strains, isolates showing more than 90% sequence identity with prototype strains are categorized as members of the *Chlamydiaceae* family. Isolates showing 80 ~ 90% sequence identity to the *Chlamydiaceae* type strains are classified into three more families termed *Parachlamydiaceae*, *Simkaniaceae*, and *Waddliaceae*. The *Chlamydiaceae* family has two genera, *Chlamydia* and *Chlamydophila*, with a total of nine species. The genus *Chlamydophila (C.*) consists of 6 species. *C. psittaci* in birds had been recognized since the 1870s as causative agent of a disease termed psittacosis (96).

Abortion in sheep caused by *C. abortus* was first described in Scotland in 1936 (130, 132). *C. felis* was isolated from cat pneumonia in 1944 and is associated with pneumonia and conjunctivitis in cats (8; 16, 127), and *C. caviae* was originally isolated from conjunctival scrapings of guinea pigs (101). *C. pecorum*, a relatively new species, is associated with polyarthritis, enteritis, pneumonia, and urogenital infections in cattle, sheep, goats, koala, and swine (6, 32, 37, 68). *C. pneumoniae* is mainly a human pathogen, but infects also koalas, horses, and frogs (69, 116)

Chlamydia (C.), the second genus of the family *Chlamydiaceae*, consists of 3 species: *C. trachomatis* is the classic human pathogen causing ocular and urogenital disease. *Chlamydia muridarum* had long been known as the mouse pneumonitis biovar of *C. trachomatis* (104). *C. suis* has been identified only recently as a common pathogen in swine associated with fertility disorders and perinatal mortality (69, 124, 149).

Hosts

Chlamydia is one of the microorganisms with the widest range of host species, affecting animal species from *Amoeba* and *Hydra* through arthropods, insects, molluscs, marsupials, birds, reptiles, amphibians and mammals including humans. Among mammals, *Chlamydophila* spp. have been isolated from ruminants, pigs, horses, koalas, dogs, rabbits, ferrets and opossums (133). *Chlamydia* spp. have been found in rodents (26) and swine (70). There are a number of reports of chlamydial infections in buffaloes (24, 46, 122).

Serological examinations show that chlamydial infections exist also in other mammals including monkeys, wild boar, hedgehogs (133), deer (36, 138), reindeer (102),

fur seals (26), and birds (96). In four species of wild ruminants (fallow deer, mouflon, red deer and Spanish ibex) from a nature reserve in Spain chlamydial infections were reported, which might act as reservoirs of chlamydial infection (20). Serological surveys also suggest the evidence of chlamydial infection in antelope (86), captive Arabian oryx (43), and snowshoe hares and muskrats in Saskatchewan, Canada (129).

Chlamydial infection and disease was also confirmed in reptiles such as chameleon, lizard, sea turtles, and crocodiles (58; 62). A pneumonia and anaemia disease syndrome in giant barred frogs of Australia is probably caused by the koala biovar of *C. pneumoniae*. Chlamydial infections have also been confirmed in another amphibian species, the African clawed frog (59, 103, 116). Chlamydial infection were reported to cause chronic gill disease in Connecticut striped bass and white perch (148), and high mortality in cultured pacu, a tropical fish species in Brazil (137).

Chlamydial infections occur also in invertebrates such as in ticks and fleas (26, 145), and lice (94). *Chlamydia*-like organisms, now classified as *Parachlamydiaceae,* have been isolated from amoebae (5), were detected in the ovaries of the spider, *Segestrai senoculata* (141), and caused fatal disease in the spider *Pisaura mirabilis* (99).

Harshbarger et al. (51) found *Chlamydia* agents in the digestive systems of hard clams and oysters from the Chesapeake Bay area of the USA. Similar organisms were detected in the digestive cells of approximately 5% of mussels from the Basque coast (15). Over a one-year period, Svardh (136) examined the prevalence of disease-associated organisms in blue mussel populations in Denmark, and among bacterial agents only chlamydiae were detected.

Epidemiology

Chlamydial diseases of animals have been described in all continents, and 21.7% of countries and regions around the world have reported incidences of animal chlamydial infections. This number is probably a substantial underestimate of the true incidence. All data suggest that chlamydial infections of animals are actually ubiquitous. Most likely, the difficulty in detecting this intracellular pathogen, and the inconsistent use of high-sensitivity detection methods have combined to underdiagnose chlamydial infection in animals. In humans, 72.6% of all countries and regions worldwide report chlamydial infections, predominantly with *C. trachomatis*, associated with sexually transmitted diseases and blindness (84, 118).

Chlamydial infections cause a wide variety of clinical diseases in animals, which are often clinically inapparent and asymptomatic. Chlamydial infections become clinically manifest as disease syndrome called ornithosis or psittacosis in birds, and that includes pneumonia, air sac inflammation, and enteritis in mammals. Other distinct chlamydial disease manifestations include abortion and conjunctivitis, encephalomyelitis and polyarthritis in mammals. When activated by stress factors, chlamydial infection may take a severe, systemic and sometimes fatal course of disease. Classification of chlamydiae had traditionally been based on host and/or disease association.

Avian chlamydiosis. Psittacosis is the term for chlamydial infection of psittacine birds or man, and ornithosis is the term for the same infection in birds other than psittacines (132). Infections with chlamydial agents have been described in 130 species of birds (12, 96), and infections of *C. psittaci* in birds are important because they cause economic loss to the poultry production and represent a biological hazard to human

health. Ornithosis in birds involves mainly the gastrointestinal tract, and the pathogen is shed in faeces or via infectious discharges from the respiratory tract. *C. psittaci* has been isolated from symptomatic and apparently healthy birds. Clinically asymptomatic and latent infections may be the predominant state for *C. psittaci* infection. Stress factors such as overcrowding, poor nutrition, viral and other bacterial infections, and transportation can precipitate overt clinical disease and mortality. Infectious chlamydiae in respiratory secretions or faeces may remain viable for several months. Transmission of disease is mainly through aerosols of faecal or feather dust. Vertical transmission through eggs has been found in chickens, ducks, seagulls and psittacine birds (126). Young birds tend to be more susceptible to infection than older birds, and some species seem to be more susceptible than others. It is also possible that feral birds might act as natural reservoirs of the agent and introduce chlamydiae into farmed bird populations such as turkeys and ducks. Wild and racing pigeons, the bird trade, and migrations of wild birds such as seagulls, finches, sparrows and waterfowl may all contribute to the dissemination and transmission of *C. psittaci* throughout avian populations (142).

Ruminant chlamydial abortion and infertility. *C. abortus* strains have been isolated in cases of abortion predominantly in sheep, goats, and cattle, but occasionally also in horses, swine, rabbits, guinea pig, and mice around the world (7, 28, 64, 93, 125). In general, chlamydial abortion is most common in lowland sheep flocks, mainly where sheep are closely confined. Usually, herds become affected after the introduction of asymptomatic carrier animals with chlamydial infection. Infection most likely occurs in uninfected sheep at lambing time by ingestion of *C. abortus*, which is excreted by infected and aborting ewes in diseased placentas, uterine discharges, and feces. In sheep,

the infection remains present at a subclinical level until the last four weeks of the next pregnancy. The major outbreak of disease in a flock tends to occur in the second lambing season after *C. abortus* infection was contracted. It has also been reported that sheep can acquire *C. abortus* infection and abort in one lambing season (131). Most affected sheep abort in the last month of gestation, and the majority of aborting ewes are young animals although sheep of all ages are susceptible to infection (154). In a flock with first-time *C. abortus* infection, up to 30% of pregnant ewes may abort. In subsequent years, as the infection becomes established as an enzootic disease, between 5-10% of pregnant ewes abort annually. *C. abortus* infection resulting in abortion leads to effective immunity in affected ewes. Chlamydial abortion in cattle and other species is similar to enzootic abortion in sheep, but much more sporadic and less common than the disease in sheep and goats. Transmission of the disease in cattle occurs similar to that in sheep, mostly by ingestion of infected tissues. However, *C. abortus* has been shown to cause seminal vesiculitis in bulls and rams, may reduce semen quality, and may be transmitted in semen (134).

C. pecorum also causes disease of the reproductive tract of cattle and pigs. This might be analogous to the insidious progress of *C. trachomatis* genital tract infection in humans (55), in which symptoms may go unnoticed for a considerable period but may lead to chronic sequelae such as pelvic inflammatory disease and infertility. In the USA, a 53% prevalence of vaginal *C. abortus* or *C. pecorum* infection has been detected in virgin heifers by quantitative PCR, suggesting that transmission is predominantly extragenital (22, 23, 65). Although *C. abortus* is primarily associated with spontaneous abortion in cattle and sheep, there is evidence that *C. pecorum* causes pregnancy wastage

(66). *C. pecorum* infection was reported to cause a severe metritis which would have resulted in at least temporary infertility (66, 83). Fertility problems have occurred in dairy cows following abortions (117), and it is possible that sporadic *C. pecorum* abortions are either undiagnosed or have been misdiagnosed as *C. abortus* abortions.

Ruminant chlamydial enteritis, pneumonia, polyarthritis, and sporadic bovine encephalomyelitis. *C. pecorum* infections are both endemic and chronic in the intestinal tract of sheep and cattle populations around the world (19, 44, 45; 67, 87). Intestinal carriage and fecal excretion onto pasture probably plays a major role in the maintenance of *C. pecorum* infection. These infections occasionally result in acute enteritis. Respiratory tract infection with *C. pecorum* may lead to severe pneumonia associated with lung consolidation. Animal diseases caused uniquely by *C. pecorum* are polyarthritis in calves and lambs, and presumably also in piglets (69, 132). Bovine encephalitis was one of the first chlamydial diseases in cattle identified by McNutt (95). This disease occurs worldwide, and *C. pecorum* has been identified as the etiologic agent of the disease termed sporadic bovine encephalomyelitis (SBE) (132).

Feline chlamydial infection. *C. felis* is endemic among domestic cats worldwide, primarily leading to conjunctivitis and rhinitis in young acts (33). The disease is transmitted through infected aerosols and secretions. Since chlamydial strains from mammals tend to be of relatively low infectivity for humans, conjunctival infection in cats is not usually considered as a major cause of symptomatic human infection. However, zoonotic infection of humans with *C. felis* has been described.

Diagnosis of chlamydial infections

Chlamydial infections in animals are usually asymptomatic and inapparent, therefore diagnosis based on clinical symptoms, and pathological lesions and differential diagnosis are of minor importance. However, if abortion in mammals or conjunctivitis in birds is observed, chlamydial infection should be suspected. Confirmation of chlamydial infection usually requires collecting an appropriate clinical sample from the animal followed by the direct detection of the organism using a suitable laboratory-based diagnostic test, which includes direct impressions smears and cytological staining; cell culture isolation of the agent; immunofluorescence tests; enzyme immunoassays; and nucleic acid amplification based tests such as nucleic acid direct hybridization or amplification assays.

Culture. For many years, the optimum method of confirming the presence of chlamydial infection had been the propagation of the infecting organism in cell culture and the demonstration of characteristic chlamydial inclusions. However, this method requires adequate transport and cold-storage facilities in order to maintain the viability of the organism prior to inoculation. Moreover, growth and isolation of the organisms in cell culture is relatively tedious, and it is difficult to maintain high quality laboratory methods consistently.

Serological tests. Serological detection is generally only suitable for prevalence surveys, less for the retrospective diagnosis of chlamydial infection. Most chlamydial infections do not elicit sufficiently high changes in antibody levels to allow for unambiguous diagnosis of a recent infection. The exception is the diagnosis of chlamydial abortion in ruminants, in which the high exposure to *C. abortus* elicits an

increase in antibody levels that is high enough to allow for unambiguous diagnosis (45, 111).

The standard method for detection of antibodies against *Chlamydiaceae* spp. in animals is the complement fixation test (CFT) using crude or partially purified preparations of *Chlamydiaceae*-specific lipopolysaccharide, but numerous ELISA methods have also been introduced. The CFT depends on the binding of anti-*Chlamydiaceae* antibodies of the host species to guinea pig complement, and has highly variable sensitivity depending on the host species and antibody isotype (70, 111). In a random survey of 40 sera from Alabama cattle herds with abortion problems, ELISAs against peptides of the *C. abortus* major outer membrane protein or against recombinant chlamydial LPS invariably detected very high antibody levels. In fact, immunoglobulin-rich sera from gnotobiotic calves challenged with bovine coronavirus had to be used as negative controls because it was impossible to find any other *Chlamydia*-negative bovine sera. In comparison, the CFT titers of all but one serum sample were negative. The single positive serum had a low titer of 1:10 (70). The high seroprevalence of chlamydial infections poses a problem of defining truly negative control sera that allow for a reliable serological cut-off in ELISA assays of antichlamydial antibodies. In cattle it was necessary to obtain sera from gnotobiotic calves as negative controls.

Chlamydial antigen detection. A key advance in the laboratory diagnosis of chlamydial infections has been the development of tests that are not dependent on the viability of the agent and are less demanding with respect to specimen transport. The initial tests were chlamydial antigen detection tests, which relied either on the direct detection of chlamydial elementary bodies in clinical material using fluorochrome-

labeled *Chlamydia*-specific monoclonal antibodies, or on the capture and detection of chlamydial antigen in an extract of clinical material using enzyme immunoassay-based procedures. These methods are still appropriate and remain in widespread use. Since the 1960s immunofluorescence using polyclonal antibodies, and since the 1980s monoclonal antibodies have been used for the detection of chlamydial antigen, both in cell culture and in clinical material. The Pathfinder® EIA (Sanofi/Kallestad) and the Boots-Celltech IDEIA® both use *Chlamydiaceae* family-specific monoclonal antibodies against the chlamydial lipopolysaccharide, and have therefore a wide diagnostic spectrum suited for use in animal diagnostics.

Nucleic acid amplification-based diagnosis. Direct antigen detection tests are gradually being superseded by newer methods based on the detection of chlamydial nucleic acid, either by direct hybridization or preferably by nucleic acid amplification. The latter use a variety of amplification reactions, including the polymerase chain reaction (PCR), ligase chain reaction (LCR), and strand displacement amplification or transcription mediated amplification. Nucleic acid-based methods generally offer superior sensitivity and specificity to the antigen detection tests, but at greater cost and a greater requirement for trained staff. However, depending on the prevalence of infection in the test population, costs may be reduced by combining different specimens. Nucleic acid amplification-based methods are now of prime importance for the diagnosis of chlamydial infections (61, 68, 81). Indeed, the development of chlamydial tests based on nucleic acid amplification technology (NAAT) has been considered the most important advance for the detection of chlamydial infections since cell culture (131). These tests amplify the target nucleic acid, DNA or RNA; or the probe after it has annealed to target

nucleic acid. Such tests are generally more sensitive than liquid or solid phase hybridization tests which do not embody an amplification process (18), and are considerably more sensitive than culture or antigen detection methods (106).

Most of the NAAT platform technologies have been specifically marketed for detection of *C. trachomatis*, but general considerations about sensitivity and specificity equally apply to the detection of the other *Chlamydiaceae* spp. Allowing for the problems of discrepant analysis, the true sensitivity of PCR and LCR is of the order of 90 to 97% (17). An integrated nucleic acid isolation and real-time PCR platform was developed to specifically detect, differentiate, and quantify all *Chlamydiaceae* spp. by fluorescence resonance energy transfer real-time PCR with high sensitivity (61, 22, 23). In this approach, step-down thermal cycling and an excess of hot-start *Taq* polymerase vastly improved the robustness and sensitivity of the real-time PCR while essentially maintaining 100% specificity. The amplification of *Chlamydiaceae* 23S rRNA allowed for the differentiation of chlamydial species and was more robust at low target numbers than amplification of the *ompA* gene. Target specific reverse transcription prior to the PCR can potentially also detect ongoing bacterial transcriptional activity (11) and increase sensitivity of the PCR. Ribosomal RNA is stable and is particularly useful for diagnosis as there may be several thousand copies per bacterial cell.

The main advantage of the nucleic acid amplification-based diagnosis for chlamydiae is that such methods combine unsurpassed sensitivity with high specificity. However, the greater sensitivity of these assays means that accidental contamination with amplified product is a problem of major importance for kit design, laboratory workflow, and personnel. Nucleic acid amplification tests tend to be more expensive than other

laboratory methods of testing for chlamydial infection. The clinic or laboratory contemplating adopting such tests therefore needs to consider not just sensitivity, specificity and the clinical requirements, but also the suitability of the test for the facilities and human resources available. Fortunately, for high throughput testing, kit manufacturers can provide instrumentation to achieve at least partial automation. Alternatively, with a little ingenuity it may be possible to adapt other programmable laboratory dispensing / assay equipment.

CHLAMYDIA PNEUMONIAE DISEASE

Chlamydia pneumoniae was only recognized in 1984 as separate chlamydial species infecting humans by nonsexual transmission (39). Since then very high prevalences of the infection have been found worldwide in the human population (112), and *C. pneumoniae* infection has been associated with several chronic inflammatory diseases. These associations have prompted intensive research efforts to separate causal involvement of the organisms with these diseases from non-causal association (73).

Disease manifestations

Respiratory infections. Pneumonia and bronchitis are the most frequently recognized illnesses associated with *C. pneumoniae*, although asymptomatic infection or unrecognized, mildly symptomatic illnesses are the most common result of infection. In a series of studies, 10% of cases of pneumonia and approximately 5% of bronchitis and sinusitis cases in adults have been attributed to the organism (41).

No set of symptoms or signs is unique to pulmonary infections with *C. pneumoniae*; however, several characteristics of the clinical presentation may help distinguish it from other causes (38, 41, 139). A subacute onset is common. Pharyngitis, sometimes with hoarseness, is often present early in the course of the illness. There may be a biphasic pattern to the illness, with resolution of pharyngitis prior to development of a more typical bronchitis or pneumonia syndrome. Cough is very common and is often prolonged. Fever is often not present at examination, but there may be a history of fever. The period from onset to clinic visit is longer for *C. pneumoniae* infections than for other acute respiratory infections. Symptoms of sinus infection commonly occur in association with *C. pneumoniae* respiratory infections.

Although the patient's leukocyte count is usually normal, the erythrocyte sedimentation rate is often elevated. A chest radiograph usually demonstrates a single subsegmental pneumonitis in milder, nonhospitalized cases. More extensive or bilateral pneumonitis may be seen in hospitalized patients. Pleural effusions have also been demonstrated in persons with more severe disease. Most cases of pneumonia are relatively mild and do not require hospitalization. Even in mild cases, however, complete recovery is slow, despite appropriate antibiotic therapy, and cough and malaise may persist for many weeks after the acute illness. Older adults appear to have, on average, a more severe clinical course than do young adults. The available evidence also suggests that underlying illnesses and concurrent infection with other bacteria, such as the pneumococci, are associated with more severe disease. Studies of patients hospitalized with *C. pneumoniae* pneumonia have found that the majority had one or more underlying illnesses (40, 89). In addition, most of the fatalities associated with *C. pneumoniae*

infection have been in persons with underlying illness and complications such as pneumococcal bacteremia (34, 40, 72).

The role of *C. pneumoniae* as an opportunistic pathogen among immunocompromised persons is not well defined. The organism has been isolated from the lungs of patients infected with the human immunodeficiency virus and has been detected by PCR in bronchoalveolar lavage specimens from human immunodeficiency virus-infected and other immunocompromised patients (34). However, whether immunocompromised persons are at increased risk of infection with *C. pneumoniae*, or more severe disease as a consequence of infection, has not been determined. It has also been suggested that *C. pneumoniae* infection may be more common among persons with chronic obstructive pulmonary disease on the basis of a study which found a higher prevalence of *C. pneumoniae* antibody among persons with that condition (9).

Severe systemic infection. Severe systemic infections with *C. pneumoniae*, while uncommon, do occur. *C. pneumoniae* has also been identified in autopsy tissue by PCR, suggesting that the organism played at least a part in the infectious process prior to death. A febrile illness in a 10-year-old boy with pneumonia, pericarditis, pleuritis, and hepatosplenomegaly has been reported (42). A commercial laboratory found very high *C. pneumoniae* IgG serum antibody, which led to further studies that resulted in a PCR demonstration of *C. pneumoniae* in stored lymph node and liver biopsy specimens.

Other syndromes. *C. pneumoniae* has also been associated with other acute illnesses. It has been isolated from patients with purulent sinusitis (52) and otitis media with effusion (105). Primary pharyngitis due to *C. pneumoniae* has been reported; however, the frequency of this infection is unclear. While *C. pneumoniae* infection has

been reported in as high as 8% of adults with pharyngitis in Finland (63), it appears to be uncommon (less than 2% of cases) in studies of young adults in the United States (50, 139). Other reported clinical syndromes include endocarditis and lumbosacral meningoradiculitis (88).

Several chronic diseases have also been presumptively associated with *C. pneumoniae* infection. Patients with *C. pneumoniae* respiratory infection have been shown to be more likely to develop asthmatic bronchitis following their respiratory illness, suggesting that *C. pneumoniae* may be a factor in the development of asthma or asthma exacerbations (47). *C. pneumoniae* has also been associated with sarcoidosis by serologic studies (114) and with erythema nodosum (27, 135). A case of Guillain-Barre´ syndrome following infection with *C. pneumoniae* has been reported (48). *C. pneumoniae* has also been implicated in reactive arthritis or Reiter's syndrome (13).

***C. pneumoniae* and atherosclerosis.** A major surprise was the association of elevated *C. pneumoniae* antibody levels with coronary atherosclerosis and heart disease (123). This association has been confirmed in numerous studies, and the organism has been detected with high frequency in atherosclerotic lesions (56). These findings have prompted major research efforts at unraveling mechanisms of disease association, and at prophylaxis and therapy of potential enhancement of coronary heart disease by *C. pneumoniae* (60).

Several pathways were proposed to explain the possibility that *C. pneumoniae*-enhanced atherosclerosis (31, 54, 113). These mechanisms include (1) direct stimulation of monocyte migration to the atheromas (92); (2) direct interference with intracellular metabolism within the plaque, as *C. pneumoniae* was able to infect all cell types present

in a plaque in vitro, thereby inducing atherogenic processes such as foam cell formation and LDL oxidation (76); (3) the lesions could be complicated by an immunopathogenic role of *C. pneumoniae*, attracting inflammatory cells causing tissue damage. T cell infiltration was demonstrated both in murine and human atherosclerotic plaques (98); (4) triggering of an autoimmune reaction to human Hsp60 by antigenic mimicry could be interfering with atherogenesis (76); and (5) apart from the atherogenic properties, *C. pneumoniae* could complicate atherosclerotic disease further by destabilizing plaques by reducing the fibrous cap area and stimulating matrix degrading metalloproteinases (29), or by enhancing thrombogenicity by stimulating coagulation factors and tissue factor expression (21).

Antibiotics were successful for the treatment of the acute pulmonary infection, but had no effect on the atherogenic properties of *C. pneumoniae* when they were administered 2 weeks after infection (121). In addition, in rabbits, antibiotics inhibited atherogenesis only slightly when they were administered 2 weeks after infection, but they were much more effective when they were administered within 5 days after infection (31, 100). Furthermore, antibiotics failed to completely eradicate *C. pneumoniae* from the organ tissues (35, 85). These findings may help to explain the conflicting outcomes seen in animal models and human trials in using antibiotics treatment.

In conclusion, the evidence for a pathogenic role of *C. pneumoniae* in atherosclerosis in mouse models seems convincing, because the results were reproducible and confirmed by different research groups. However, the precise mechanisms of this relationship remain unclear, although many hypotheses exist. Attempts to eradicate *C. pneumoniae* from the body, both by the immune system and by antibiotic treatment,

generally encountered many difficulties which could be related to the unusual gram-negative, obligate intracellular characteristics of the bacterium. The value of the currently available antibiotics should not be overestimated, because they were only effective in preventing the long-term atherogenic effects of *C. pneumoniae* infection when they were given during the acute infection, which is often asymptomatic or aspecific in humans. Therefore, the focus of future research should merely shift back to basic research. The precise mechanisms by which *C. pneumoniae* is interfering with atherogenesis should be further elucidated to enable more specific strategies to interfere with this process, e.g. by immunosuppressive agents. In addition, the role of other infectious pathogens should be further examined, and especially the impact of the pathogen burden as a whole. The development of an effective vaccine would be the final strategy to prevent chlamydial disease and its complications, but not to prevent the impact of the pathogen burden.

PATHOGENESIS

It has been well known that host immune responses against infection are different depending on the type of pathogen. In 1995, Ferrick et al. (30) reported two different types of $CD4^+$ T-helper cells in C3H/HeJ mice. Intraperitoneal infection with intracellularly replicating *Listeria monocytogenes* bacteria made one fraction of peritoneal $CD4^+$ T-helper cells produce IFN-γ. At peak production on day 5, the number of IFN-γ producing cells was 10 fold higher than of $CD4^+$ T-helper cells producing IL-4. Conversely, infection with the extracellular parasite *Nippostrongylus brasiliensis* prompted $CD4^+$ T-helper cells to produce IL-4 at about 10-fold excess over IFN-γ on day

10. These experiments differentiated $CD4^+$ T-helper cells into two types designated as Th1 or Th2 cells. Th1 cells generate cellular immunity against intracellular pathogens, and Th2 cells promote humoral immunity against extracellular pathogens. Th1 and Th2 cells are not derived from distinct lineages but develop from the same T helper cell precursors in dependence on the cytokine milieu (120). The Th1 response is defined by the production of IL-2 and IFN-γ, while the cytokine profile of the Th2 response is IL-4, IL-5, IL-6, IL-10, and IL-13. Both types of cells produce IL-3, TNF-α and granulocyte-macrophage colony stimulating factor (GM-CSF) (74).

Like for other intracellular pathogens, the main protective immune response against infection with *Chlamydiaeceae* spp. is cellular Th1 immunity, although there are contradictory reports about the effect of the Th2 response against chlamydial infection. Yang et al. (153) reported that B cell-deficient C57BL/6 mice generated by knocking out the transmembrane portion of the β-chain gene showed three-fold higher mortality and higher chlamydial lung burden over 30 days after lung infection with *C. muridarum* (*C. trachomatis* mouse pneumonitis biovar MoPn). Interestingly, the knockout mice also showed a two-fold reduced DTH response, determined by footpad swelling 13 days after infection, as compared to wild type mice. *In vitro* re-stimulated splenic T cells from knockout mice completely or partially failed to produce cytokines such as IFN-γ, IL-6, and IL-10. The results show that B cells are necessary not only for producing antibody against *C. muridarum* but also for the initiation of efficient T cell responses (DTH) against pulmonary chlamydial infection, and this is related to impaired cytokine production. Hawkins et al. (53) produced a *C. trachomatic*-specific $CD4^+$ Th2 cell clone (Th2-MoPn) and a $CD4^+$ Th1 cell clone (Th1-MoPn) for use in a MoPn genital tract

infection model. They transferred these cells into *C. muridarum*-susceptible BALB/c mice that had been infected with *C. muridarum* 10 days earlier. Mice that received Th1-MoPn cells cleared the infection to a basal level within 50 days after infection, while mice that received Th2-MoPn cells, non-specific Th1-cells, or control mice showed continuous high levels of MoPn in their genital tracts for up to 80 days after infection, even in the presence of significantly higher anti- *C. muridarum* IgG and IgA levels than the Th1-MoPn recipient mice. To track cell migration patterns, they labeled T cells with fluorescent dye and transferred them to BALB/c mice on day 7 after vaginal infection. Eighteen hours later, they found significantly fewer Th2-MoPn cells than Th1-MoPn cells in the genital tract, but similar numbers of cells were in mesenteric lymph nodes and iliac lymph nodes.

It is difficult to know whether immune responses to chlamydial antigens are linked to the immunopathological mechanism that operates in chlamydial-chronic diseases. Halme et al. (49) measured IgM level and *in vitro* proliferative response against *C. pneumoniae* of peripheral blood lymphocytes from 291 patients who had consulted a doctor because of respiratory tract symptoms and acute fever. Among them, only 16 patients were diagnosed as *C. pneumoniae*-specific IgM positive and nine of the 16 were in the positive range of cell-mediated immune responses. This implies that our understanding of immune mechanisms in natural human chlamydial infection is incomplete.

Experimental infection models offer advantages over epidemiological studies in the analysis of the host immune response against chlamydial infection. Penttila et al. (110) reported on the immune response of BALB/c mice against lung infection of *C.*

pneumoniae. Although BALB/c mice is a mouse strain susceptible to intracellular infection, primary infection in their model peaked during the first 2 weeks then gradually decreased over 27 days after infection. Mice with secondary infection showed a 100-fold lower bacterial burden in their lungs than mice with primary infection. The expression level of IFN-γ in cells from secondary infected lung tissues increased significantly, while IL-4 and IL-10 level were low. After secondary infection, the influx of immune cells was significantly increased.

Genetic factors are known to affect the immune response by modulating either resistance or susceptibility against various diseases such as malaria, leprosy, tuberculosis, AIDS, mucocutaneous leishmaniasis, and hepatitis B. Several human case-control studies in Africa showed that polymorphisms in the promoter region of the TNF-α gene and the IL-10 1082G allele are associated with trachomatous scarring. In addition, various HLA genes, class I allele HLA-A31, HLA class II DQA0102, DQA1010, DQB0501, DQAq0401, and DQB10402 allele have been linked to differential outcomes of *C. trachomatis* genital disease sequelae (Mahdi, 2002). Yang et al. (150) showed different immune responses of the C57BL/6 and BALB/c mouse strains against *C. muridarum*. C57BL/6 mice showed lower weight loss with faster weight recovery, lower mortality, and faster clearance rate of *C. muridarum* than BALB/c mice. Twenty-five days after intranasal infection with 10^5 IFU of MoPn, C57BL/6 mice completely cleared the organism, while BALB/c mice still had a titer of about 10^4 IFU/lung. C57BL/6 mice showed stronger delayed-type hypersensitivity reaction (DTH) to footpad injection of *C. muridarum* antigens than BALB/c mice, but the IgG1antibody titer was higher in

BALB/c mice. The IFN-γ and IL-10 ratio of the two strains showed exactly opposite patterns, with a Th1 response in C57BL/6 mice and Th2 response in BALB/c mice.

In summary, complex mechanisms underlie the disease outcome of chlamydial infection, and we need to consider host genetic factors as well as the bacteria to understand the mechanisms of ubiquitously present chlamydial infections in animals as well as the human population.

Models of disease

Three animal models of *C. pneumoniae* infection, mouse, rabbit, and monkey, have been evaluated. The most susceptible animals are mice, which are susceptible to inoculation by intranasal (71; 77, 152, 153), intravenous (77, 153), subcutaneous (77, 153), and intracerebral (77) routes. Lung infection induced by intranasal inoculation runs a prolonged course. Organisms are recoverable from lungs for 42 days, and the lung pathology persists for over 60 days (152).

The lung pathology in mice is characterized by patchy interstitial pneumonitis, with polymorphonuclear leukocyte infiltration in the early stage and with mononuclear cell infiltration in the late stage (152). Ultrastructural examination revealed *C. pneumoniae* inclusions in ciliated bronchial epithelial cells and interstitial macrophages (151). This is similar to pneumonitis induced in mice with *C. trachomatis*, except infection with *C. trachomatis* is cleared in 14 days. A striking pathologic feature is the accumulation of lymphoid cells in the perivascular and peribronchial areas, which appear on day 11 and persist through day 60 following the primary infection. For *C. trachomatis*, formation of lymphoid cell foci is observed only in chronic or repeated

ocular and salpingeal reinfection in both humans (140) and monkeys (107, 108, 109). Human lung pathology in *C. pneumoniae* infection has not been well described, and whether the pathology is similar to that in mice develops in humans is unknown.

C. pneumoniae has been shown to spread systemically in mice following intranasal inoculation (153). Isolation of *C. pneumoniae* from spleen and peritoneal macrophages is as frequent as from lungs in intranasally inoculated mice. This finding that *C. pneumoniae* infection in mice is a systemic disease suggests that it may be a systemic infection in humans.

C. pneumoniae has been shown to be of low virulence in baboons (*Papio cynocephalus anubus*) and rhesus (*Macaca cyclopid*) and cynomolgus monkeys. Nasopharyngeal, oropharyngeal, or intratracheal inoculation of baby baboons (10) and cynomolgus monkeys (57) with *C. pneumoniae* resulted in no disease attributable to the experimental infection, although the organisms were recoverable from the nasopharynx. Unlike that of *C. trachomatis*, inoculation of *C. pneumoniae* into conjunctiva results in only mild inflammation (77).

New Zealand White rabbits are susceptible to intranasal and intratracheal inoculation with *C. pneumoniae* (97). Respiratory disease in the rabbit model is characterized by moderate multifocal interstitial pneumonia with bronchiolitis and vasculitis. Single inoculation results in a self-resolving pneumonitis, 3 weeks in duration, composed of heterophils initially and then changing to predominately mononuclear cells. With repeated inoculations, scattered microgranulomas consisting of a central core of macrophages surrounded by activated lymphocytes develop and persist through day 42 of infection. Organisms could be cultured from the upper respiratory tract during the early

stages of the disease but never from lung tissue. However, lung tissue was intermittently positive by PCR through day 42. Chlamydial DNA was also detected by PCR in spleen tissue and peripheral blood mononuclear cells, indicating systemic disease similar to that in the mouse model.

ANALYTICAL PROBLEMS IN CHLAMYDIAL RESEARCH

Pathogen detection

A general problem in *Chlamydia* research and evaluation of clinical samples is the sensitive, quantitative, and reproducible detection of low numbers of chlamydial organisms typically associated with the chronic and subclinical infections. Real-time quantitative PCR approach is the most sensitive and specific way to quantify chlamydia in specimens. General rules for real-time PCR apply also to the performance of real-time PCR for detection of chlamydiae.

A major challenge in successful routine use of real-time PCR is the consistent output of high quality results. Vaerman et al. (144) conclude that it is today's challenge "to design experimental protocols that are rigorously validated. Each step of any real-time PCR based assay must be controlled, from sampling to PCR, including manipulations like extraction and reverse transcription. The evaluation of analytical parameters such as linearity, precision, accuracy, specificity, recovery, limit of detection, robustness, reference interval (and so on) helps us to achieve this goal. Statistical tools such as control charts allow us to study, in the real-time PCR process, the impact of various factors that change over time."

In order to obtain consistent and contamination-free real-time PCR results, separate laboratories should be designated for sample processing and nucleic acid extraction, for assembly of real-time PCRs, for the real-time PCR instrument, and for contamination-free disposal of closed PCR vessels.

Specimen collection and processing for real-time PCR falls largely into 2 categories: i) specimens for high sensitivity real-time PCR of low-copy targets such as chlamydiae, for which specimen quantity may be limiting, or ii) specimens for genetic typing for which specimen quantity is not limiting. Specimens for low-copy targets require careful preservation of nucleic acids, removal of PCR inhibitors, and highest recovery during nucleic acid extraction (4). Frequently, the limiting factor in detection of low-copy targets is target preservation and recovery in nucleic acid extraction, not the real-time PCR assay (22). For genetic typing of high-copy targets, it is important that PCR inhibitors are quantitatively removed during nucleic acid extraction while sample preservation and recovery rates are of less concern.

It is a misconception that immediate freezing is the best approach for nucleic acid preservation. In fact, nucleic acids in frozen samples become exposed to nucleases during thawing, and low-copy targets may easily be lost. It is imperative to collect low-copy samples specifically for PCR analysis in nucleic acid preservatives such as guanidinium isothiocyanate buffer before freezing (22). In most cases, it will make good sense to collect any sample specifically for real-time PCR. This requires good communication and clear instructions between laboratory and clinical personnel (57). Other factors that affect the stability and property of samples should also be considered. This may include anticoagulants, stabilizing agents, temperature, timing before initial

processing, sterility, and even the endogenous degrading properties of specific sample types (57).

In real-time PCR assays, optimal extraction of nucleic acids from a wide range of clinical samples is one of the most underappreciated, but nevertheless challenging and important steps. Proper extraction must efficiently release nucleic acids from samples, remove PCR inhibitors, avert the degradation of nucleic acids, and ensure adequate concentration of the nucleic acids after extraction. In some cases, concentration of target organisms by physical means increases assays sensitivity, but it is important to ascertain the enrichment effect (22). Such methods include immunomagnetic, centrifugal, or filter concentration (3, 80, 115).

The presence of inhibitory substances in the samples may strongly influence PCR performance and detection sensitivity. PCR inhibitors typically interfere with the action of DNA polymerase (3), but may also degrade nucleic acids, or interfere with the cell lysis procedure (147). Bile salts and complex polysaccharides in feces (78), heme, immunoglobin G, and lactoferrin in blood (1, 2), collagen in food samples (75), and humic substances in soil (143) have been identified as PCR-inhibitors.

Nucleic acid preparations used as samples in real-time PCR assays include total nucleic acids, purified DNA, total RNA, and poly $(A)^+$ RNA. An abundance of quality-assured commercial kits are available for extraction of nucleic acids, and it is strongly advisable to use such kits in the clinical laboratory. It is imperative, however, to validate recovery and removal of PCR inhibitors of any nucleic acid extraction method prior to routine use (115). Also, compatibility of the nucleic acid storage buffer with the real-

time PCR, and reproducibility of results after freeze-thaw cycles of extracted nucleic acids should be evaluated (146).

Huang et al (61) reported a hot-start quantitative PCR in the glass capillary quantitative PCR format of the Light-Cycler®, which could detect as few as single copies of DNA of *Chlamydia* spp. by SYBR® Green fluorescence of the dsDNA product and by fluorescence resonance energy transfer (FRET) hybridization probes. The PCRs were seen to have 15-fold more sensitivity than the cell culture quantitative assay of *C. psittaci* B577 infectious stock. The number of chlamydial genomes detected by *C. psittaci* B577 FRET PCR correlated well with cell culture determination of inclusion forming units (IFUs). When infected tissue samples were analyzed by cell culture and PCR, the correlation coefficient between IFUs and chlamydial genomes was higher with *C. psittaci* B577 FRET PCR than with *Chlamydia* omp1 SYBR Green PCR (61). Thus, real-time PCR is an effective approach for high throughput and sensitive detection and quantification of chlamydial nucleic acids in clinical and experimental specimens.

Analysis of mouse models of chlamydial disease

A problem in the analysis of mouse models of chlamydial infection and disease is the consistent evaluation of multiple functional parameters in infected tissue. Determination of parameters such as reactive immune cells requires rapid processing of live tissue, thus limiting the number of specimens. Analysis of transcript levels offers an attractive option for screening or simultaneous examination of numerous outcomes associated with known gene functions. Nucleic acids in specimens can reliably be stabilized in specimens by homogenization in concentrated solutions of guanidinum

isothiocyate (22). Of all methods used to quantify mRNA, real-time reverse transcriptase PCR is considered the most sensitive and accurate one (14). Typically, separate real-time RT-PCR assays are used to quantify analyte mRNA and the mRNA of a constantly transcribed internal reference gene (also termed housekeeping gene). Thus, presently reverse transcriptase real-time PCR is still a cumbersome technique that requires multiple reactions per single specimen and has a high potential for operator errors.

RESEARCH OBJECTIVES

The overall objective of this research was to evaluate multivariate influences on the outcome of *C. pneumoniae* lung infection in mice. To this end, analysis of multiple transcripts in murine lung tissue was required. An initial objective of this research was therefore to develop accurate real-time RT-PCR methodology that allowed the simultaneous quantification of analyte and reference transcript in a single reaction. To acccomplish these goals, the following research objectives were identified:

1. Develop a single-tube, one-step, duplex real-time RT-PCR method to accurately quantify 25 mRNA species by use of fluorescently-labeled oligonucleotide probes and amplicon detection by fluorescence emitted after fluorescence resonance energy transfer (FRET).
2. To analyze multivariate influences of mouse strain, immune status, time post inoculation, and dietary protein and antioxidants on the outcome of experimental intranasal *C. pneumoniae* infection of 320 inbred mice. The parameters disease, expressed as lung weight increase over mock-infected mice, and lung *C. pneumoniae* burden were to be associated with the categorical parameters mouse strain, immune status, and time post inoculation, and with relative expression of 25 mRNAs in mouse lung tissue.

REFERENCES

1. **Akane, A., K. Matsubara, H. Nakamura, S. Takahashi, and K. Kimura.** 1994. Identification of the heme compound copurified with deoxyribonucleic acid (DNA) from bloodstains, a major inhibitor of polymerase chain reaction (PCR) amplification. J. Forensic. Sci. **39:**362-372.
2. **Al-Soud, W. A., L. J. Jonsson, and P. Radstrom.** 2000. Identification and characterization of immunoglobulin G in blood as a major inhibitor of diagnostic PCR. J. Clin. Microbiol. **38:**345-350.
3. **Al-Soud, W. A., P. –G. Lantz, A. Bäckman, P. Olcén, and P. Rådström.** 1998. A sample preparation method which facilitates detection of bacteria in blood cultures by the polymerase chain reaction. J. Microbiol. Meth. **32:**217-224.
4. **Al-Soud, W. A., and P. Radstrom.** 2001. Purification and characterization of PCR-inhibitory components in blood cells. J. Clin. Microbiol. **39:**485-493.
5. **Amman, R., N. Springer, W. Schönhuber, W. Ludwig, E. N. Schmid, K. D. Muller, and R. Michel.** 1997. Obligate intracellular bacterial parasites of *Acanthamoebae* related to *Chlamydia* spp. Appl. Environ. Microbiol. **63:**115-121.

6. **Anderson, I. E., S. I. Baxter, S. Dunbar, A. G. Rae, H. L. Phi, M. J. Clarkson, and A. J. Herring.** 1996. Analyses of the genomes of chlamydial isolates from ruminants and pigs support the adoption of the new species *Chlamydia pecorum*. Int. J. Sys. Bacteriol. **46:**245-251.

7. **Appleyard, W. T., I. D. Aitken, and I. Anderson.** 1983. Outbreak of chlamydial abortion in goats. Vet. Rec. **113:**63.

8. **Baker, J. A**. 1944. Virus causing pneumonia in cats and producing elementary bodies. J. Exp. Med. **79:**159.

9. **Beaty, C. D., J. T. Grayston, S. P. Wang, C. C. Kuo, C. S. Reto, and T. R. Martin.** 1991. *Chlamydia pneumoniae*, strain TWAR, infection in patients with chronic obstructive pulmonary disease. Am. Rev. Respir. Dis. **144:**1408-1410.

10. **Bell, T. A., C. C. Kuo, S. P. Wang, and J. T. Grayston.** 1989. Experimental infection of baboons (Papio cynocephalus anubis) with *Chlamydia pneumoniae* strain 'TWAR'. J. Infect. **19:**47-49.

11. **Birch, L., C. E. Dawson, J. H. Cornett, and J. T. Keer.** 2001. A comparison of nucleic acid amplification techniques for the assessment of bacterial viability. Lett. Appl. Microbiol. **33:**296-301.

12. **Bonnet, F., P. Morlat, I. Delevaux, A. M. Gavinet, M. Parrens, N. Bernard, D. Lacoste, and J. Beylot.** 2000. A possible association between *Chlamydiae psittacci* infection and temporal arteritis. Joint Bone Spine. **67:**550-552.

13. **Braun, J., S. laitko, and J. Treharne.** 1994. *Chlamydia pneumoniae* – a new causative agent of reactive arthritis and undifferentiated oligoarthritis. Ann. Rheum. Dis. **53:**100-105.

14. **Bustin, S. A.** 2000. Absolute quantification of mRNA using real-time reverse transcription polymerase chain reaction assays. J. Mol. Endocrinol. **25:**169-193.

15. **Cajaraville, M. P., and E. Angulo.** 1991. *Chlamydia*-like organisms in digestive and duct cells of mussels from the Basque coast. J. Invertebr. Pathol. **58:**381-386.

16. **Cello, R. M.** 1967. Ocular infections in animals with PLT (*Bedsonia*) group agents. Am. J. Opthalmol. **63:**1270.

17. **Cheng, H., M. Macaluso, S. H. Vermund, and E. W. Hook.** 2001. Relative accuracy of nucleic acid amplification tests and culture in detecting *Chlamydia* in asymptomatic men. J. Clin. Microbiol. **39:**3927-3937.

18. **Chernesky, M. A.** 1999. Nucleic acid tests for the diagnosis of sexually transmitted diseases. FEMS Immunol. Med. Microbiol. **24:**437-446.

19. **Clarkson, M. J., and H. L. Philips.** 1997. Isolation of faecal chlamydia from sheep in Britain and their characterization by cultural properties. Vet. J. **153:**307-310.

20. **Cubero-Pablo, M. J., M. Plaza, L. Perez, M. Gonzalez, and L. Leon-Vizcaino.** 2000. Seroepidemiology of chlamydial infections of wild ruminants in Spain. J. Wildl. Dis. **36:**35-47.

21. **Dechend, R., M. Maass, J. Gieffers, R. Dietz, C. Scheidereit, A. Leutz, and D. C. Gulba.** 1999. *Chlamydia pneumoniae* infection of vascular smooth muscle and endothelial cells activates NF-kappaB and induces tissue factor and PAI-1 expression: a potential link to accelerated arteriosclerosis. Circulation. **100:**1369-1373.

22. **DeGraves, F. J., D. Gao, H. R. Hehnen, T. Schlapp, and B. Kaltenboeck.** 2003. Quantitative detection of *Chlamydia psittaci* and *C. pecorum* by high-sensitivity real-time PCR reveals high prevalence of vaginal infection in cattle. J Clin. Microbiol. **41:**1726-1729.

23. **DeGraves, F. J., T. Kim, J. Jee, T. Schlapp, H. R. Hehnen, and B. Kaltenboeck.** 2004. Reinfection with *Chlamydophila abortus* by uterine and indirect cohort routes reduces fertility in cattle preexposed to *Chlamydophila*. Infect. Immun. **72:**2538-2545.

24. **Dhingra, P. N., L. P. Agarwal, V. M. Mahajan, and S. C. Adalakha.** 1980. Isolation of chlamydia from pneumonic lungs of buffaloes, cattle and sheep. Zbl Veterinarmedizin B. **27:**680-682.

25. **Eb, F., J. Orfila, and J. F. Lefebvre.** 1976. Ultrastructural study of the development of the agent of ewe's abortion. J. Ultrast. Res. **56:**177-185.

26. **Eddie, B., F. J. Radovsky, D. Stiller, and N. Kumada.** 1966. Psittacosis-lymphogranuloma venereum (PL) agents (Bedsonia, *Chlamydia*) in ticks, fleas, and native mammals in California. Am. J. Epidemiol. **90:**449-460.

27. **Erntell,. M., K. Ljunggren, T. Gadd, and K. Persson.** 1989. Erythema nodosum--a manifestation of *Chlamydia pneumoniae* (strain TWAR) infection. Scand. J. Infect. Dis. **21:**693-696.

28. **Everett, K. D., R. M. Bush, and A. A. Andersen.** 1999. Emended description of the order *Chlamydiales*, proposal of *Parachlamydiaceae* fam. Nov. and *Simkania* fam.nov., each containing one monotypic genus, revised taxonomy of the family

Chlamydiaceae, including a new genus and fire new species, and standards for the identification of organisms. Int. J. Syst. Bacteriol. **49:**415-440.

29. **Ezzahiri, R., F. R. Stassen, H. A. Kurvers, M. M. van Pul, P. J. Kitslaar, and C. A. Bruggeman.** 2003. *Chlamydia pneumoniae* infection induces an unstable atherosclerotic plaque phenotype in LDL-receptor, ApoE double knockout mice. Eur. J. Vasc. Endovasc. Surg. **26:**88-95.

30. **Ferrick, D. A., M. D. Schrenzel, T. Mulvania, B. Hsieh, W. G. Ferlin, and H. Lepper.** 1995. Differential production of interferon-gamma and interleukin-4 in response to Th1- and Th2-stimulating pathogens by gamma delta T cells in vivo. Nature. **373:**255-257.

31. **Fong, I. W., B. Chiu, E. Viira, D. Jang, M. W. Fong, R. Peeling, and J. B. Mahony.** 1999. Can an antibiotic (macrolide) prevent *Chlamydia pneumoniae*-induced atherosclerosis in a rabbit model? Clin. Diagn. Lab. Immunol. **6:**891-4.

32. **Fukushi, H., and K. Hirai.** 1992. Proposal of *Chlamydia pecorum* sp. nov. for Chlamydia strains derived from ruminants. Int. J. Syst. Bacteriol. **42:**306-308.

33. **Gaillard, E. T., A. M. Hargis, D. J. Prieur, J. F. Evermann, and A. S. Duillon.** 1984. Pathogenesis of feline gastric chlamydial infection. Am. J. Vet. Res. **45:** 2314-2321.

34. **Gaydos, C. A., P. M. Roblin, M. R. Hammerschlag, C. L. Hyman, J. J. Eiden, J. Schachter, and T. C. Quinn.** 1994. Diagnostic utility of PCR-enzyme immunoassay, culture, and serology for detection of *Chlamydia pneumoniae* in symptomatic and asymptomatic patients. J. Clin. Microbiol. **32:**903-905.

35. **Gieffers, J., H. Fullgraf, J. Jahn, M. Klinger, K. Dalhoff, H. A. Katus, W. Solbach, and M. Maass.** 2001. *Chlamydia pneumoniae* infection in circulating human monocytes is refractory to antibiotic treatment. Circulation. **103:**351-356.

36. **Giovannini, A., F. M. Cancellotti, C. Turilli, and E. Randi.** 1988. Serological investigations for some bacterial and viral pathogens in fallow deer (*Cervus dama*) and wild boar (*Sus scrofa*) of the San Rossore Preserve, Tuscany, Italy. J. Wildl. Dis. **24:**127-132.

37. **Girjes, A. A., W. A. Ellis, M. F. Lavin, and F. N. Carrick FN.** 1993. Immuno-dot blot as a rapid diagnostic method for detection of chlamydial infection in koalas (*Phasolarctos cinereus*). Vet. Rec. **133:**136-141.

38. **Grayston, J. T., C. C. Kuo, L. A. Campbell, and E. P. Benditt.** 1993. *Chlamydia pneumoniae*, strain TWAR and atherosclerosis. Eur. Heart J. **14 Suppl K:**66-71.

39. **Grayston, J. T., C. Mordhorst, A. L. Bruu, S. Vene, and S. P. Wang.** 1989. Countrywide epidemics of *Chlamydia pneumoniae*, strain TWAR, in Scandinavia, 1981-1983. J. Infect. Dis. **159:**1111-1114.

40. **Grayston, J. T., S. P. Wang, C. C. Kuo, and L. A. Campbell.** 1989. Current knowledge on *Chlamydia pneumoniae*, strain TWAR, an important cause of pneumonia and other acute respiratory diseases. Eur J Clin Microbiol Infect. Dis. **8:**191-202.

41. **Grayston, J. T.** 1992. Infections caused by *Chlamydia pneumoniae* strain TWAR. Clin. Infect. Dis.**15:**757-761.

42. **Grayston, J. T.** 1994. *Chlamydia pneumoniae* (TWAR) infections in children. Pediatr. Infect. Dis. J. **13:**675-684.

43. **Greth, A., D. Calvez, M. Vassart, and P. C. Lefevre.** 1992. Serological survey for bovine bacterial and viral pathogens in captive Arabian oryx (Oryx leucoryx Pallas, 1776). Revue Scientifique et Technique. **11:**1163-1168.

44. **Griffiths, P. C., H. L. Philips, M. Dawson, and M. J. Clarkson.** 1992. Antigenic and morphological differentiation of placental and intestinal isolates of *Chlamydia psittaci* of ovine origin. Vet. Micobiol. **30:**165-177.

45. **Griffiths, P. C., J. M. Plater, M. W. Horigan, M. P. M. Rose, C. Venables, and M. Dawson.** 1996. Serological diagnosis of ovine enzootic abortion by comparative inclusion immunofluorescence, recombinant lipopolysaccharide enzyme linked immunosorbent assay, and complement fixation test. J. Clin. Microbiol. **34:**1512-1518.

46. **Gupta, P. P., B. Singh, and P. N. Dhingra.** 1976. *Chlamydial pneumonia* in a buffalo calf. Zbl. Veterinärmedizin B. **23:**779-781.

47. **Hahn, D. L., T. Anttila, and P. Saikku.** 1996. Association of *Chlamydia pneumoniae* IgA antibodies with recently symptomatic asthma. Epidemiol. Infect. **117:**513-7.

48. **Haidl, S., T. Anttila, and P. Saikku.** 1992. Guillain-Barre syndrome after *Chlamydia pneumoniae* infection. N. Engl. J. Med. **326**:576-577.

49. **Halme, S., J. Latvala, R. Karttunen, I. Palatsi, P. Saikku, and H. M. Surcel.** 2000. Cell-mediated immune response during primary *Chlamydia pneumoniae* infection. Infect. Immun. **68:**7156-7158.

50. **Hammerschlag, M. R., T. Reznik, P. M. Roblin, J. Ramirez, J. Summersgill, and S. Bukofzer.** 2003. Microbiological efficacy of ABT-773 (cethromycin) for the treatment of community-acquired pneumonia due to *Chlamydia pneumoniae*. J. Antimicrob. Chemother. **51:**1025-1028.

51. **Harshbarger, J. C., S. C. Chang, and S. V. Otto.** 1977. *Chlamydiae* (with phages), mycoplasmas, and rickettsiae in Chespeake Bay bivalves. Science. **196:**666-668.

52. **Hashigucci, K., and T. Matsunobu.** 2003. Etiology of acute pharyngitis in adults: the presence of viruses and bacteria. Nippon Jibiinkoka Gakkai Kaiho. **106:**532-539.

53. **Hawkins, R. A., R. G. Rank, and K. A. Kelly.** 2002. A *Chlamydia trachomatis*-specific Th2 clone does not provide protection against a genital infection and displays reduced trafficking to the infected genital mucosa. Infect. Immun. **70:**5132-5139.

54. **Herrera, V. L., L. Shen, L. V. Lopez, T. Didishvili, Y. X. Zhang, and N. Ruiz-Opazo.** 2003. *Chlamydia pneumoniae* accelerates coronary artery disease progression in transgenic hyperlipidemia-genetic hypertension rat model. Mol. Med. **9:**135-142.

55. **Hitchcock, P. J.** 1999. Future directions of chlamydial research. In: Chlamydia, Intracellular Biology, Pathogenesis and Immunity. Stephens, R.S. (ed.), ASM Washington, D.C., U.S.A., 297-311.

56. **Hoefer, D., G. Poelzl, J. Kilo, C. Hoermann, J. I. Mueller, G. Laufer, and H. Antretter.** 2005. Early detection and successful therapy of fulminant *Chlamydia pneumoniae* myocarditis. ASAIO J. **51:**480-481.

57. **Holland, N. T., M. T. Smith, B. Eskenazi, and M. Bastaki.** 2003. Biological sample collection and processing for molecular epidemiological studies. Mutat. Res. **543:**217-234.

58. **Homer, B. L., E. R. Jacobson, J. Schumacher, and G. Scherba.** 1994. Chlamydiosis in mariculture-reared green sea turtles (*Chelonia mydas*). Vet. Pathol. **31:**1-7.

59. **Howerth, E. W.** 1984. Pathology of naturally occurring chlamydiosis in African clawed frogs (*Xenopus laevis*). Vet. Pathol. **21:**28-32.

60. **Hruba, D., K. Roubalova, P. Kraml, and M. Andel.** 2004. Signs of active infection with *Chlamydia pneumoniae* in patients with coronary heart disease. Cas. Lek. Cesk. **143:**830-835.

61. **Huang, J., F. J. DeGraves, D. Gao, P. Feng, T. Schlapp, and B. Kaltenboeck.** 2001. Quantitative detection of *Chlamydia* spp. by fluorescent PCR in the LightCycler. BioTechniques. **30:**150-157.

62. **Huchzermeyer, F. W.** 1997. Public health risks of ostrich and crocodile meat. Revue Scientifique et Technique. **16:**599-604.

63. **Huovinen, P., R. Lahtonen, T. Ziegler, O. Meurman, K. Hakkarainen, A. Miettinen, P. Arstila, J. Eskola, and P. Saikku.** 1989. Pharyngitis in adults: the presence and coexistence of viruses and bacterial organisms. Ann. Intern. Med. **110:**612-616.

64. **Jain, S. K., B. S. Rajya, G. C. Mohanty, O. P. Paliwal, M. L. Mehrotra, and R. L. Sab.** 1975. Pathology of chlamydial abortion in ovine and caprine. Curr. Sci. **44:**209-210.

65. **Jee, J., F. J. Degraves, T. Kim, and B. Kaltenboeck.** 2004. High prevalence of natural *Chlamydophila* species infection in calves. J. Clin. Microbiol. **42:**5664-5672.

66. **Jones, G. E.** 1999. Chlamydial diseases of the reproductive tract of domestic ruminants. In: Sexually Transmitted Diseases and Adverse Outcomes of Pregnancy. Hitchcock, P.J., MacKay, H.T., Wasserheit, J.N. and Binder, R. (eds.). American Society for Microbiology, Washington, D.C., U.S.A., 293-309.

67. **Jones, G. E., J. C. Low, J. Machell, and K. Armstrong.** 1997. Comparison of five tests for the detection of antibodies against chlamydial (enzootic) abortion of ewes. Vet. Rec. **141:**164-168.

68. **Kaltenboeck, B., K. G. Kousoulas, and J. Storz.** 1991. Detection and strain differentiation of *Chlamydia psittaci* mediated by a two-step polymerase chain reaction. J. Clin. Microbiol. **29:**1969-1975.

69. **Kaltenboeck, B., K. G. Kousoulas, and J. Storz.** 1993. Structures of and allelic diversity and relationships among the major outer membrane protein (*ompA*) genes of the four chlamydial species. J. Bacteriol. **175:**487-502.

70. **Kaltenboeck, B., N. Schmeer, and R. Schneider.** 1997. Evidence for numerous *omp*1 alleles of porcine *Chlamydia trachomatis* and novel chlamydial species obtained by PCR. J. Clin. Microbiol. **35:**1835-1841.

71. **Kaukoranta-Tolvanen, S. S., A. L. Laurila, P. Saikku, M. Leinonen, L. Liesirova, and K. Laitinen.** 1993. Experimental infection of *Chlamydia pneumoniae* in mice. Microbiol. Pathog. **15:**293-302.

72. **Kauppinen, T. P.** 1994. Assessment of exposure in occupational epidemiology. Scand. J. Work. Environ. Health. **20:**19-29.

73. **Kazmierski, R., E. Podsiadly, S. Tylewska-Wierzbanowska, and W. Kozubski.** 2005. Association between carotid atherosclerosis, inflammatory markers and *Chlamydia pneumoniae* infection. Neurol. Neurochir. Pol. **39:**277-286.

74. **Kelso, A., P. Groves, and A. B. Troutt, and K Francis.** 1995. Evidence for the stochastic acquisition of cytokine profile by $CD4^+$ T cells activated in a T helper type 2-like response in vivo. Eur. J. Immunol. **25:**1168-1175.

75. **Kim, C. H., M. Khan, D. E. Morin, W. L. Hurley, D. N. Tripathy, M. Jr. Kehrli, A. O. Oluoch, and I. Kakoma.** 2001. Optimization of the PCR for detection of *Staphylococcus aureus nuc* gene in bovine milk. J. Dairy Sci. **84:**74-83.

76. **Kol, A., and P. Libby.** 1998. The mechanisms by which infectious agents may contribute to atherosclerosis and its clinical manifestations. Trends Cardiovascul. Med. **8:**191-199.

77. **Kuo, C. C., H. H. Chen, S. P. Wang , and J. T. Grayston.** 1986. Identification of a new group of *Chlamydia psittaci* strains called TWAR. J. Clin. Microbiol. **24:**1034-1037.

78. **Lantz, P. –G., M. Matsson, T. Wadström, and P. Rådström.** 1997. Removal of PCR inhibitors from human faecal samples through the use of an aqueous two-phase system for sample preparation prior to PCR. J. Microbiol. Meth. **28:**159-167.

79. **Li, D., A. Vaglenov, T. Kim, C. Wang, D. Gao, and B. Kaltenboeck.** 2005. High-yield culture and purification of *Chlamydiaceae* bacteria. J. Microbiol. Meth. **61:**17-24.

80. **Lindqvist, R., B. Norling, and S. T. Lambertz.** 1997. A rapid sample preparation method for PCR detection of food pathogens based on buoyant density centrifugation. Lett. Appl. Microbiol. **24:**306-310.

81. **Lisby, G.** 1999. Application of nucleic acid amplification in clinical microbiology. Mol. Biotechnol. **12:**75-99.

82. **Louis, C., G. Nicolas, F. Eb, J. F. Lefebvre, and J. Orfila.** 1980. Modifications of the envelope of *Chlamydia psittaci* during its developmental cycle: freeze-fracture study of complementary replicas. J. Bacteriol. **141:**868-875.

83. **Magnino, S., P. G. Vigo, P. C. Griffiths, J. M. Plater, C. Bazzocchi, L. De-Guili, M. Donati, R. Cevenini, C. Bandi, C. Bergami, and M. Fabbi.** 2000. Molecular characterization of chlamydial strains isolated from Italian dairy cattle affected with endometritis. In: Proceedings of the European Society for Chlamydia Research, vol. 4. Saikku, P. (ed.). Societa Editrice Esculapio, Bologna, Italy, 272.

84. **Mak, R. P., L. van Renterghem, and A. Traen.** 2005. *Chlamydia trachomatis* in female sex workers in Belgium: 1998-2003. Sex. Transm. Infect. **81:**89-90.

85. **Malinverni, R., C. C. Kuo, L. A. Campbell, A. Lee, and J. T. Grayston.** 1995. Effects of two antibiotic regimens on course and persistence of experimental *Chlamydia pneumoniae* TWAR pneumonitis. Antimicrobiol. Agents Chemother. **39:**45-49.

86. **Mansell, J. L., K. N. Tang, C. A. Baldwin, E. L. Styer, and A. D. Liggett.** 1995. Disseminated chlamydial infection in antelope. J. Vet. Diagn. Invest.. **7:**397-399.

87. **Markey, B. K., M. S. McNulty, D. Todd, and D. P. Mackie.** 1993. Comparison of ovine abortion and non-abortion isoates of *Chlamydia psittaci* using inclusion morphology, polyacrylamide gel electrophoresis, restriction endonuclease analysis and reactivity with monoclonal antibodies. Vet. Microbiol. **35:**141-159.

88. **Marrie, T. J.** 1990. Epidemiology of community-acquired pneumonia in the elderly. Semin. Respir. Infect. **5:**260-268.

89. **Marrie, T. J., J. T. Grayston, S. P. Wang, and C. C. Kuo.** 1987. Pneumonia associated with TWAR strain of *Chlamydia*. Ann. Intern. Med. **172:** 1330-1335.

90. **Matsumoto, A.** 1982. Surface projections of *Chlamydia psittaci* elementary bodies as revealed by freeze-deep-etching. J. Bacteriol. **151:**1040-1042.

91. **Matsumoto, A.** 1988. Structural characteristics of chlamydial bodies. In: Microbiology of Chlamydia. (Baron, A. L. ed). CRC Press, Boca Raton, Fl., USA, 21-45.

92. **May, A. E., V. Redecke, S. Gruner, R. Schmidt, S. Massberg, T. Miethke, B. Ryba, C. Prazeres da Costa, A. Schomig, and F. J. Neumann.** 2003. Recruitment of *Chlamydia pneumoniae*-infected macrophages to the carotid artery wall in noninfected, nonatherosclerotic mice. Arterioscler. Thromb. Vasc. Biol. **23:**789-794.

93. **McCauley, E. H., and E. L. Tieken.** 1968. Psittacosis-lymphogranuloma venereum agent isolated during an abortion epizootic in goats. J. Am. Vet. Med. Assoc. **152:**1758 -1765.

94. **McKercher, D. G., E. M. Wada, S. K. Ault, and J. H. Theis.** 1980. Preliminary studies on transmission of *Chlamydia* to cattle by ticks (*Ornithodorus coriaceus*). Am. J. Vet. Res. **41:**922.

95. **McNutt, S.H., and E. F. Waller.** 1940. Sporadic bovine encephalomyelitis. Cornell Veterinarian. **30:**437-448.

96. **Meyer, K. F.** 1965. Ornithosis. In: Disease of Poultry, 5th ed., Biester HE, Schwarte LH (eds), Iowa State University Press, Ames, Iowa, USA, 675.

97. **Moazed, T. C., C. Kuo, D. L. Patton, J. T. Grayston, L. A. Campbell.** 1996. Experimental rabbit models of *Chlamydia pneumoniae* infection. Am. J. Pathol. **148:**667-676.

98. **Moazed, T. C., C. C. Kuo, J. T. Grayston, and L. A. Campbell.** 1998. Evidence of systemic dissemination of *Chlamydia pneumoniae* via macrophages in the mouse. J. Infect. Dis. **177:**1322-1325.

99. **Morel, G.** 1978. Isolement de deux *Chlamydiales* (rickettsies) chez un arachnide: l'araignee *Pisaura mirabilis*. Experientia. **34:**344.

100. **Muhlestein, J. B.** 1998. Bacterial infections and atherosclerosis. J. Investig. Med. **46:**396-402.

101. **Murray, E. S.** 1964. Guinea pig inclusion conjunctivitis virus. 1. Isolation and identification as a member of the psittacosis-lymphogranuloma-trachoma group. J. Infect. Dis. **114:**1-12.

102. **Neuvonen, E.** 1976. Occurrence of antibodies to group specific *Chlamydia* antigen in cattle and reindeer sera in Finnish Lapland. Acta Veterinaria Scandinavica. **17:**363-369.

103. **Newcomer, C. E., M. R. Anver, J. L. Simmons, B. W. Jr. Wilcke, and G. W. Nace.** 1982. Spontaneous and experimental infections of *Xenopus laevis* with *Chlamydia psittaci*. Lab. Anim. Sci. **32:**680-686.

104. **Nigg, C.** 1942. Unidentified virus which produces pneumonia and systemic infection in mice. Science. **95:**49-50.

105. **Ogawa, H., K. Hashiguchi, and Y. Kazuyama.** 1992. Recovery of *Chlamydia pneumoniae*, in six patients with otitis media with effusion. J. Laryngol. Otol. **106:**490-492.

106. **Ostergaard, L.** 1999. Diagnosis of urogenital *Chlamydia trachomatis* infection by use of DNA amplification. Acta Pathologica Microbiologica Scandinavica (APMIS), Supplements. **89:** 5-36.

107. **Patton, D. L., C. C. Kuo, S. P. Wang, R. M. Brenner, M. D. Sternfeld, S. A. Morse, and R. C. Barnes.** 1987. Chlamydial infection of subcutaneous fimbrial transplants in cynomolgus and rhesus monkeys. J. Infect. Dis. **155:**229-235.

108. **Patton, D. L., and C. C. Kuo.** 1989. Histopathology of *Chlamydia trachomatis* salpingitis after primary and repeated reinfections in the monkey subcutaneous pocket model. J. Reprod. Fertil. **85:**647-656.

109. **Patton, D. L., and H. R. Taylor.** 1986. The histopathology of experimental trachoma: ultrastructural changes in the conjunctival epithelium. J. Infect. Dis. **153:**870-878.

110. **Penttila, J. M., R. Pyhala, M. Sarvas, and N. Rautonen.** 1998. Expansion of a novel pulmonary $CD3^-$ $CD4^+$ $CD8^+$ cell population in mice during *Chlamydia pneumoniae* infection. Infect. Immun. **66:**3290-3294.

111. **Perez-Martinez, J. A., N. Schmeer, and J. Storz.** 1986. Bovine chlamydial abortion: serodiagnosis by modified complement-fixation and indirect inclusion fluorescence tests and enzyme-linked immunosorbent assay. Am. J. Vet. Res. **47:**1501-1506.

112. **Pether, J. V., and S. P. Wang, and J. T. Grayston.**1989. *Chlamydia pneumoniae*, strain TWAR, as the cause of an outbreak in a boys' school previously called psittacosis. Epidemiol. Infect. **103:**395-400.

113. **Pislaru, S. V., M. van Ranst, C. Pislaru, Z. Szelid, G. Theilmeier, J. M. Ossewaarde, P. Holvoet, S. Janssens, E. Verbeken, and F. J. van de Werf.** 2003. *Chlamydia pneumoniae* induces neointima formation in coronary arteries of normal pigs. Cardiovasc. Res. **57:**834-842.

114. **Puolakkainen, M., L. A. Campbell, C. C. Kuo, M. Leinonen, C. Gronhagen-Riska, and P. Saikku.** 1996. Serological response to *Chlamydia pneumoniae* in patients with sarcoidosis. J. Infect. **33:**199-205.

115. **Radstrom, P., R. Knutsson, P. Wolffs, M. Dahlenborg, and C. Lofstrom.** 2003 Pre-PCR processing of samples. Methods Mol. Biol. **216:**31-50.

116. **Reed, D. E., S. D. Lincoln, R. P. Kwapien, T. L. Chow, and C. E. Whiteman.** 1975. Comparison of antigenic structure and pathogenicity of bovine intestinal chlamydia isolate with an agent of epizootic bovine abortion. Am. J. Vet. Res. **36:**1141.

117. **Reed, K. D., G. R. Ruth, J. A. Meyer, and S. K. Shukla.** 2000. *Chlamydia pneumoniae* infection in a breeding colony of African clawed frogs (*Xenopus tropicalis*). Emerg. Infect. Diseases. **6:**196-199.

118. **Resnikoff, S., D. Pascolini, D. Etya'ale, I. Kocur, R. Pararajasegaram, G. P. Pokharel, and S. P. Mariotti.** 2004. Global data on visual impairment in the year 2002. Bulletin of the World Health Organization. **82:**844-51.

119. **Rockey, D. D., and A. Matsumoto.** 2000. The chlamydial developmental cycle. In: Prokaryotic Development. Brun YV, Shimkets LJ, (eds.). ASM Press, Washington D. C., 403-425.

120. **Romagnani, S.** 1996. Development of Th 1- or Th 2-dominated immune responses: what about the polarizing signals? Int. J. Clin. Lab. Res. **26:**83-98.

121. **Rothstein, N. M., T. C. Quinn, G. Madico, C. A. Gaydos, and C. J. Lowenstein.** 2001. Effect of azithromycin on murine arteriosclerosis exacerbated by *Chlamydia pneumoniae*. J. Infect. Dis. **183:**232-238.

122. **Rowe, L. W., R. S. Hedger, and C. Smale.** 1978. The isolation of a *Chlamydia psittaci*-like agent from a free-living African buffalo (*Syncerus caffer*). Vet. Rec. **103:**13-14.

123. **Saikku, P., M. Leinonen, K. Mattila, M. R. Ekman, M. S. Nieminen, P. H. Makela, J. K. Huttunen, and V. Valtonen.** 1988. Serological evidence of an association of a novel Chlamydia, TWAR, with chronic coronary heart disease and acute myocardial infarction. Lancet. **2(8618):**983-986.

124. **Schiller, I., R. Koesters, R. Weilenmann, R. Thoma, B. Kaltenboeck, P. Heitz, and A. Pospischil.** 1997. Mixed infections with porcine *Chlamydia trachomatis / pecorum* and infections with ruminant *Chlamydia psittaci* serovar 1 associated with abortions in swine. Vet. Microbiol. **58:**251-260.

125. **Schiller I, Koesters R, Weilenmann R, Thoma R, Kaltenboeck B, Heitz P, and S. Pospischil.** 1997. Mixed infections with porcine *Chlamydia trachomatis / pecorum* and infections with ruminant *Chlamydia psittaci* serovar 1 associated with abortions in swine. Vet. Microbiol. **58:**251-260.

126. **Shewen, P. E.** 1980. Chlamydial infection in animals: a review. Can. Vet. J. **21:**2-11.

127. **Shewen, P. E., R. C. Povey, and M. R. Wilson.** 1978. Feline chlamydial infection. Can. Vet. J.. **19:** 289-292.

128. **Soloff, B., R. G. Rank, and A. L. Barron.** 1982. Ultrastructural studies of chlamydial infection in guinea-pig urogenital tract. J. Comp. Pathol. **92:**547.

129. **Spalatin, J., C. E. Fraser, R. Connell, R. P. Hanson, and D. T. Berman.** 1966. Agents of psittacosis-lymphogranuloma venereum group isolated from muskrats and snowshoe hares in Saskatchewan. Can. J. Comp. Med. Vet. Sci. **30:**260-264.

130. **Stamp, J. T., J. A. A. Watt, and R. B. Cockburn.** 1952. Enzootic abortion in ewes. Complement fixation test. J. Comp. Pathol. **62:**93-101.

131. **Stary, A.** 2000. Diagnosis of genital *Chlamydia trachomatis* infections. In: Proceedings of the Fourth Meeting of the European Society for Chlamydia Research Saikku, P. ed., published Esculapio, Bologna, 94-97.

132. **Storz, J.** 1971. *Chlamydia* and *Chlamydia*-Induced Diseases. Springfield, IL, USA: Charles C. Thomas, Publisher, 358 pp.

133. **Storz, J.** 1988. Overview of animal diseases induced by chlamydial infections. In: Microbiology of *Chlamydia*, Barron AL, ed. CRC Press, Boca Raton, Florida, USA, 167-192.

134. **Storz, J., E. J. Carroll, E. H. Stephenson, L. Ball, and A. K. Eugster.** 1976. Urogenital infection and seminal excretion after inoculation of bulls and rams with chlamydiae. Am. J.Vet. Res. **37:**517-520.

135. **Sundelof, B., H. Gnarpe, and J. Gnarpe.** 1993. An unusual manifestation of *Chlamydia pneumoniae* infection: meningitis, hepatitis, iritis and atypical erythema nodosum. Scand. J. Infect. Dis. **25:**259-61.

136. **Svardh, L.** 1999. Bacteria, granulocytomas, and trematode metacercariae in the digestive gland of *Mytilus edulis*: seasonal and interpopulation variation. J. Invertebr. Pathol. **74:** 275-280.

137. **Szakolczai, J., F. Vetesi, and S. R. Pitz.** 1999. Epitheliocystis disease in cultured pacu (*Piaractus mesopotamicus*) in Brazil. Acta. Veterinaria. Hungarica. **47:**311-318.

138. **Taylor, S. K., V. G. Vieira, E. S. Williams, R. Pilkington, S. L. Fedorchak, K. W. Mills, J. L. Cavender, A. M. Boerger-Fields, and R. E. Moore.** 1996. Infectious keratoconjunctivitis in free-ranging mule deer (*Odocoileus hemionus*) from Zion National Park, Utah. J. Wildl. Dis. **32:**326-330.

139. **Thom, D. H., J. T. Grayston, L. A. Campbell, C. C. Kuo, V. K. Diwan, and S. P. Wang.** 1994. Respiratory infection with Chlamydia pneumoniae in middle-aged and older adult outpatients. Eur. J. Clin. Microbiol. Infect. Dis. **13:**785-792.

140. **Thygeson, P., C. Dawson, L. Hanna, E. Jawetz, and M. Okumoto.** 1960. Observations on experimental trachoma in monkeys produced by strains of virus propagated in yolk sac. Am. J. Ophthalmol. **50:**907-918.

141. **Traciuc, E.** 1985. Normal and parasitized stages of spiders. II. Development of *Chlamydia*-like microorganisms infesting ovaries of *Segestria senoculata*. Archives Roumaines de Pathologie Experimentale et de Microbiologie. **44:**293-299.

142. **Travnicek, M., L. Cislakova, W. Deptula, M. Stosik, and M. R. Bhide.** 2002. Wild pigeons and pheasants--a source of *Chlamydophila psittaci* for humans and animals. Ann. Agri. Environ. Med. **9:**253-255.

143. **Tsai, Y. L., and B. H. Olson.** 1992. Rapid method for separation of bacterial DNA from humic substances in sediments for polymerase chain reaction. Appl. Environ. Microbiol. **58:**2292-2295.

144. **Vaerman, J. L., P. Saussoy, and I. Ingargiola.** 2004. Evaluation of real-time PCR data. J. Biol. Regul. Homeost. Agents. **18:**212-214.

145. **Weyer, F.** 1970. Zur Frage der Rolle von Arthropoden als Reservoir des Psittakoseerregers. Z. Tropenmedizin und Parasitologie. **21:**146.

146. **Whitcombe, D., J. Theaker, S. P. Guy, T. Brown, and S. Little.** 1999. Detection of PCR products using self-probing amplicons and fluorescence. Nat. Biotechnol. **17:**804-807.

147. **Wilson, I. G.** 1997. Inhibition and facilitation of nucleic acid amplification. Appl. Environ. Microbiol. **63:**3741-3751.

148 **Wolke, R. E., D. S. Wyand, and L. H. Khairallah.** 1970. A light and electron microscopic study of epitheliocystis disease in the gills of Connecticut striped bass (*Morone saxatilis*) and white perch (*Morone americanus*). J. Comp. Pathol. **80:**559-563.

149. **Woollen, N., E. K. Daniels, T. Yeary, H. W. Leipold, and Phillips.** 1990. Chlamydial infection and perinatal mortality in a swine herd. J. Am. Vet. Med. Assoc. **197:**600-601.

150. **Yang, X., K. T. HayGlass, and R. C. Brunham.** 1996. Genetically determined differences in IL-10 and IFN-gamma responses correlate with clearance of *Chlamydia trachomatis* mouse pneumonitis infection. J. Immunol. **156:**4338-4344.

151. **Yang, Z. P., P. K. Cummings, D. L. Patton, and C. C. Kuo.** 1994. Ultrastructural lung pathology of experimental *Chlamydia pneumoniae* pneumonitis in mice. J. Infect. Dis. **170:**464-467.

152. **Yang, Z. P., C. C. Kuo, and J. T. Grayston.** 1993. A mouse model of *Chlamydia pneumoniae* strain TWAR pneumonitis. Infect. Immun. **61:**2037-2040.

153. **Yang, Z. P., C. C. Kuo, and J. T. Grayston.** 1995. Systemic dissemination of *Chlamydia pneumoniae* following intranasal inoculation in mice. J. Infect. Dis. **171:**736-738.

154. **Young, S., H. D. Parker, and B. D. Firehammer.** 1958. Abortion in sheep due to a virus of the psittacosis-lymphogranuloma group. J. Am. Vet. Med. Assoc. **133:**374-379.

CHAPTER 2: One-Step Duplex Reverse Transcriptase PCRs Simultaneously Quantify Analyte and Housekeeping Gene mRNAs

INTRODUCTION

Of all methods used to quantify mRNA, real-time reverse transcriptase PCR is considered the most sensitive and accurate one (1). In addition to its wide use in laboratory research, real-time RT-PCR has the potential for broad application in diagnosis of functional defects in disease. Absolute quantification of mRNA is generally impractical and unnecessary, because consistently transcribed housekeeping genes effectively serve as internal standards for relative quantification of the transcripts of genes of interest (1, 2, 3, 4, 5). Fluorescent probes in real-time PCR have remedied specificity problems inherent to the quantification of amplification products by double-stranded DNA-binding fluorescent dyes (2). Nevertheless, reverse transcriptase PCR is still a cumbersome technique that requires multiple reactions per single specimen. In many RT-PCR methods, genomic DNA must be removed to avoid false positive amplification. Separation of reverse transcription and PCR into a two-step RT-PCR is necessary if multiple targets should be quantified relative to housekeeping gene transcripts. Finally, one-step RT-PCR, which combines reverse transcription and amplification into one reaction, determines absolute, but not relative, amounts of single

targets. These absolute quantities of different gene transcripts cannot be related to each other because variations in reverse transcription and amplification efficiency cannot be controlled between different single-target one-step RT-PCRs. Collectively, these limitations increase the sample size required for the reaction, and decrease sensitivity and specificity, thus preventing routine clinical diagnostic use of this powerful technique, and rendering laboratory research applications cumbersome.

In this study, we combined two independent real-time PCR methods into a single reaction, termed duplex PCR, allowing simultaneous amplification and quantification of transcripts of both an analyte and a housekeeping gene. We present data that indicate the validity of such a real-time duplex PCR method that also performs reverse transcription in this single reaction prior to amplification. The present study examines in detail the properties of such real-time one-step duplex RT-PCR methods that remove major technical limitations of real-time reverse transcriptase PCR.

MATERIALS AND METHODS

Extraction of Total Nucleic Acids and RNase Treatment

Macrophages elicited via intraperitoneal thioglycollate injection from male A/J and C57BL/6J mice were plated in 24-well-plates, stimulated with *C. pneumoniae* lysate, and removed by use of a cell scraper (6). Total nucleic acids were extracted from sedimented cells by use of High Pure PCR Template Preparation Kit (Roche Molecular Biochemicals, Indianapolis, IN) as described and eluted in 10 mM Tris-HCl, pH 8.5, 0.1 mM EDTA ($T_{10}E_{0.1}$) (7). For selected analyses, RNA in total nucleic acids was

hydrolyzed at 37ºC for 30 min with DNase-free RNase (Invitrogen, Carlsbad, CA) at 12.5 μg/ml.

All experimental animal procedures utilized in this research followed NIH guidelines and were reviewed and approved by the Auburn University Animal Care and Use Committee.

Design of Primers and Probes

Primers and FRET probes were obtained from QIAGEN, Valencia, CA, and are shown in Table 1. Oligonucleotides were designed to span exon boundaries, thus only allowing amplification from, and detection of, cDNA but not genomic DNA. The length of the amplification products is between 160 and 220 bp. All oligonucleotides were designed by use of the Vector NTI software (InforMax Inc., Frederick, MD) for a calculated T_m of 71° to 73° assuming 190 mMol salt concentration and 100 pM oligonucleotide concentration. Carboxyfluorescein (6-FAM) probes were 3' labeled and used unpurified as FRET energy donor probes excited by 488 nm light. Bodipy 630/650 and Cy5.5 probes were 5'-labeled, 3'-phosphorylated, HPLC-purified and used as acceptor probes (8). Fluorescence emitted from Bodipy 630/650 probes served for detection of the analyte gene Arginase I and Arginase II mRNAs (10, 11, 12) at 640 nm, and from Cy5.5 probes for detection of the PBGD and HPRT housekeeping genes (3, 4, 5, 13, 14) at 705 nm in each duplex PCR (Arginase I + HPRT, Arginase II + PBGD).

Reaction Mix for Real-Time One-Step Duplex Reverse Transcriptase PCR

The PCR buffer was 20 mM Tris-HCl, pH 8.4, 50 mM KCl, 4.5 mM $MgCl_2$, 0.05 % Nonidet P-40, 0.05 % Tween-20, 0.03 % acetylated bovine serum albumin, and 200 μM each dATP, dCTP, dGTP, and 600 μM dUTP. Reactions were performed in glass capillaries with 15 μl of 1.33 x master mixture and 5 μl of sample nucleic acids or standards. Each 20 μl reaction contained 2.0 U Platinum *Taq* DNA polymerase (Invitrogen, Carlsbad, CA), 0.2 U heat-labile uracil-N-glycosylase (Roche Molecular Biochemicals, Indianapolis, IN), and 0.0213 U ThermoScript™ reverse transcriptase (Invitrogen, Carlsbad, CA). PBGD primers were used at 0.8 μM, all other primers at 1 μM, Bodipy 630/650 and Cy5.5 probes at 0.2 μM, and 6-FAM probes at 0.1 μM. Master mixes were prepared freshly from 10x PCR buffer, 5x oligonucleotide mix, 50x nucleotide mix, and enzymes. For convenient pipetting, ThermoScript™ RT was used as 1:140 dilution in storage buffer. Standard reactions containing 10,000, 1,000, 100, or 10 copies of each target were performed with each run.

Thermal Cycling

All PCRs were performed on the LightCycler® real-time PCR platform (Roche Molecular Biochemicals, Indianapolis, IN) using LightCycler® Software version 3.5. Thermal cycling was preceded by a 20-minute reverse transcription reaction at 55°C followed by 5 min incubation at 95°C. Thermal cycling consisted of 18 high-stringency step-down cycles followed by 25 relaxed-stringency fluorescence acquisition cycles. The 18 high-stringency step-down thermal cycles for the Arginase I- HPRT duplex PCR were 6 x 15 sec @ 95°C, 60 sec @ 75°C; 9 x 15 sec @ 95°C, 60 sec @ 73°C; 3 x 15 sec @

95°C, 30 sec @ 71°C, 30 sec @ 72°C. The high-stringency step-down thermal cycles for the Arginase II-PBGD duplex PCR were 6 x 15 sec @ 95°C, 60 sec @ 72°C; 9 x 15 sec @ 95°C, 30 sec @ 70°C, 30 sec @ 72°C; 3 x 15 sec @ 95°C, 30 sec @ 68°C, 30 sec @ 72°C. The relaxed-stringency fluorescence acquisition cycling for both duplex PCRs consisted of 25 x 15 sec @ 95°C, 8 sec @ 58°C followed by fluorescence acquisition, 30 sec @ 65°C, and 30 sec @ 72°C.

Single target (simplex) PCRs for Arginase I, Arginase II, HPRT, and PBGD used a lower Platinum *Taq* DNA polymerase quantity of 1.5 U per 20 µl reaction, but otherwise the respective identical protocols. *Chlamydia pneumoniae* 23S rRNA FRET real-time PCR was performed as described (7).

All types of duplex PCR were analyzed by agarose gel electrophoresis, the presence of two correctly-sized amplification products and absence of aberrant products was verified, and both amplification products of each duplex PCR were DNA sequenced.

Color Compensation

A color compensation file was created in a calibration cycling protocol with 4 samples in PCR buffer without enzymes (1: blank; 2: 1 µM fluorescein probe; 3: 1 µM Bodipy 630/650 probe; 4: 1 µM Cy5.5 probe). The thermal protocol for calibration of color compensation was 1 x 30 sec @ 95°C; 40 x 0 sec @ 95°C, 10 sec @ 55°C, 10 sec @ 72°C, and 1 temperature gradient step from 5 sec @ 40°C to 0 sec @ 95°C followed by 1 x 30 sec @ 40°C. After calibration cycling, data were saved as color compensation file and imported for analysis of duplex RT-PCR data.

PCR Standards

Templates for standard reactions were prepared from RT-PCRs that contained 200 μM dTTP instead of dUTP. This rendered the standards insensitive to cleavage by uracil-N-glycosylase, which was used to prevent PCR product carry-over. PCR products were isolated by 4 % MetaPhor agarose gel electrophoresis, extracted by glass matrix binding and elution (Roche Molecular Biochemicals, Indianapolis, IN), quantified by PicoGreen DNA fluorescence assays (Molecular Probes, Eugene, OR), verified by DNA sequencing, and used at 10^4, 10^3, 10^2, 10, and 0 copies per 5 μl in a background of 100 ng purified pGEM plasmid DNA (Promega, Madison, WI) in $T_{10}E_{0.1}$.

For evaluation of the quantification of the duplex PCR standards at different target ratios and concentrations, each of 10^4, 10^3, 10^2 or 10 copies of analyte standards (Arginase I and Arginase II) were combined with each of 10^4, 10^3, 10^2 or 10 copies of housekeeping gene standards (HPRT, PBGD), and each combination was quantified as duplicates in 2 independent duplex PCRs. The copy numbers of each target in relation to the copies of the respective other target as found in the assays were determined, related to actual standard copy numbers, and equations for correction factors were deduced by linear least-square regression analysis (STATISTICA 6.1 software [StatSoft, Tulsa, OK]). For analysis of samples by duplex RT-PCR, standard reactions containing 10^4, 10^3, 10^2 or 10 copies of both DNA templates were performed without reverse transcription and used to quantify the concentrations of specimen mRNAs, which had been subjected to reverse transcription. The negative control was 100 ng purified pGEM plasmid DNA in 5 μl $T_{10}E_{0.1}$, mouse macrophage total nucleic acid positive for the respective targets served as the control for reverse transcription.

RESULTS

Prior to characterizing the real-time one-step duplex RT-PCR assays, we undertook extensive efforts to optimize the methodology, starting from previously established reaction chemistries and step-down thermal cycling (7, 9). Concentrations of reverse transcriptase, *Taq* polymerase, primers, and all steps in the thermal cycling protocols were calibrated. Of particular importance for fine-tuning the reactions were the amount of reverse transcriptase, the relative numbers and annealing temperatures of high-stringency step-down cycles (beginning at 70°C-75°C), and the relaxed-stringency fluorescence acquisition cycles including fluorescence acquisition at 58°C after 8 sec equilibration followed by 30 sec annealing at 63°C-65°C (data not shown). For all duplex RT-PCRs gel electrophoresis demonstrated correct amplification products, and DNA sequencing results of the amplified fragments precisely matched the mRNA sequences.

Specificity of one-step duplex reverse transcriptase quantitative PCR (RT-qPCR)

To evaluate the ability of the one-step RT-qPCRs to discriminate between genomic DNA and mRNA targets, we amplified total nucleic acids isolated from mouse macrophages stimulated with lysed *C. pneumoniae* bacteria. Sample nucleic acids were or were not treated with RNase, and were amplified in the presence or absence of reverse transcriptase. Only *C. pneumoniae* DNA, but not the 4 mRNA targets were amplified in the absence of reverse transcriptase (data not shown). RNase treatment of total nucleic

acids abolished amplification of the mRNA targets, but not of *C. pneumoniae* DNA. These results validated the application of the one-step RT-PCR using exon-spanning primers and probes to the analysis of total nucleic acid specimens.

Evaluation of Target Quantification

DNA standards containing equal amounts of both targets had served to establish real time one-step duplex RT-PCR. A fundamental question in duplex PCR is how the targets interact during amplification and fluorescent detection when they are present in unequal ratios. To examine these interactions, we performed for each of the 4 possible pairs of analyte (Arginase I, Arginase II) and housekeeping genes (HPRT, PBGD) a matrix of standard duplex reactions in the absence of reverse transcriptase in which 10^4, 10^3, 10^2, or 10 copies of one target were combined with 10^4, 10^3, 10^2, or 10 copies of the respective other target. Figure 1 shows as an example the results for the Arginase II-PBGD duplex PCR. These reactions, termed standard performance, demonstrated that targets in approximately 300-fold or lower abundance than the other target in a duplex PCR were amplified less efficiently and under-reported (Fig. 1). This was true for all targets in all combinations, but varied depending on thermal cycling conditions. In the final protocols, we adjusted the thermal cycling parameters such that amplification of the analyte genes was more efficient than that of the housekeeping genes, as evident in Figure 1 and plots A and C of Figure 2 for Arginase II in comparison to PBGD. The rationale for this approach was that highest sensitivity for amplification of housekeeping gene mRNA was not necessary because a minimum of 20-30 copies of housekeeping

gene mRNA is required for accurate normalization. Thus copy numbers of housekeeping gene mRNAs lower than 20, even if quantified precisely, still would not allow accurate determination of analyte mRNA copies, which presumably will show a wider concentration range than housekeeping gene mRNA.

To evaluate the relative shifts in amplification efficiencies and data reporting, we plotted for each duplex PCR the results of 2 replicates of duplicate reactions as logarithm of target ratio determined in the assay versus the ratio of actual/assay-determined targets. The equation for the least square best fit regression line allows determination of an assay-specific correction factor for each target and its ratio to the respective other target. The data plotted for the Arginase II-PBGD duplex PCR in Figure 2 clearly indicate for both analyte and housekeeping gene targets a reduced amplification efficiency at low abundance (log target ratio < 0; correction factors > 1), and increased efficiency at high abundance (log target ratio > 0; correction factors □ 1). For PBGD, the correction factor at –2.5, which is the lowest acceptable logarithm of target ratios, is higher than that of Arginase II (1.238 vs. 1.168), reflecting the adjustment of thermal PCR parameters in favor of the analyte Arginase II. Similar relationships between correction factors and target ratios were found for the Arginase I-HPRT duplex PCR. Plots of logarithm actual target copies versus logarithm assay-determined corrected target copies in Figure 2 reveal linear fits with narrow confidence intervals over the 3 log range of standard targets tested. These corrected assay data of all duplex PCRs correlated better with actual copy numbers than the uncorrected assay results (data not shown). It is important to notice that only log target ratios between –2.5 to 2.5 were used to calculate the correction factors. Higher and lower values were excluded because of the assay inaccuracy for the respective lower

target. Therefore, the duplex PCRs as described allow the reliable determination of 10-10,000 copies of each target over a 100,000-fold range ($10^{-2.5}$ – $10^{2.5}$, equal to 1/320 - 320) of target copy ratios.

Color Compensation

The LightCycler® real-time PCR platform acquires fluorescent signals in FRET duplex-PCR at 3 emission wavelengths, and residual signal of short wavelength peaks may obscure fluorescence peaks in the long wavelength channels. To compensate for such fluorescence spill-over, we acquired signals for a color compensation file according to the LightCycler® instructions, and used this file to electronically compensate for fluorescence spill-over during analysis of the results of duplex PCRs.

During attempts to combine the Arginase I analyte target with the PBGD housekeeping gene target in a duplex PCR, we noticed extensive increases in the PBGD fluorescent signal at 705 nm emission wavelength at 10-fold or higher copy ratios of Arginase I to PBGD standards (Fig. 3). To evaluate if this excessive signal resulted from fluorescent spill-over from the 640 nm Arginase I emission peak, we removed either the Bodipy 630/650-labeled Arginase I FRET acceptor probe or the Cy5.5-labeled PBGD FRET acceptor probe from the duplex PCR. Removal of the PBGD probe, but not of the Arginase I probe, eliminated the excessive signal in the PBGD emission channel. These data proved unequivocally that the excessive signal at 705 nm was not caused by lack of compensation of fluorescence spill-over, but was generated directly by the PBDG Cy5.5-labeled FRET acceptor probe.

The minimum combination of reaction components necessary to create the aberrant PBGD signal were Arginase I template, Arginase I and PBGD primers, the Cy5.5-labeled PBGD probe, and either the Arginase I or the PBGD fluorescein probe. These reactions were analyzed by agarose gel electrophoresis, sequence alignments of the Arginase I DNA fragment with primers and probes, and DNA sequencing (data not shown). A 146 bp product was identified in addition to the 212 bp Arginase I fragment. Only the presence of large amounts of the Arginase I fragment was associated with production of this aberrant fragment. This 146 bp fragment was primed at the 5' end by the downstream PBGD primer (17 bp match), and downstream by the upstream PBGD primer (10 bp match) or downstream Arginase I primer, resulting in a nested PCR from the original Arginase I amplification product. Both the PBGD Cy 5.5 and fluorescein probes match both the sense and antisense strands with 13 to 15 bp. Annealing of both PBGD probes to the non-coding strand creates the thermodynamically most stable hybrids, and separates the fluorescein and Cy 5.5 labels by 3 basepairs. If the Arginase I fluorescein probe is combined with the PBGD Cy 5.5 probe, the fluorescent labels are separated by 23 bp on the non-coding strand. Both combinations of the PBGD Cy 5.5 probe are sufficient to generate a 705 nm FRET signal under the conditions described. Thus, the muPBDGCY5.5 probe, annealing to high numbers of regular and aberrant Arginase I amplification fragments in the Arginase I-PBGD duplex PCR, interacted with both Arginase I and PBGD fluorescein probes to produce excessive PBGD signal. Therefore, co-amplification of Arginase I and PBGD targets in a duplex PCR was not compatible.

Subsequent removal experiments of all probes in the duplex PCRs described here revealed that fluorescent signals of the appropriate emission channels, and target quantification, did not differ in the reactions from PCRs performed with the complete set of probes. Also, equations deduced from standard performance reactions of these reactions, as well as for the Arginase I signal in the Arginase I-PBGD, closely resembled those deduced here for both Arginase II-PBDG duplex PCR channels (Fig. 3). Thus, electronic color compensation reliably and quantitatively corrected fluorescence spill-over, and excessive signal such as observed in the Arginase I-PBGD duplex PCR was the result of sequence-specific interaction between DNA targets and probes. Also, relative over- and under-reporting in dependence on target ratios in standard performance reflected intrinsic properties of PCR assay chemistry, presumably competition between targets for rate limiting *Taq* polymerase, rather than insufficient electronic signal correction.

Reproducibility of Real-Time One-step Duplex RT-PCR

To assess the reproducibility and accuracy of the established duplex RT-PCR methods over a range of target concentrations and ratios, we analyzed serial dilutions of total nucleic acid samples from *C. pneumoniae*-stimulated murine peritoneal macrophages. The raw numbers of mRNA copies of each target determined for 2 samples in both duplex RT-PCRs were multiplied with the appropriate correction factors, and copies of analyte mRNA were expressed as normalized copy numbers per 1,000 copies of the respective housekeeping gene mRNAs. The corrected copy numbers of HPRT and PBGD mRNAs, per 5 µl of the undiluted samples, were approximately 3,000

and 1,200, respectively. The results in Figure 4 indicate that the transcript levels of both Arginase I and Arginase II relative to HPRT and PBGD, respectively, remain nearly constant over a 64-fold range of sample nucleic acid concentrations. The increased standard deviation of analyte gene mRNAs per 1,000 housekeeping gene mRNA in proportion to sample dilution indicates reduced accuracy at low copy numbers. The results of this analysis validate the reproducibility of both real-time one-step duplex RT-PCR methods within the range of target mRNA concentrations (10-10,000 copies per 5 µl) and ratios ($10^{-2.5}$ – $10^{2.5}$, equal to 1/320 - 320) established in the standard performance reactions.

DISCUSSION

The present study built on LightCycler® real-time PCR chemistry and step-down thermal cycling strategies developed earlier (7, 9), and adapted these methods to one-step reverse transcription, high-sensitivity amplification, and simultaneous real-time quantitative detection of two mRNA targets. This method provides a number of advantages over alternative approaches for mRNA quantification by real-time PCR (1, 2). Most importantly, it simultaneously quantifies a target transcript of specific interest together with a second mRNA, typically an internal control mRNA of an essential gene present in all somatic cells in approximately constant steady-state equilibrium (4, 5). Thus, one-step duplex RT-PCR generates results that allow calculation of the copy numbers of a target transcript in relation to a constant number of internal control transcripts of a housekeeping gene from the data of a single assay (normalization: relative quantification). This approach reduces inaccuracies such as differences in PCR

efficiencies that cannot be avoided in methods that separate mRNA quantification into sample reverse transcription and single target amplifications. Furthermore, reverse transcription in one-step duplex RT-PCR is primed by a gene-specific primer that also primes in PCR, likely improving the efficiency of production of target-length cDNA over reverse transcription that uses random oligonucleotide or oligo (dT) primers. Finally, the obvious simplicity of the one-step method likely will translate into enhanced precision by minimizing the number of experimental steps and sample transfers.

Additional advantages come from the choice of exon-spanning primers and probes, which prevents amplification or detection of genomic DNA. This approach allows PCR-quantification of mRNA in total nucleic acid specimens, and eliminates the need for DNase treatment of RNA samples and the controls necessary to assure amplification of cDNA, but not of genomic DNA (1). The one-step duplex RT-PCR methods in this study minimally detect 10 copies of analyte cDNA. However, our unpublished data of limiting standard and sample dilutions suggest that well calibrated one-step duplex RT-PCRs will detect a single copy of analyte cDNA in the presence of 20-30 copies of housekeeping gene cDNA. Thus, by virtue of the sensitive quantification of mRNAs in minute specimen volumes in a single assay, the greatest benefits of the one-step duplex RT-PCR most likely will apply to clinical specimens. Such specimens typically provide limited amounts of extracted total nucleic acids that are subjected to numerous analyses and might contain low concentrations of mRNA (15, 16, 17).

The appropriate choice of quantitative, and qualitative positive and negative standards for real-time one-step duplex RT-PCRs is critical. Reactions of standard dilution buffer without target fragments, with and without reverse transcription, serve as

negative amplification controls. Control for reverse transcription, in our hands, was best provided by known positive specimens. For quantitative determination, the interaction between the targets in duplex RT-PCRs during amplification and fluorescent signal detection is an important consideration. The matrix of standard performance reactions validates the method and determines equations for correction factors. Quantitative standards in the approach described in this study contain equal numbers of both double-stranded target DNA fragments, not RNA standards, and are amplified without reverse transcriptase. The number of standard molecules is therefore absolute, not created by variable-rate reverse transcription of RNA standards. Reverse transcriptase generates sample cDNA, but also reduces PCR efficiency by creating variable amounts of background DNA. Therefore, the approach described here relates target quantification in samples, that are variable in their PCR inhibition, to absolute target standards without reverse transcriptase-mediated inhibition. Background inhibition in duplex RT-PCR of unknown specimens affects amplification of both targets. Thus, analyte mRNA quantification relative to housekeeping gene mRNA remains unaffected by variable background PCR inhibition in specimens. Because of the PCR inhibitory background created by reverse transcription, careful calibration of each batch of reverse transcriptase is very important for overall performance of real-time one-step duplex RT-PCRs.

The acceptable range of 1/320 to 320-fold ($10^{-2.5}$ – $10^{2.5}$) target ratios in duplex RT-PCR specifies the limits of the analytical range of a real-time duplex RT-PCR. In essence, mRNA levels of analyte and housekeeping genes must be similar, and transcription levels of analytic targets will dictate the choice of housekeeping gene. In this study we sought to use housekeeping genes with low transcription levels for

appropriate evaluation of genes typically transcribed at low levels. Additional housekeeping genes will be needed for duplex RT-PCRs determining high-concentration analyte mRNAs (4, 5). Amplification fragments in such duplex PCR methods should be between 100-200 base pairs in length, and the T_m of primers and probes should be as high as 74°C, to allow for highly stringent thermal cycling conditions. Duplex RT-PCRs designed according to these guidelines can be conveniently established by first fine-tuning step-down cycling in 2°C annealing temperature steps starting approximately at the primer T_m, such that a signal for 10^4 target copies appears between cycles 6-8 of the subsequent fluorescence acquisition cycles. During these cycles, the 8 sec fluorescence acquisition step at 58°C is critical and should not be modified. Omission of this step and fluorescence acquisition at higher temperature results in delayed, but steep increases of the fluorescent signal over only 2-3 cycles from threshold and saturation signal, vastly reducing PCR accuracy. Efficiency of fluorescence acquisition cycles can be calibrated by adjusting the annealing temperature following fluorescence acquisition to a temperature between 61°C and 67°C. Quantification of more than 10^4 target copies is less challenging, and the total number of step-down cycles must be reduced by 3-4 cycles for each 10-fold increase of expected targets, or the specimen be appropriately diluted such that less than 10^4 target copies are present per PCR.

In summary, we have established sensitive real-time PCR methodology for accurate quantification of eukaryotic analyte mRNA relative to a housekeeping gene in a single assay. The overall method discriminates cDNA from genomic DNA sequences and entails reverse transcription of both target mRNAs from total nucleic acids, followed by PCR amplification, real-time signal detection and quantification, and correction of

assay results by factors deduced from reactions that evaluate quantification at variable ratios of the target standards. We have used this approach to develop, with ease, more duplex PCRs quantifying analyte mRNAs relative to PBGD and HPRT as well as additional housekeeping gene transcripts. We anticipate that real-time one-step duplex RT-PCR methods will accelerate the functional analysis of clinical specimens for gene transcription in the context of disease.

Table 1: Oligonucleotide primers and probes used in this study.

Primer/ Probe	Sequence (5'→3')[a]	cDNA bp Location	T_m[b]	RT-PCR Product, Genbank Accession Number
muARG1UP	GTGGAGACCACAGTCTGGCAGTTGGA	372-397 exon 3,	72.6°C	Mouse Arginase I 212 bp BC 013341
muARG1DN	GCAGGGAGTCACCCAGGAGAATCCT	583-559 exon 5	71.9°C	
muARG1BOD	Bodipy 630/650-GAAGGAACTGAAAGGAAAGTTCCCAGATGT-Phos	526-555 exon 4, 5	71.5°C	
muARG1FLU	CATGGGCAACCTGTGTCCTTTCTCC -6-FAM	500-524 exon 4	71.9°C	
muARG2UP	TTTCTCTCGGGGACAGAAGAAGCTAGGA	96-123 exon 1	72.0°C	Mouse Arginase II 160 bp BC 023349
muARG2DN	CAGATTATTGTAGGGATCATCTTGTGGGACA	255-225 exon 3	71.6°C	
muARG2BOD	Bodipy 630/650-TCTTCAGCAAGCCAGCTTCTCGAATGG-Phos	143-169 exon 2	72.8°C	
muARG2FLU	GGTGGCATCCCAACCTGGAGAGC-6-FAM	171-193 exon	72.6°C	
muPBGDUP	CGGCCACAACCGCGGAAGAA	20-39 exon 1,	71.7°C	Mouse PBGD 164 bp M28663, M28664 M28665, M28666
muPBGDDN	GTCTCCCGTGGTGGACATAGCAATGA	183-158 exon 4,	73.0°C	
muPBGDCY5.5	Cy5.5-TCGAATCACCCTCATCTTTGAGCCGT-Phos	90-68 exon 3,	72.1°C	
muPBGDFLU	CAGCTGGCTCTTACGGGTGCCCA-6-FAM	66-41 exon 3	71.0°C	
muHPRTUP	TCCCAGCGTCGTGATTAGCGATGA	102-125 exon 1,	72.7°C	Mouse HPRT 172 bp NM 013556
muHPRTDN	AATGTGATGGCCTCCCATCTCCTTCATGACAT	273-242 exon 3	72.9°C	
muHPRTCY5.5	Cy5.5-GATTATGGACAGGACTGAAAGACTTGCTCG-Phos	210-239 exon 2,	71.7°C	
muHPRTFLU	GGATTTGGAAAAAGTGTTTATTCCTCATGGAC-6-FAM	177-208 exon 2	72.7°C	

[a] Bodipy 630/650, amine-reactive Bodipy fluorophone attached to 5' terminus; Cy5.5, CE phosphoramidite attached to 5' terminus; 6-FAM, 6-carboxyfluorescein attached to 3'-O-ribose; Phos, phosphate group attached to the 3' terminus.

[b] T_m was calculated for 190 mM salt concentration and 100 pM probe concentration.

FIGURES

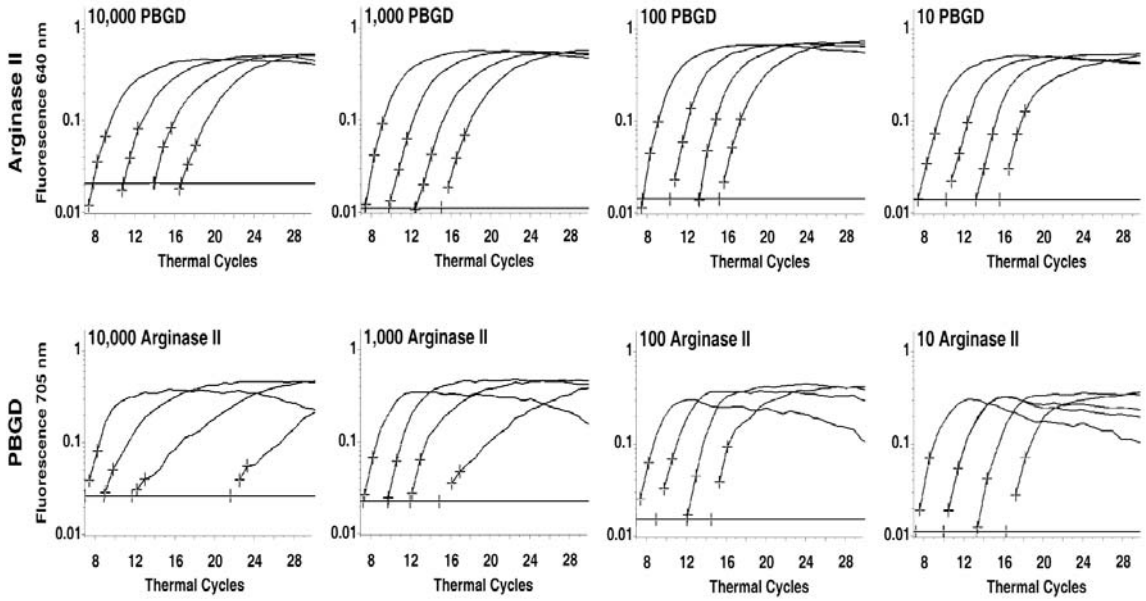

Figure 1. The relative copy number of each target affects real-time duplex PCR amplification of Arginase II and PBGD standards. To evaluate the performance of the duplex PCR standard at different target ratios and concentrations, a matrix of reactions (standard performance) was performed in which 10^4, 10^3, 10^2, or 10 copies per reaction of the Arginase II template were combined with 10^4, 10^3, 10^2, or 10 copies of the PBGD template. **Upper row**: fluorescent signals for 10^4 (left curve), 10^3, 10^2, and 10 copies (right curve) of the Arginase II template at simultaneous amplification of 10^4, 10^3, 10^2, or 10 copies of PBGD; **lower row**: signals for 10^4 - 10 copies of the PBGD template at simultaneous amplification of 10^4 - 10 copies of Arginase II. Thermal cycling is calibrated to maximize amplification efficiency of the Arginase II analyte target at high or low PBGD copy numbers. Conversely, low copy numbers of the PBGD housekeeping

gene target amplify poorly in the presence of high numbers of Arginase II templates. This approach ensures valid results at low Arginase II transcript levels. Highest sensitivity for detection of housekeeping gene mRNA is not required because results by definition are inaccurate below 20 copies of the reference housekeeping gene mRNA.

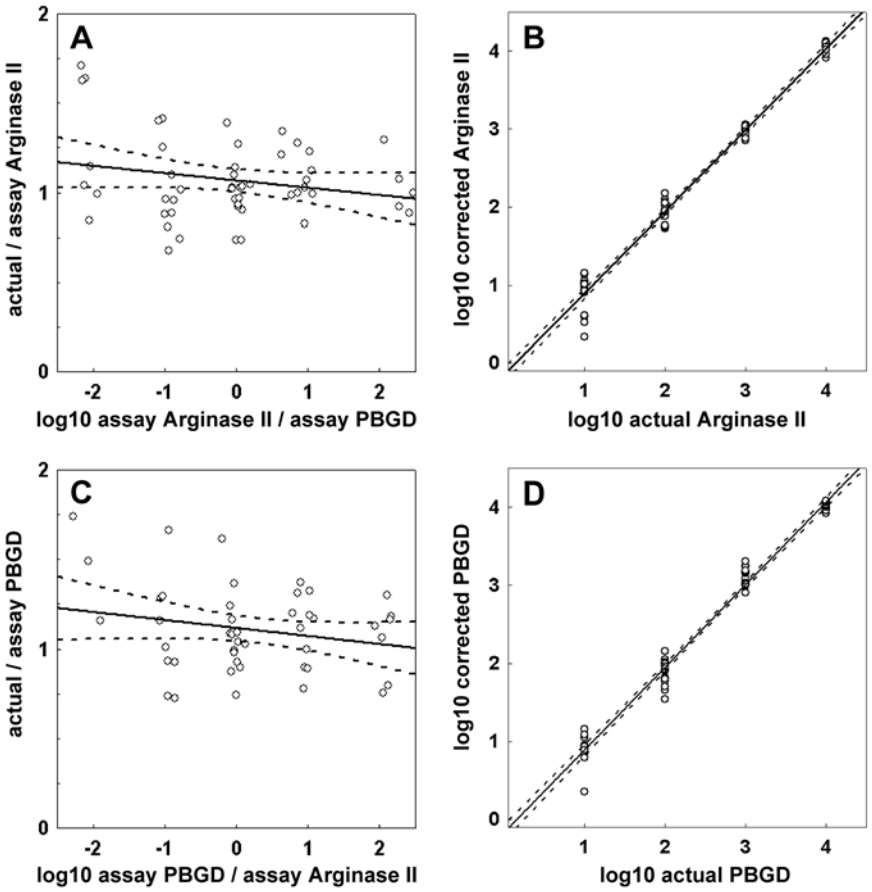

Figure 2. Factors deduced from the standard performance reactions effectively correct the assay data of Arginase II and PBGD. Paired Arginase II–PBGD data from 4 standard performance reactions as shown in Fig. 1 were used to evaluate the amplification of both targets relative to the known concentration of each standard. Least square regression analysis obtained for each target a linear equation describing the relation between the logarithm of Arginase II/PBGD copy numbers (and inverse ratio) and actual (true) copies divided by copies as determined in the assay (assay copies). The factor actual/assay copies is required for correction of assay copies to the true number of

target copies in dependence on the number of copies of the respective other target. The regression equation deduced in plot A (actual/assay Arginase II = 1.066 - 0.0408 x log10 assay Arginase II/assay PBGD) was used to calculate correction factors for each pair of data from each sample in plot B. Assay PBGD data in plot D were corrected using the regression equation (actual/assay PBGD = 1.1143-0.0494 x log10 assay PBGD/assay Arginase II) deduced in plot C.

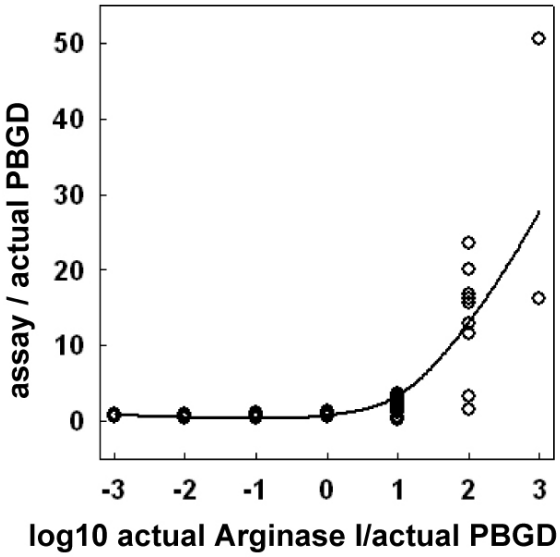

Figure 3. Arginase I templates interact with the PBGD Cy5.5 probe to produce an excessive PBGD signal at high Arginase I/PBGD template ratios. During method development, Arginase I-PBGD duplex PCRs showed very high PBGD signals, resulting in PBGD over-reporting, if a 10-fold or higher excess of Arginase I templates over PBGD templates was added to the reactions. Omission of the Bodipy 630/650-labeled Arginase I probe from the duplex PCR did not eliminate this signal, but removal of the Cy5.5-labeled PBGD probe did. The minimum reaction components necessary to create the aberrant PBGD signal were the combined Arginase I template, Arginase I and PBGD primers, the Cy5.5-labeled PBGD probe, and either the Arginase I or the PBGD fluorescein probe. Subsequent analyses revealed that muPBGDDN primed a 146 bp nested PCR fragment from large amounts of the original Arginase I fragment. Both PBGD probes, or the Arginase I fluorescein probe and the PBGD Cy5.5 probe, form thermodynamically sufficiently stable hybrids with the non-coding strand, separating the

fluorescein and Cy 5.5 labels by 3 or 23 basepairs, respectively. This resulted in the aberrant 705 nm FRET signal, which made co-amplification of Arginase I and PBGD targets in a duplex PCR incompatible.

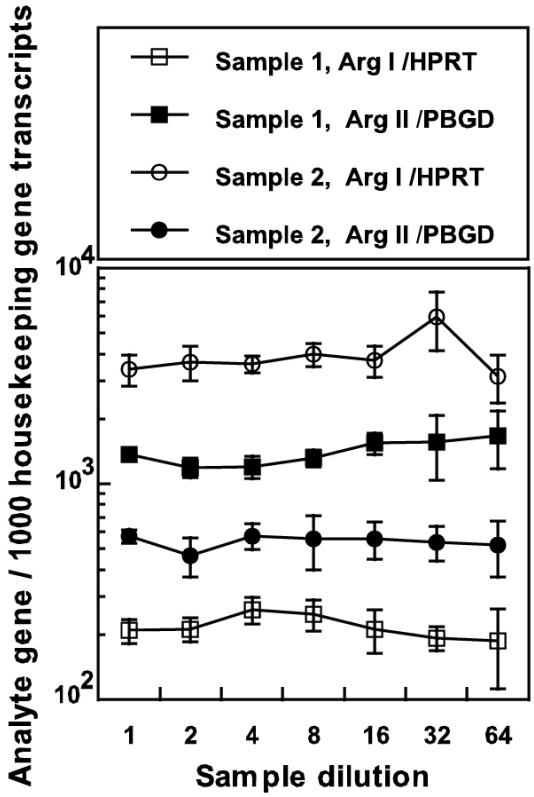

Figure 4. Relative copy numbers of analyte and housekeeping genes in real-time one-step duplex RT-PCRs remain constant in assays of sample dilutions. To test the overall performance of duplex RT-PCRs, quadruplicates of undiluted (1:1) and serial 1:2 dilutions of two total nucleic acid specimens from *C. pneumoniae*-stimulated murine macrophages were amplified for Arginase I and HPRT, and Arginase II and PBGD mRNAs. Data are represented as means ± standard deviation. The results indicate that the ratios of analyte to housekeeping mRNAs as determined by duplex RT real-time PCR remain nearly constant over a 64-fold range of specimen nucleic acid concentrations.

REFERENCES

1. **Bustin, S. A.** 2000. Absolute quantification of mRNA using real-time reverse transcription polymerase chain reaction assays. J. Mol. Endocrinol. **25:**169-193.

2. **Bustin, S. A.** 2002. Quantification of mRNA using real-time reverse transcription PCR (RT-PCR): trends and problems. J. Mol. Endocrinol. **29:**23-29.

3. **Kuhne, B. S. and P. Oschmann.** 2002. Quantitative real-time RT-PCR using hybridization probes and imported standard curves for cytokine gene expression analysis. BioTechniques **33:**1078-1089.

4. **Thellin, O., W. Zorzi, B. Lakaye, B. D. Borman, B. Coumans, G. Hennen, T. Grisar, A. Igout, and E. Heinen.** 1999. Housekeeping genes as internal standards: use and limits. J. Biotechnol. **75:**291-295.

5. **Vandesompele, J., K. D. Preter, F. Pattyn, B. Poppe, N.Y. Roy, A. D. Paepe, and F. Spleleman.** 2002. Accurate normalization of real-time quantitative RT-PCR data by geometric averaging of multiple internal control genes. Genome Biology **3:**research0034.1-0034.11.

6. **Huang, J., F. J. DeGraves, S. D. Lenz, D. Gao, P. Feng, D. Li, and B. Kaltenboeck**. 2002. The quantity of nitric oxide released by macrophages regulates *Chlamydia*-induced disease. Proc. Natl. Acad. Sci. USA. **99:**3914-3919.

7. **DeGraves, F.J., D. Gao, and B. Kaltenboeck.** 2003. High-sensitivity quantitative PCR platform. BioTechniques **34:**106-115.

8. **Ahsen, N. Von., M. Oellerich, and E. Schutz.** 2000. A method for homogeneous color-compensated genotyping of factor V (G1691A) and methylenetetrahydrofolate reductase (C677T) mutations using real-time multiplex fluorescence PCR. Clin. Biochem. **33:**535-539.

9. **Huang, J., F.J. DeGraves, D. Gao, T. Schlapp, and B. Kaltenboeck.** 2001. Quantitative detection of *Chlamydia spp*. by fluorescent PCR in the LightCycler®. BioTechniques **30:**150-157.

10. **Iyer, R.K., J. M. Bando, C. P. Jenkinson, J. G. Vockley, P. S. Kim, R. M. Kern, S. D. Cederbaum, and W. W. Grody**. 1998. Cloning and characterization of the mouse and rat type II arginase genes. Mol. Genet. Metab. **63:**168-175.

11. **Shi, O., D. Kepka-Lenhart, S. M. Jr. Morris, and W.E. O'Brien**. 1998. Structure of the murine arginase II gene. Mammalian Genome **9:**822-824.

12. **Strausberg, R. L., E. A. Feingold, L. H. Grouse, et al**. 2002. Generation and initial analysis of more than 15,000 full-length human and mouse cDNA sequences. Proc. Natl. Acad. Sci. USA. **99:**16899-16903.

13. **Beaumont, C., C. Porcher, C. Picat, Y. Nordmann, and B. Grandchamp.** 1989. The mouse porphobilinogen deaminase gene. Structural organization, sequence, and transcriptional analysis. J. Biol. Chem. **264:**14829-14834.

14. **Melton, D. W., D. S. Konecki, J. Brennand, and C. T. Caskey**. 1984. Structure, expression, and mutation of the hypoxanthine phosphoribosyltransferase gene. Proc Natl. Acad. Sci. USA. **81:**2147-2151.

15. **Culp, T. D. and N. D. Christensen.** 2003. Quantitative RT-PCR assay for HPV infection in cultured cells. J. Virol. Methods **111:**135-144.

16. **Huber, R., E. Kunisch, B. Gluck, R. Egerer, S. Sickinger, and R. W. Kinne.** 2003. Comparison of conventional and real-time RT-PCR for the quantitation of jun protooncogene mRNA and analysis of junB mRNA expression in synovial membranes and isolated synovial fibroblasts from rheumatoid arthritis patients. Zeitschrift für Rheumatologie. **62:**378-389.

17. **Smith A. B., V. Mock, R. Melear, P. Colarusso, and D. E. Willis.** 2003. Rapid detection of influenza A and B viruses in clinical specimens by LightCycler® real time RT-PCR. J. Clin. Virol. **28:**51-58.

CHAPTER 3: Multivariate Analysis of *Chlamydia pneumoniae* Lung Infection in Two Inbred Mouse Strains

INTRODUCTION

Chlamydia pneumoniae is an obligate intracellular bacterial pathogen. It is the most common chlamydial pathogen affecting humans, and typically causes a mild acute respiratory infection. It is likely that *C. pneumoniae* infection can also result in chronic, persistent infection with several possible disease outcomes, including coronary heart disease and Alzheimer's disease (22, 43). Epidemiological data on this important pathogen provide a strong incentive to explore factors that potentially prolong or exacerbate *C. pneumoniae* infections, to understand the molecular mechanisms of chlamydial disease, and eventually to supply information useful for vaccine development.

It is well documented that people who have recovered from either an ocular or a genital infection with *C. trachomatis* or from respiratory infection with *C. pneumoniae* can be reinfected at the same site (33, 70, 79). It has also been established for both genital and ocular infections with *C. trachomatis* that the major pathologic changes are associated with the tendency for individuals to become re-infected, although the number of the organisms actually cultured upon re-infection is often low. It is quite possible that the pathology can be elicited solely by exposure to chlamydial antigen in the challenge inoculum, via delayed-type hypersensitivity DTH (70).

It has become apparent that cell-mediated immunity (CMI) is a significant factor in the resolution of chlamydial infection. In both primate and murine models, the mononuclear infiltrate in the genital tract has been characterized and found to be composed of a large number of T cells. Mice have large numbers of T cells in the genital tract following *C. muridarum* infection, and these cells are predominantly of the $CD4^+$ phenotype (34). The ability of B-cell-deficient mice to resolve the infection suggested that the T cell role was as a mediator of CMI rather than as a helper cell in the production of antibody (57). Perry and colleagues (1997) showed that T cell-deficient mice were unable to resolve *C. muridarum* infection. An important role for $CD4^+$ cells in the resolution of upper genital tract disease in mice was demonstrated by Landers et al (1991), who depleted mice of $CD4^+$ cells by treatment with anti-L3T4 antibody. When they challenged these mice by intra-uterine injection with *C. muridarum*, they found an increased number of organisms in the oviduct as well as an increased incidence of hydrosalpinx in the depleted animals in comparison to control animals. Further proof of the protective function of T cells was provided by successfully curing *C. muridarum*-infected nude mice through the adoptive transfer of T-cell lines (56). Rothfuchs et al (2004) reported that macrophage-, $CD4^+$, or $CD8^+$ T cell-derived IFN-γ is essential for protection against *C. pneumoniae* lung-infection in IFN-γ deficient C57BL/6 mice while NK cells were not needed for innate resistance against *C. pneumoniae* in their knockout mouse model.

Other protective mechanisms have been proposed that are active in a protective immune response to chlamydial-infection. Yang et al (1998) found that B cell-deficient C57BL/6 mice have a significantly higher mortality rate and *C. trachomatis* growth in

their lungs than control mice. On the other hand, Hawkins et al. transferred *C. muridarum*-specific CD4Th2 and CD4Th1 clones to *C. trachomatis* infected mice, and found that the $CD4^+$ Th2 clones did not provide protection against genital infection of *C. trachomatis* (24).

While there is consensus about the need for Th1-cell derived IFN- γ for protection of chlamydiae, the mechanisms of chlamydial disease are largely unknown (82). Traditionally, chlamydial diseases have been described as mononuclear tissue infiltrates that frequently can be macroscopically observed as granulomas. It is thought that these lesions develop after numerous episodes of re-infection, and that they represent a DTH response to chlamydial antigens.

Many *Chlamydia* researchers use knockout cell lines or nude mice to investigate the relationship between immune response-related genes and disease outcome. This is a useful approach for observation of the function of the target gene since the differential outcome in the absence of the gene can be observed. However, knockout approaches create completely new phenotypes that typically do not exist in natural populations. For these reasons, knockout approaches fail to model multifactorial diseases with redundant regulatory pathways. Many factors affect the outcome of chlamydial disease (1, 4, 6, 7). Thus, strictly quantitative examination of determinants and disease outcome in genetically unaltered hosts is required to understand potentially subtle interactions between genetic regulatory mechanisms that may result in different outcomes of chlamydial infection.

It was the goal of this investigation to elucidate mechanisms that differentiate between the progression of chlamydial infection towards granulomatous disease versus

mechanisms that result in resolution of the infection without sequelae. In this study, a lung inoculation model of *C. pneumoniae* was used because of the readily quantifiable disease characterized by interstitial mononuclear infiltrates, which can be measured as increase in lung weight over the lung weight of naïve mice (29). The influence of host genetics was addressed by use of two inbred mouse strains with differential susceptibility to chlamydial infection. The dependence of chlamydial disease on pre-existing immunity to *C. pneumoniae* and on the time after challenge were examined by challenging naïve or immune mice and sacrificing them on day 3 or 10 after challenge inoculation. We report here a simple model using 3 transcript parameters measured early after challenge infection that can predict with high accuracy the late disease outcome. This model also elucidates genetic mechanisms that determine the outcome of chlamydial lung infection.

MATERIALS AND METHODS

Experimental Design.

A balanced multivariate experiment was designed to evaluate the contribution of the genetic background of two mouse strains (A/J or C57BL/6), in the presence or absence of an established immune response against *C. pneumoniae* (immune or naïve), and at different temporal progression of the infection (day 3 or 10 post inoculation) to the outcome of *C. pneumoniae* infection (Table 1). To exclude a confounding sex influence, only female mice were used. Groups of 10 mice received 4 weeks prior to challenge a low-dose immunizing *C. pneumoniae* inoculum (immune) or a mock inoculum (naïve). From two weeks before *C. pneumoniae* challenge until sacrificing all mice (Harlan Sprague & Dawley) received one of the following four diets ad libitum: high-protein &

high-antioxidants diet (HH), high-protein & low-antioxidants diet (HL), low-protein & high-antioxidants diet (LH), or low-protein & low-antioxidants diet (LL) (Table 2). Mice were sacrificed 3 or 10 days after *C. pneumoniae* challenge. The whole experiment consisted of 32 different groups of two mouse strains, four diets, two immune conditions, and two time points, comprising a total of 320 mice (Table 1).

Chlamydia pneumoniae.

C. pneumoniae strain CDC/ CWL-029 (ATCC VR-1310) was grown, purified and quantified as described (20). Briefly, Buffalo Green Monkey Kidney cells (Diagnostic Hybrids, Inc. Athens, OH) were used as host cells for propagation of chlamydiae. For purification, EBs in supernatant culture medium were concentrated by sedimentation, followed by low-speed centrifugation for removal of host cell nuclei, and by step-gradient centrifugation of the supernatant in a 30% RenoCal-76 - 50% sucrose step-gradient. Sediments of purified infectious EBs were suspended in sucrose-phosphate-glutamate (SPG) buffer and stored in aliquots at -80°C.

Animals and diets.

Inbred A/J and C57BL/6 female mice were obtained from Harlan, Sprague and Dawley (Indianapolis, IN) at 5 weeks of age. Udel "shoebox" type cages with spun fiber filter top were maintained in static air or ventilated cage racks. Five animals were housed per cage in a temperature-controlled room with a 12-hour light/dark cycle. They were allowed ad libitum access to water and one of four diets. Mice were fed a 19% protein/1.33% L-arginine standard rodent maintenance diet. All animal protocols

followed NIH guidelines and were approved by the Auburn University Institutional Animal Care and Use Committee (IACUC).

Two weeks before challenge infection and during challenge infection, mice were fed one of 4 custom diets (Table 2) containing either 24% protein/1.8% L-arginine or 14% protein/0.7% L-arginine and either high or low antioxidants (low: 3.56 g vitamin C + 0.85 g vitamin E acetate/kg diet; high: 6.42 g vitamin C + 1.57 g vitamin E acetate/kg diet). Diets were manufactured by Harlan Teklad (Madison, WI, USA). The composition of the four custom diets is listed in Table 2.

***C. pneumoniae* lung challenge infection**.

Mouse intranasal inoculation was performed as described (29). For intranasal inoculation, mice received a light isoflurane inhalation anesthesia. Six week-old mice received a low dose challenge of 5×10^6 *C. pneumoniae* viable elementary bodies in 30 µl SPG buffer (immune mice) or a mock inoculum of 30 µl SPG buffer (naïve mice). Beginning at 8 weeks of age, all mice were fed a standardized custom diet containing either 24% protein/1.8% arginine or 14% protein/0.7% arginine and either high or low antioxidants (Table 2). Four weeks after the priming inoculation, at 10 weeks of age, the mice were challenged by intranasal inoculation of 1×10^8 *C. pneumoniae* bacteria and sacrificed by CO_2 inhalation 3 or 10 days later. Lungs were weighed, snap frozen in liquid nitrogen, and stored at -80°C until further processing. Percent lung weight increase was based on naïve lung weights of 138.4 mg for adult A/J mice and 133 mg for adult C57BL/6 mice.

Mouse lung nucleic acid extraction.

Mouse lungs were homogenized in guanidinium isothiocyanate Triton X-100-based RNA/DNA stabilization reagent in disposable tissue grinders (Fisher Scientific, Atlanta, GA) to create a 10% (wt/vol) tissue suspension. This suspension was used for total nucleic acid extraction by the High Pure® PCR template preparation kit (Roche Applied Science, Indianapolis, IN) (10, 29) and for mRNA extraction using oligo $(dT)_{20}$ silica beads.

For total nucleic acid extraction, 100 µl of 10% lung suspension was mixed with 240 µl of DNA/RNA stabilization reagent and 40 µl of 10% proteinase K solution and incubated for 1 hr at 72°C at 600 rpm in a shaking heater. This suspension was mixed with 100 µl isopropanol and centrifuged through glass fiber filter tubes for 1 min at 5,000 × g to bind total nucleic acids. After two washing steps with 500 µl wash buffer for 1 min at 13,000 × g, total nucleic acids bound to the glass fiber filter were incubated with 100 µl of 10 mM Tris-HCl, pH 8.5, 0.1 mM EDTA (10) for 5 min at 72°C and eluted by centrifugation for 1 min at 13,000 × g.

For mRNA extraction, a suspension of oligo $(dT)_{20}$-coated silica beads (25 mg/ml in dH_2O; 1 µm particle size, Kisker GbR, Steinfurt, Germany) was used. First, 100 µl of 10% lung suspension was mixed with 10 µl oligo $(dT)_{20}$ silica bead suspension diluted in 230 µl dilution buffer (0.1 M Tris-HCl, pH 7.5, 0.2 M LiCl, 20 mM EDTA). For mRNA binding, samples were incubated at 72°C for 3 minutes followed by room temperature for 10 minutes. The silica beads were sedimented by centrifugation at 13,000 × g for 2 minutes, supernatants removed by decanting, the beads resuspended in 100 µl DNase buffer (20 mM Tris-HCl, pH 7.0, 1 M NaCl, 10 mM $MnCl_2$) containing 100 U of RNase-

free bovine pancreatic DNase I (Roche Applied Science, Indianapolis, IN) and incubated for 15 minutes at room temperature. Subsequently, beads were washed three times with wash buffer (10 mM Tris-HCl, pH 7.5, 0.2 M LiCl, 1 mM EDTA) by vigorous vortexing for 2 minutes followed by sedimentation at 13,000 x g, and mRNA was eluted by resuspension of the beads in 200 µl DEPC-treated ddH_2O followed by incubation at 72°C for 7 minutes, centrifugal sedimentation, and removal of the supernatant mRNA. The purified total nucleic acid and mRNA samples were stored at -80°C until used for real-time PCR assays.

Analysis of lung nucleic acids by real-time PCR.

The primers and probes used in all PCR assays were obtained from Operon, Alameda, CA, and the sequences are listed in Table 3.

C. pneumoniae and host cell DNA: The copy number of *C. pneumoniae* genomes per lung were determined by *Chlamydia* genus-specific 23S rRNA FRET (fluorescence resonance energy transfer) qPCR (15). Copy numbers of murine genomes per lung, as markers of total number of cells, were determined by real-time amplification and quantification of an intron sequence of the porphobilinogen deaminase gene (PBGD). The qPCRs were performed in 20 µl volumes consisting of 15 µl reaction master mixture and 5 µl sample aliquot in glass capillaries in a LightCycler® real-time thermal cycler. The PCR buffer was 4.5 mM $MgCl_2$, 50 mM KCl, 20 mM Tris-HCl, pH 8.4, supplemented with 0.05% each Tween-20 and Nonidet P-40, and 0.03% acetylated bovine serum albumin (Roche Applied Science, Indianapolis, IN). Nucleotides were used at 0.2 mM (dATP, dCTP, dGTP) and 0.6 mM (dUTP). For each 20 µl total reaction

volume, 1.5 U hot-start Platinum *Taq* DNA polymerase (Life Technologies, Grand Island, New York) and 0.2 U heat-labile uracil-DNA glycosylase (Roche Molecular Biochemicals, Indianapolis, IN) was used. Heat-labile uracil DNA glycosylase is active at room temperature and is inactivated at 50°C. This allows the use of UNG carry-over prevention in one-step RT-qPCR. Thermal cycling consisted of a 2 min denaturation step at 95°C followed by 18 high-stringency step-down thermal cycles, 40 low-stringency fluorescence acquisition cycles, and melting curve determination between 50°C and 80°C. The parameters for the 23S rRNA qPCR were 6x 12 sec at 64°C, 8 sec at 72°C, 0 sec at 95°C; 9x 12 sec at 62°C, 8 sec at 72°C, 0 sec at 95°C; 3x12 sec at 60°C, 8 sec at 72°C, 0 sec at 95°C; 40x 8 sec at 54°C and fluorescence acquisition, 8 sec at 72°C, 0 sec at 95°C (10, 16). The parameters for the PBGD intron qPCR were 40x 8 sec at 58°C and fluorescence acquisition, 8 sec at 72°C, 0 sec at 95°C.

Transcripts: One-step duplex RT-qPCR was performed in a LightCycler as described (29). In one-step RT-qPCR, RT reaction and PCR amplification for one of the 23 analyte transcripts and an internal reference gene transcript (porphobilinogen deaminase, PBGD, for 22 analyte transcripts; or hypoxanthine guanine phosphoribosyl transferase, HPRT, for Arginase 1 analyte transcript) were performed in the same tube. All analyte transcript numbers are expressed as copies per 1000 reference transcripts. The murine analyte transcripts for which one-step duplex PCRs were developed include cellular markers, chemokines and cytokines, and inflammatory effectors and regulators (Tables 3a-c, 4a, b).

Statistical Analysis.

All statistical analyses were performed with the Statistica 7.0 software package (StatSoft, Inc., Tulsa, OK). Data of *C. pneumoniae* genome and transcripts numbers were logarithmically transformed. Normal distribution of data was confirmed by Shapiro-Wilk's W test, and homogeneity of variances by Levene's test. Data were analyzed by mean plots ± 95% confidence intervals in factorial analysis of variance (ANOVA). Comparisons of means under the assumption of no *a priori* hypothesis were performed by the Tukey honest significant difference (HSD) test. Differences at $p \leq 0.05$ in the Tukey HSD were considered significant.

The influences of the main effects mouse strain, immune status or time after inoculation on the 27 parameters were visualized in column plots of the Log_2 transformed ratios of mean values at both effect levels. Correlations between day-3 or day-10 group means of 25 cellular marker or transcript levels and day-3 or day-10 group means of the main outcomes lung weight increase or *C. pneumoniae* lung load were visualized in column plots.

Multivariate partial least squares regression (PLS; 28) was used to extract, by linear combination of independent cellular marker and transcript variables, up to 3 latent factors (components) for modeling of the outcomes lung weight increase or *C. pneumoniae* lung load. The modeling power (r^2) of these components, and the relative contribution of the independent variables to these components was calculated.

The dichotomous independent variables mouse strain, immune status, time after inoculation, diet protein, and diet antioxidants were used for single-component PLS modeling of disease (lung weight increase) and *C. pneumoniae* load outcomes of the 32

groups derived from all combinations of these variables. The relative contribution of the main variables to disease and *C. pneumoniae* lung load was calculated from factor scores derived by multiplication of weight by loading scores of all principal and their interaction factors. In the single component PLS model weight and loading scores were identical, and the factor scores were derived as the square of the weight score. The percent contribution of each main variable to the overall outcome (sum of all factor scores) was calculated from the sum of the fractional factor scores for each variable.

The influence of group mean day-3 transcripts levels on group mean day-10 disease or *C. pneumoniae* lung load outcomes was modeled using multiple regression and PLS analyses. Initially, all day-3 transcript parameters were used to calculate a multiple regression model for day-10 disease outcome. Using forward stepwise regression and increasing stringency for entering and removing parameters, models of reduced complexity were calculated that used only few parameters while still possessing high explanatory power. Finally, a best-fit simple model using 3 transcript parameters was established. The day-10 *C. pneumoniae* lung load outcome could be modeled with similar, high accuracy by use of numerous combinations of day-3 transcripts.

To understand the predictive interaction of the transcript parameters, the stepwise algorithm towards a simple best-fit multiple regression day-10 disease model was emulated in manual PLS analysis. Components that contributed r^2 increases of less than 0.05 to the day-10 disease model were eliminated, followed by elimination of variables that contributed less than 10% to the weighted sum of the remaining factor scores. The reduced set of variables and components was used again for PLS analysis, followed by further elimination. To avoid overfitting, all possible 3-way combinations of the

remaining variables were used to construct a best-fit final day-10 disease model with three transcripts and three components. These transcripts were identical to those used in the simplest 3-parameter multiple regression model, and the r^2 of the models was identical. These day-3 transcripts were then used to compute a day-10 *C. pneumoniae* lung load model. This model did not have the highest explanatory power, but was calculated to visualize the complex, partially opposite effects of day-3 transcript levels on the day-10 disease and *C. pneumoniae* lung load outcomes. The validity of both models was confirmed by models derived from partial data sets of the even or odd cases of the complete data. These models were deployed to predict the respective complementary data sets.

RESULTS

In this study, multivariate regulation of disease and chlamydial burden was examined in a *C. pneumoniae* mouse lung challenge model. Specifically, the simultaneous influence of host (mouse strain), its anti-*C. pneumoniae* immune status, and the time after inoculation, and the full factorial combinations of these variables, on disease as measured by lung weight increase and on *C. pneumoniae* lung load was analyzed. In addition, the influence of transcription of 25 genes on these outcomes was evaluated. To maximize the analytical accuracy, these parameters were directly derived from the mouse lung as the key affected organ. Transcripts were quantified by one-step duplex real-time RT-PCR in which analyte and reference transcripts were simultaneously amplified. In contrast to microarray experiments that target a high number of genes in a small number of animals, this investigation targeted a smaller amount of transcripts, but

with higher accuracy, and allowed outcome comparisons at multiple factor levels (overall 32 groups in this study) with appropriate statistical power (n=10/factor level). Multiple regression and partial least square regression algorithms were used to model the relative contributions of different factors and transcripts to disease and *C. pneumoniae* lung load.

The main factors mouse strain, immune status, and time after challenge inoculation result in opposite outcomes for lung disease and elimination of *C. pneumoniae*.

After lung challenge inoculation with *C. pneumoniae*, mice were sacrificed on day-3 or day-10, and lungs were processed to determine 29 outcome parameters which included lung weight increase, *C. pneumoniae* lung load by real-time PCR, 25 transcript concentrations by one-step duplex real-time RT-PCR, and two ratios of critical transcripts. Transcripts of interleukin-4 (IL-4) and C-reactive protein (CRP) were not detected in any specimen, and were therefore not included in analyses.

Analysis of the complete data from 160 A/J mice and 160 C57BL/6 mice for the main effect mouse strain on disease and *C. pneumoniae* load showed that A/J mice had an overall mean lung weight increase of 14.1 % (disease) that was highly significantly lower than the 35.9 % lung weight increase observed in C57BL/6 mice (Figure 1, $p < 10^{-4}$). In contrast, the $10^{5.5}$ *C. pneumoniae* genome load per lung in A/J mice of was highly significantly higher than the $10^{4.7}$ *C. pneumoniae* genomes per C57BL/6 mouse ($p < 10^{-4}$). We conclude that A/J mice had a highly significant reduction in disease as compared to C57BL/6 mice, but a highly significant increase in more chlamydial organisms per lung. Thus, A/J mice prioritized minimizing disease at the cost of reduced pathogen

elimination while C57BL/6 mice prioritized elimination of *C. pneumoniae* at the cost of increased disease.

Figure 2 shows the interaction of the main factors mouse strain, immune status, and time post inoculation to produce the outcomes shown in Figure. 1. Naïve C57BL/6 mice had significantly higher lung weight increases than naïve A/J mice on days 3 and 10 pi ($p \leq 0.028$), and immune C57BL/6 mice on day-10 pi ($p = 0.0004$). Between days 3 and 10 pi, disease (lung weight increase) decreased from 31.8 % to 16.6 % in immune A/J mice, and increased from 43.0 % to 59.9 % in immune C57BL/6 mice. This indicated that disease was enhanced by the host immune response in a host-restricted and time-dependent fashion.

Conversely, naive A/J mice had a lung burden of $10^{5.58}$ *C. pneumoniae* genomes that was highly significantly higher than the $10^{3.80}$ genomes of C57BL/6 mice ($p < 10^{-4}$). On day 10 pi naive A/J mice carried $10^{5.83}$ *C. pneumoniae* genomes as compared to the significantly lower load of $10^{4.69}$ genomes of C57BL/6 mice ($p = 0.013$). The *C. pneumoniae* lung load declined from $10^{6.75}$ to $10^{3.82}$ in immune A/J mice, and decreased from $10^{6.05}$ to $10^{4.24}$ in C57BL/6 immune mice from day-3 to day-10 ($p < 10^{-4}$). Overall, the observation is of interest that early after inoculation on day 3 pi immune mice of both strains showed highly significantly higher lung *C. pneumoniae* loads than naïve mice ($p < 10^{-4}$).

In partial least square analysis all 5 binomial factors (mouse strain, immune status, time pi, dietary protein, dietary antioxidants) and their 26 full factorial combinations were used to model disease (lung weight increase; $r^2 = 0.57$, $r = 0.76$, $p < 10^{-4}$) and total *C. pneumoniae* lung burden ($r^2 = 0.54$, $r = 0.73$, $p < 10^{-4}$) in best possible

fits of all data (n = 320) or of the groups means (n = 32; lung weight increase and *C. pneumoniae* lung burden: $r^2 = 1$) that differed in their explanatory power (r^2). The relative contribution of the main factors to disease and *C. pneumoniae* lung load was identical in both models and was calculated from the sum of all fractional factor scores of the single PLS component (Table 5). These data showed that immune status and mouse strain were the main contributors to disease, while time after inoculation, immune status, and mouse strain are the main influences on *C. pneumoniae* lung load. Dietary protein and antioxidants only marginally affected the main outcomes of *C. pneumoniae* challenge, and for that reason were not considered in the following analyses.

The 3 main binomial variables (mouse strain, immune status, time pi) and their full factorial combinations were applied in a simplified 7-parameter full factorial PLS model to predict lung weight increase and *C. pneumoniae* lung burden (Figure 3). The relative contributions of each parameter to lung weight increase and lung *C. pneumoniae* load are shown in Figure 4. This 7-parameter PLS model highly produced a highly significant prediction of lung weight increase and *C. pneumoniae* lung burden with high accuracy. Consistent with data shown in Figures 1 and 2, host genetics (mouse strain) was the only factor contributing strongly, and with opposite effect, to both disease and *C. pneumoniae* lung load. Disease (lung weight increase) was exclusively driven by immune status and mouse strain, in this order of importance. *C. pneumoniae* lung load was ~50% dependent on the interaction of immune status with time after challenge inoculation, followed by time pi, mouse strain, and the interaction of mouse strain with immune status. These results are consistent with data shown in Figure 2.

Marker transcript levels differ significantly for the main factors influencing outcomes of *C. pneumoniae* challenge infection.

Figures 5-12 show the summary information about the dependence of disease and *C. pneumoniae* burden and of 25 gene copy or transcript concentration parameters on main factors mouse strains, immune status and time after inoculation. C57BL/6 mice had generally higher transcript levels than A/J for most cellular markers except for T cell maturation markers (Figure 5, A). Most cytokines, inflammatory modulators, and cellular markers were significantly lower in naïve than in immune mice (Figure 5, B), and significantly higher on day-3 pi than on day-10 pi (Figure 5, C).

In Figures 6-12, that present detailed transcript data, most transcript concentrations showed a strong interaction between immune status and time pi for both mouse strains. Typically, transcript levels decreased between days 3 and 10 pi in immune mice, and increased in naïve mice. This trend is evident for both A/J and C57BL/6 mice in parameters PBGD intron, lactoferrin, F4/80, NKp46, CD45RB, CD45RO, perforin1, Arg1, Arg2, Nos2, Cybb, Ptgs2, IL-6, TNF-α, IFN-γ, Cxcl2, IL-10, and Ccl2. Serpine 1 decreases in both naïve and immune mice between day 3 and 10 pi, and CD19 does not show a significant trend.

Transcripts of the pan T cell marker CD3δ in immune A/J mice were highly significantly increased over naïve A/J mice ($p < 10^{-4}$), but did not change significantly between days 3 and 10 pi (Figure 7, A). In contrast, they increased in naïve C57BL/6 mice ($p = 0.007$), but highly significantly decreased in immune C57BL/6 mice (Figure 7,

B; $p < 10^{-4}$). Concentrations and immune-time interactions of the functional T cell markers Tim3 and GATA3 are fundamentally different between A/J and C57BL/6 mice (Figure 7, C-H). They decreased between days 3 and 10 pi in immune A/J mice, and increased in immune C57BL/6 mice. This resulted in higher ratios of Tim3/GATA3 or a stronger Th1 shift in immune C57BL/6 mice than in immune A/J mice both on day 3 ($p < 10^{-4}$) and on day 10 pi ($p < 0.038$).

Trends for Arg2 transcripts, the macrophage-specific arginase and an indicator of macrophage activation status, were similar in A/J and C57BL/6 mice, with increases between day 3 and 10 in naïve mice, and decreases in immune mice. However, the overall expression of Arg2 was higher in C57BL/6 mice. The specific activation status of macrophages, as measured by the ratio of the arginase 2 transcript over the macrophage marker transcript F4/80 (Arg2/F480), was highly significantly lower on day 3 pi in A/J mice than in C57BL/6 mice ($p < 0.009$). It increased from day 3 to day 10 significantly in A/J mice ($p < 10^{-3}$), and decreased significantly in C57BL/6 mice ($p < 0.037$).

Early transcript levels on day 3 associate with opposite late *C. pneumoniae* infection outcomes on day 10.

To survey the association of genetic parameters with the disease and *C. pneumoniae* load outcomes, correlation coefficients (r) of the day-3 and day-10 parameters with the day-3 and day-10 outcomes of all animals, and of the day-3 group means with the group means of the day-10 outcomes were plotted (Figure 13). For the early outcomes, most day-3 parameters significantly positively correlated to both day-3 disease (lung weight increase) and day-3 *C. pneumoniae* lung load (Figure 13, A). In

contrast, for the late day-10 peak disease or *C. pneumoniae* lung load outcome, the correlation of day-10 parameters to day-10 outcomes was highly variable (Figure 13, C). High day-10 CD3δ transcript concentrations significantly associated with low day-10 *C. pneumoniae* lung load. Importantly, Th1 inflammatory markers Tim3, Tim3/GATA3, and arginase1 significantly and strongly positively correlated on day 10 with disease, clearly indicating that *C. pneumoniae* disease associates with a delayed-type hypersensitivity response. Several transcript concentrations such as those of F4/80, arginase 2, Cybb, IL-6, Cxcl2, IL-10, and Ccl2 correlated positively with *C. pneumoniae* lung load, and tended to also negatively correlate with disease. However, a significant correlation to both outcomes was observed only for transcripts of the cytokine Ccl2 (Figure 13, C). Thus, at the late post-challenge time point these parameters were associated with reduced chlamydial elimination but also a tendency to reduced disease.

To identify candidate mechanisms operative in precipitating late peak disease, or protection from it, correlations of the 16 group means of day-3 transcript parameters with the 16 corresponding group means of the day-10 outcomes were evaluated (Figure 13, B). Virtually all day-3 transcripts correlated significantly and negatively with day-10 *C. pneumoniae* lung burden, indicating that all early inflammatory mechanisms eliminated chlamydiae. Most day-3 transcripts did not significantly correlate with day-10 disease. The exception were lactoferrin, NKp46, Tim3/GATA3, Arg2, and Arg2/F4/80, which were all significantly associated with increased day-10 disease. The inverse regressions of day-3 lactoferrin, NKp46, and Arg2 transcripts to day-10 disease (lung weight increase) and *C. pneumoniae* lung load are shown in Figure 14. Importantly, these data suggest that an exaggerated contribution of innate immunity to the early response to *C.*

pneumoniae challenge (lactoferrin, NKp46), and excessive Th1 immunity (Tim3/GATA3) and macrophage activation (Arg2, Arg2/F4/80) are involved in precipitation of late disease.

Host-dependent levels of early Th1 and Th2 responses, and their balance, highly significantly model the late disease and load outcomes of *C. pneumoniae* lung infection.

To better understand the contributions and interactions of host gene expression on *C. pneumoniae* disease mechanisms, day-10 disease or *C. pneumoniae* lung load outcomes were modeled by stepwise multiple regression analysis. An initial model predicting day-10 lung weight increase from the 16 group means of all day-3 transcript parameters was iteratively refined to models of reduced complexity to a final simple best-fit model using the 3 transcript parameters Tim3, GATA3, and Arg2 that explained 85% of the data (Figure 15 A). These day-3 transcripts were then used to compute a day-10 *C. pneumoniae* lung load model (Figure 15 C). This model did not have the highest explanatory power, but was calculated to visualize the complex, partially opposite effects of day-3 transcript levels on the day-10 disease and *C. pneumoniae* lung load outcomes. The validity of both models was confirmed by the similarity of models derived from partial data sets of the even or odd cases of the complete data.

To dissect the interaction of the transcript parameters, the 3-parameter multiple regression model for day-10 lung weight increase was emulated by partial least square regression (PLS) analysis. The rearrangement of the transcripts into new composite variables produced three components with potential biological significance (Figure 15 B).

These components were termed Th1 inflammation, Th1:Th2 balance, and Th2 inflammation because of the absolute factor scores and the relative values with which Tim3, GATA3, and Arg2 contributed to these latent variables. Day-3 Tim3 and Arg2 transcripts, but not GATA3, contributed positively to component 1, which was therefore termed Th1 inflammation, and which explained 55% of the day-10 lung weight increase. Component 2 explained an additional 11% of the data, and was termed Th1:Th2 balance because both Tim3 and GATA3 contributed, but not Arg2. Component 3 explained additional 19% of the data. It was negatively determined by Tim3, strongly positively by GATA3, and weakly positively by Arg2, and was therefore named Th2 inflammation.

Day-3 Tim3, GATA3, and Arg2 transcripts predicted day-10 *C. pneumoniae* load in a single-component PLS model with an $r^2 = 0.72$ (Figure 15 C). Components 2 and 3 were not used in PLS modeling because they contributed each only 0.01 to the overall r^2 value. The single component model indicated that high levels of transcripts of Tim3, GATA3, and Arg2 correlated with low *C. pneumoniae* lung loads (Figure 15, D).

Figure 16 visualizes the complex interaction of Tim3, GATA3, and Arg2 lung transcript concentrations that produce the day-10 outcomes as shown in Figure 2 and modeled by PLS regression, i.e., high disease vs. A/J mice in C57BL/6 mice, particularly those with immunity to *C. pneumoniae*, and ineffective *C. pneumoniae* elimination in naïve A/J mice vs. immune A/J mice and all C57BL/6 mice. The striking difference in disease outcome between the 2 mouse strains in naïve, but particularly in immune animals, correlates with consistently higher Arg2 transcripts in C57BL/6 mice, and with highly increased GATA3 transcripts in immune A/J mice. In contrast, decreased day-10 *C. pneumoniae* load correlates with increased Tim3 and Arg2 transcripts.

DISCUSSION

This investigation analyzed the simultaneous effect of multiple determinants on two measures of the outcome of murine *C. pneumoniae* lung infection, 1) disease expressed as lung weight increase and 2) the burden of *C. pneumoniae* bacteria in the lung. The overriding result is that optimum outcomes for both measures appear incompatible, and that the infected host has to prioritize the outcomes. C57BL/6 mice showed under all conditions of infection higher disease than A/J mice, but generally eliminated the infectious organisms more efficiently than A/J mice. Thus, A/J mice prioritized minimizing disease at the cost of reduced pathogen elimination while C57BL/6 mice prioritized elimination of *C. pneumoniae* at the cost of increased disease. Therefore, the host genetic makeup was the decisive factor that determined if the infection resulted in severe or marginal disease. This is consistent with a body of reports about host genetic restriction of responses to chlamydial antigens or infection (9, 11, 13, 73, 84, 86).

Another important result is the observation that disease was always more severe in animals that had established immunity against *C. pneumoniae* as compared to animals that had not been previously exposed to the bacteria. Conversely, immune animals reduced *C. pneumoniae* bacteria by about 100- to 1000-fold between 3 and 10 days after inoculation while naïve animals did not achieve net reduction of the bacteria during this time. It is the adaptive immune response that maximizes disease but also accomplishes the indispensable requirement of eliminating the bacteria from the infected host. Thus, the interaction of acquired immunity with the host genetic background is the critical determinant for disease severity.

Finally, maximum disease required some time to develop, and was observed late on day 10 after inoculation, but not early on day 3. This indicates that disease is enhanced by the immune response in a time-dependent and host-restricted fashion. The corollary of this observation is that host regulation of the early response to the *C. pneumoniae* inoculum is the key disease determinant.

To pinpoint genetic mechanisms regulating disease, or protection from it, the transcription of genes involved in immune regulation and inflammation was quantitatively analyzed. Most of the transcripts decreased significantly between day 3 and day 10 in immune mice, increased significantly in naïve mice, were on day 3 higher in immune than in naïve mice, and on day 10 higher in naïve than in immune mice (Figure 5). Obvious observations were the high transcript levels of markers of naïve and memory T cells, CD45RB and CD45RO, respectively, in A/J mice, immune mice, and on day 3 rather than on day 10 pi. Of interest were also the consistently increased concentrations of cytokine (particularly of IL-6 and IFN-γ) and inflammatory effector transcripts in day-3 immune mice (Figure 5). Correlations of day-3 transcript concentrations with day-3 disease or *C. pneumoniae* load outcomes were concordant for both outcomes, and day-10 transcript correlations were variable with both outcomes, but mostly discordant (Figure 13).

Most revealing was the projection from day-3 transcription to day-10 outcomes of the *C. pneumoniae* challenge: virtually all correlations of day-3 transcript means were discordant for the day-10 outcome means. Consistent with the incompatibility of simultaneous low disease and chlamydial load, high day-3 expression of marker transcripts of neutrophils and natural killer cells (lactoferrin, NKp46) was associated with

high day-10 lung weight increase and low *C. pneumoniae* lung burden. Similarly, high transcript concentration of the macrophage-specific arginase 2, an indicator of macrophage activation, and high ratios of Tim3 to GATA3, and of arginase 2 to F4/80 transcripts on day-3 associated with enhanced day-10 disease, but reduced chlamydial lung loads. These data strongly suggested that an exaggerated contribution of innate immunity to the early response to *C. pneumoniae* challenge (lactoferrin, NKp46), and excessive Th1 immunity (Tim3/GATA3) and macrophage activation (Arg2, Arg2/F4/80) are involved in precipitation of late disease. In fact, disease-resistant A/J mice had significantly lower levels of these markers, and also higher IL-10 transcripts, than C57BL/6 mice (Figure 5), indicating an overall anti-inflammatory Th2 bias of the response to *C. pneumoniae* infection in A/J mice.

A best-fit multiple regression model of the day-10 lung weight increase was found by iteratively using all possible combinations of three day-3 transcript concentrations. Using parameters Tim3, GATA3, and arginase 2, this model predicted peak disease on day 10 pi with 85% explanatory power. PLS analysis dissected the interaction of these parameters by combining them into three components that we termed Th1 inflammation, Th1:Th2 balance, and Th2 inflammation because of the relative contribution of Tim3, GATA3, and Arg2 to these latent variables. Tim3, GATA3, and arginase 2 also predicted the day-10 *C. pneumoniae* lung loads with an r^2 of 0.72 in a single-component PLS model in which all day-3 transcripts negatively correlated with bacterial load.

Examination of absolute concentrations of the critical predictive determinants reveals how the interaction of apparently unrelated gene transcription patterns produces opposite disease outcomes - minimal disease in A/J mice and severe disease in C57BL/6

mice, particularly in those with adaptive immunity to *C. pneumoniae*. Tim3 mRNA is largely identical between the mouse strains, but is approximately 2-fold increased in immune over naïve mice. GATA3 is highly significantly increased in immune A/J mice, and arginase 2 is consistently higher in C57BL/6 mice, and higher in immune than in naïve mice.

These data suggested a primary role for GATA3 in *C. pneumoniae* disease regulation. Based on transcript data in this study, the following regulatory cascade was envisioned: by inducing early after *C. pneumoniae* challenge a Th1:Th2 balance in immune A/J mice, GATA3 mitigates the Th1-driven macrophage activation and inflammation (3, 31, 36) and permits production of high levels of Th1, but also Th2, cytokines by a robust T cell population. In contrast, low GATA3 activity allows an early strong Th1 polarity in immune C57BL/6 mice, resulting in high Th1, but not Th2, cytokine production, and excessive macrophage activation. The ensuing intense inflammation requires down-regulation by reduction of the $CD4^+$ T cell population and Th1 cytokine production driving inflammation because little Th2 anti-inflammatory cytokines are released. Thus, high early IFN-γ production required for elimination of chlamydiae is balanced by IL-10 in immune A/J, but not in C57BL/6 mice.

These results do not negate the importance of Th1 immunity in protection against chlamydiae, emphasized in a large body of investigations that identified $CD4^+$ T cells and their production of IFN-γ as indispensable for clearance of chlamydial infections (34, 38, 53, 56, 57, 60). However, the results reported here clarify that Th2 immunity is not exclusively counterproductive for resolution of chlamydial infection (24), but is also a required component that controls inflammation elicited by the Th1 component of the anti-

chlamydial immune response. In fact, the data presented in this study are consistent with the fact that suppressed, but strongly Th1-polarized immunity is the pathogenetic principle in chlamydial infection. Thus, host genetic control of induction and maintenance of Th2 immunity and GATA3 expression (80, 88), the balance with Th1 responsiveness (68), and the avoidance of immunosupression associated with excessive Th1 immunity (14, 18) appear the main routes of inquiry that will provide answers to the vexing problem of molecular mechanisms of chlamydial pathogenesis.

Tables

Table 1. Balanced multivariate design of the *C. pneumoniae* challenge experiments.

Mouse[a] Strain	Immune Status	Sacrificing Day[b]	Diet	
			Protein	Antioxidants
A/J	naive	3	high	low
				high
			low	low
				high
C57BL/6			high	low
				high
			low	low
				high
A/J		10	high	low
				high
			low	low
				high
C57BL/6			high	low
				high
			low	low
				high
A/J	immune	3	high	low
				high
			low	low
				high
C57BL/6			high	low
				high
			low	low
				high
A/J		10	high	low
				high
			low	low
				high
C57BL/6			high	low
				high
			low	low
				high

[a] Ten mice (2 cages of 5 mice) were used for each combination of experimental categorical variables.

[b] Day 10 or 3 is the time to sacrificing of mice after challenge inoculation.

Table 2. Composition of four custom rodent diets.

Components (g/kg)	HH[a]	HL	LH	LL
Casein	275.90	275.90	160.92	160.92
L-Cystein	4.41	4.41	2.41	2.41
L-Arginine HCl	9.37	9.37	2.46	2.46
Corn Starch	302.82	306.30	426.88	430.36
Maltodextrin	132.00	132.00	132.00	132.00
Sucrose	100.00	100.00	100.00	100.00
Soybean Oil	70.00	70.00	70.00	70.00
Cellulose (fiber)	50.00	50.00	50.00	50.00
Mineral Mix, AIN-93G-MX	35.00	35.00	35.00	35.00
Calcium Phosphate Monobasic	--	--	2.02	2.02
Calcium Carbonate	2.31	2.31	0.12	0.12
Vitamin Mix, AIN-93-VX	12.00	12.00	12.00	12.00
Choline Bitartrate	2.50	2.50	2.50	2.50
TBHQ (antioxidant)	0.01	0.01	0.01	0.01
Vitamin E Acetate (500 U/g)	0.72	0.10	0.72	0.10
Stay-C 35	2.86	--	2.86	--
Food Color (soluble)	0.10	0.10	0.10	0.10

[a] HH, high-protein & high-antioxidant: 24% protein, 1.8% L-arginine, Vit. E + Vit. C

HL, high-protein & low-antioxidant: 24% protein, 1.8% L-arginine

LH, low-protein & high-antioxidant: 14% protein, 0.8% L-arginine, Vit. E + Vit. C

LL, low-protein & low-antioxidant: 14% protein, 0.8% L-arginine.

Table 3a. Oligonucleotide primers and probes used in real-time PCRs.

gene name length exon	primers probes[a]	Sequence (5'→3')[a]
Chlamydia 23S rRNA 168 bp	UP	GGGGTTGTAGGGTYGAGRAIAWRRGATC
	DN	GAGAGTGGTCTCCCCAGATTCARACTA
	BOD	BOD-CCTGAGTAGRRCTAGACACGTGAAAC-P
	FLU	ACGAAARAACAARAGACKCTAWTCGAT-6-FAM
PBGD intron 176 bp	UP	CCTAGTAGAGACACACCTGAATTGCTATTGTGA
	DN	TTCATAGCCAAGACTACTGCTTACTGCCTG
	BOD	BOD-TGAGCTGGGAAGCTTGCTTATCTCCT-P
	FLU	TGGGCAGGCTGCCTGAGATAAGG-FAM
Lactoferrin 189 bp exon 4-6	UP	CCTGCATCCCTTGAGGAAGCGGTA
	DN	TCCAGCATTGTCTCTCAGACACCTCAAG
	BOD	BOD-GAGGAGCCATACTCAGGTTATGCTGGA-P
	FLU	AGCCAACAAATGTGCCTCTTCCCC-6-FAM
F4/80 229 bp exon 7-9	UP	CAAAGACCTAGAGGTGACATGTGAAGATATTGA
	DN	TTGCTGTATCTGCTCACTTTGGAGTATCAAGT
	BOD	BOD-CTGCAAAAGGATCCTCTTCAAGTGTAAGGA-P
	FLU	GAAGGCTCCCAAGGATATGGAAACTTCA-6-FAM
NKp46 180 bp exon 3-6	UP	TGGCTCTTACAACGACTATGCATGGTCT
	DN	GATCCCAGAAGGCGGAGTCCTTTTG
	BOD	BOD-GAGTTTGACCTTTCAACCAATGAATCAGGA-P
	FLU	CCTACCGACCCTACTTCTTCTCTTGATTATTG-6-FAM
CD3δ 215 bp exon 2-4	UP	TGCAAGTCCATTACCGAATGTGCCA
	DN	ATCTTCACGATCTCGAAGAGGCTGATACAG
	BOD	BOD-CTTCTGGGGCTGCTGAGGTTCAAG-P
	FLU	TTTGCAGGACATGAGACCGGAAGG-6-FAM
Tim3 200 bp exon 2-5	UP	CTGAAATTAGACATCAAAGCAGCCAAGGT
	DN	GTTCTGATCGTTTCTCCAGAGTCCTTAATTTC
	BOD	BOD-GGAACAAAAATTTCCACATGGGCTGA-P
	FLU	ACAGACACTGGTGACCCTCCATAATAACAA-6-FAM
GATA3 171 bp exon 3-5	UP	AAGCCCAAGCGAAGGCTGTCG
	DN	TTTCTTCATAGTCAGGGGTCTGTTAATATTATGAAG
	BOD	BOD-GCAATGCCTGTGGGCTGTACTACAAG-P
	FLU	GAACGCTAATGGGGACCCGGTC-6-FAM

[a] UP, upstream primer; DN, downstream primer; BOD, amine-reactive Bodipy fluorophore attached to 5' terminus; FLU, 6-FAM, 6-carboxyfluorescein attached to 3'-O-ribose; P, Phosphate group attached to the 3' terminus; I=deoxy inosine; K=G/T; R=A/G; W=A/T; Y=C/T.

Table 3b. Oligonucleotide primers and probes used in real-time PCRs.

gene name length exon	primers probes[a]	Sequence (5'→3')[a]
CD45RB 209 bp exon 2-7	UP	CACAGAAGTCTTTGTCACAGGGCAAACA
	DN	GAGTTGTGAGGCTGGCACCTGGTG
	BOD	BOD-CGTGGATAACACACCATCACTGGGTGTA-P
	FLU	TGTGGGGACAGGTGAGGCAGCA-6-FAM
CD45RO 157 bp exon 2-9	UP	CACAGAAGTCTTTGTCACAGGGCAAACA
	DN	GTTCCCAAACATGGCAGCACATGTT
	BOD	BOD-GGCTGGCACCATCACTGGGTGTA-P
	FLU	GCCCAGAGTGGATGGTGTAAGAGTTGTG-6-FAM
Perforin 1 194 bp exon 1-3	UP	ATGTGAACCCTAGGCCAGAGGCAAAC
	DN	TCTGAGCGCCTTTTTGAAGTCAAGGT
	BOD	BOD-CGCATGTACAGTTTTCGCCTGGTACAA-P
	FLU	GACCAGTACAACTTTAATAGCGACACAGTAGAGTG-6-FAM
CD19 198 bp exon 4-7	UP	GGTCATTGCAAGGTCAGCAGTGTGG
	DN	GGAGGCGTCACTTTGAAGAATCTCCTG
	BOD	BOD-CCTGAGAAGGAAAAGGAAGCGAATGACT-P
	FLU	GTGGCTTTTCTCTATTGTCAAAGAGCCTTTA-6-FAM
Arg1 212 bp exon 3-5	UP	GTGGAGACCACAGTCTGGCAGTTGGA
	DN	GCAGGGAGTCACCCAGGAGAATCCT
	BOD	BOD-GAAGGAACTGAAAGGAAAGTTCCCAGATGT-P
	FLU	CATGGGCAACCTGTGTCCTTTCTCC-6-FAM
Arg2 160 bp exon 1-3	UP	TTTCTCTCGGGGACAGAAGAAGCTAGGA
	DN	CAGATTATTGTAGGGATCATCTTGTGGGACA
	BOD	BOD-TCTTCAGCAAGCCAGCTTCTCGAATGG-P
	FLU	GGTGGCATCCCAACCTGGAGAGC-6-FAM
Nos2 189 bp exon 12-15	UP	GCTACGCCTTCAACACCAAGGTTGTCT
	DN	CAAACACAGCATACCTGAAGGTGTGGTT
	BOD	BOD-GCAATGGGCAGACTCTGAAGAAATCTCTG-P
	FLU	GCACATTTGGGAATGGAGACTGTCCC-6-FAM
Cybb 176 bp exon 5-7	UP	CTATTCAATGCTTGTGGCTGTGATAAGCA
	DN	CCTGCACAGCCAGTAGAAGTAGATCTTTTTG
	BOD	BOD-CAACTGCTATCTTAGGTAGTTTCCAGGCATC-P
	FLU	TCTTCACTGGCTGTACCAAAGGGTCCA-6-FAM
IL-4 226 bp exon 2-5	UP	TCACAGGAGAAGGGACGCCATGCA
	DN	GTGCAGCTTATCGATGAATCCAGGCA
	BOD	BOD-GTGAGCTCGTCTGTAGGGCTTCCAA-P
	FLU	CTCACAGCAACGAAGAACACCACAGAG-6-FAM

[a] UP, upstream primer; DN, downstream primer; BOD, amine-reactive Bodipy fluorophore attached to 5' terminus; FLU, 6-FAM, 6-carboxyfluorescein attached to 3'-O-ribose; P, Phosphate group attached to the 3' terminus; I=deoxy inosine; K=G/T; R=A/G; W=A/T; Y=C/T.

Table 3c. Oligonucleotide primers and probes used in real-time PCRs.

gene name length exon	primers probes[a]	Sequence (5'→3')[a]
Ptgs2 176 bp exon 5-7	UP	AGGACTGGGCCATGGAGTGGACTTA
	DN	CAGGGATGTGAGGAGGGTAGATCATCTC
	BOD	BOD-GTATCCCCCCACAGTCAAAGACACTCA-P
	FLU	AATTGAAATATCAGGTCATTGGTGGAGAGG-6-FAM
IL-6 210 bp exon 1-3	UP	GTTCCTCTCTGCAAGAGACTTCCATCCA
	DN	CCATTGCACAACTCTTTTCTCATTTCCAC
	BOD	BOD-ACCAGCATCAGTCCCAAGAAGGCAA-P
	FLU	TTGTGAAGTAGGGAAGGCCGTGGTTGT-6-FAM
TNF 177 bp exon 2-5	UP	GCCACCACGCTCTTCTGTCTACTGAACT
	DN	CTCCACTTGGTGGTTTGCTACGACGT
	BOD	BOD-TTGGGAACTTCTCATCCCTTTGGGGA-P
	FLU	CCATAGAACTGATGAGAGGGAGGCCA-6-FAM
Ifng 166 bp exon 3-4	UP	CCTTCTTCAGCAACAGCAAGGCGAA
	DN	CAGCAGCGACTCCTTTTCCGCTTC
	BOD	BOD-GGGTTGTTGACCTCAAACTTGGCAATAC-P
	FLU	TGAATGCTTGGCGCTGGACCTG-6-FAM
Cxcl2 241 bp exon 2-5	UP	ACGTGTTGGCTCAGCCAGATGCAGTTAA
	DN	TGGACCCATTCCTTCTTGGGGTCA
	BOD	BOD-TGTCCCAAAGAAGCTGTAGTTTTTGTCACC-P
	FLU	AGAGCTACAAGAGGATCACCAGCAGCAG-6-FAM
IL-10 227 bp exon 2-4	UP	GCACTGCTATGCTGCCTGCTCTTACTG
	DN	CAACCCAAGTAACCCTTAAAGTCCTGCAT
	BOD	BOD-CCAGCTGGACAACATACTGCTAACCGACT-P
	FLU	CCAGGTGAAGACTTTCTTTCAAACAAAGG-6-FAM
Ccl2 193 bp exon 2-4	UP	ACGTGTTGGCTCAGCCAGATGCAGTTAA
	DN	TGGACCCATTCCTTCTTGGGGTCA
	BOD	BOD-TGTCCCAAAGAAGCTGTAGTTTTTGTCACC-P
	FLU	AGAGCTACAAGAGGATCACCAGCAGCAG-6-FAM
Serp1 222 bp exon 5-8	UP	CGCCTCCTCATCCTGCCTAAGTTCTC
	DN	TGAGATGACAAAGGCTGTGGAGGAAGAC
	BOD	BOD-TAGCACAGGCACTGCAAAAGGTCAGG-P
	FLU	AGTCTTTCCGACCAAGAGCAGCTCTCT-6-FAM
CRP 189 bp exon 1-3	UP	GGACTCCTTGTCCTTGATCTTTCAGACAA
	DN	ACACATAGGAAGTATCTGACTCCTTGGGAAA
	BOD	BOD-TCATGAAGACATGTTTAAAAAGGCCTTTGT
	FLU	ATCATGATCAGCTTCTCTCGGACTTTTG-6-FAM

[a] UP, upstream primer; DN, downstream primer; BOD, amine-reactive Bodipy fluorophore attached to 5' terminus; FLU, 6-FAM, 6-carboxyfluorescein attached to 3'-O-ribose; P, Phosphate group attached to the 3' terminus; I=deoxy inosine; K=G/T; R=A/G; W=A/T; Y=C/T.

Table 4a. Functional significance, GenBank accession number, and key references of transcripts of cellular marker genes.

Specific marker & definition	GenBank accession number & references
PBGD intron The 3rd enzyme of the heme biosynthetic pathway	J04981 Beaumont et al. (2).
Lactoferrin Neutrophil secreted antimicrobial-globular protein	NM_008522 Shirsat et al. (66). Rogan et al. (59).
F4/80 Macrophage surface antigen with unknown function	NM_010130 Lin et al. (40). Schaller et al. (64).
NKp46 NK cell natural cytotoxicity triggering receptor 1	NM_010746 Vankayalapati et al. (75). Pessino et al. (54). Sivori et al. (67).
CD3δ T cell-specific, expressed T cell receptor component	NM_013487 Elsen et al. (17). Dave et al. (12). Kappes et al. (32).
Tim 3 CD4 Th1 cell surface protein	AF450241 Monney et al. (44). Khademi et al. (35). Veillard et al. (76).
GATA-3 CD4 Th2 cell-specific GATA-3 transcription factor	X55123 Ko et al. (37). Nawijin et al. (47). Zheng et al. (85). Pai et al. (52). Zhu et al. (88).
CD45RB Naïve T cell surface protein	NM_011210 Hermiston et al. (25). Saga et al. (62).
CD45RO Memory T cell surface protein	NM_011210 Hermiston et al. (25). Saga et al. (62).
Perforin 1 CD8 CTL and NK cell secreted cytolytic granule protein	J04148 Trapani et al. (72). Podack et al. (55). White et al. (78).
CD19 B cell surface protein	NM_009844 Zhou et al. (87). Sato et al. (63). Gardby et al. (20). Gardby et al. (21).

Table 4b. Functional significance, GenBank accession number, and key references of inflammatory regulator gene transcripts.

Specific marker & definition	GenBank accession number and references
Arginase1 Liver isoform, cytosolic enzyme	NM_007482 Takiguchi et al. (69) Mori et al. (45).
Arginase2 Extra-hepatic (macrophage) isoform, mitochondrial enzyme	NM_009705 Shi et al. (65). Mori et al. (45).
NOS2 Macrophage produced Nitric oxide synthase 2	NM_010927 Lyons et al. (41). Okamoto et al.(51).
Cybb Cytochrome b-245, beta polypeptide (formerly $gp91^{phox}$ subunit of the phagocyte oxidative burst NADPH oxidase)	NM_007807 Bjorgvinsdottir et al. (3). Chamseddine et al. (10).
Ptgs2 Prostaglandin-endoperoxide synthase 2 (cyclooxygenase-2, COX-2)	NM_01198 O'Banion et al. (49). Ejuma et al. (16). Hodges et al. (26).
IL-6 Interleukin-6	NM_031168 Van Snikc et al. (74). McLoughlin et al. (42).
TNF-α Tumor necrosis factor	NM_013693 Fransen et al. (19). Botha et al. (6). Jendro et al. (31).
IFN-γ Interferon gamma	NM_008337 Gray et al. (23).
Cxcl2 C-X-C motif ligand 2 (formerly macrophage inflammatory protein-2, MIP-2, homolog to human IL-8)	NM_009140 Tekamp-Olson et al.(71). Hodges et al. (26).
IL-10 Interleukin-10	NM_010548 Kim et al. (36). Murray et al. (46).
Ccl2 C-C motif ligand 2 (monocyte chemotactic protein-1, MCP-1)	NM_011333 Boring et al. (4). Rutledge et al. (61).
Serpine1 Serine proteinase inhibitor E 1 (formerly plasminogen activator inhibitor-1, PAI-1)	NM_008871 Yamamoto et al. (80). Rebecca et al.(58).
IL-4 Interleukin-4	NM_021283 Noma et al. (48). Butler et al. (8).
CRP C-reactive protein	NM_007768 Ohnishi et al. (50).

Table 5. Percent absolute contribution of the main factors to disease (lung weight increase) and lung *C. pneumoniae* load in the full factorial PLS model.

Factor	Contribution to Disease, %	Contribution to lung *C. pneumoniae*, %
Mouse strain	37.8	21.4
Immune status	46.3	29.1
Time post inoculation	8.6	41.9
Dietary protein	4.6	4.7
Dietary antioxidants	2.7	2.9

Figures

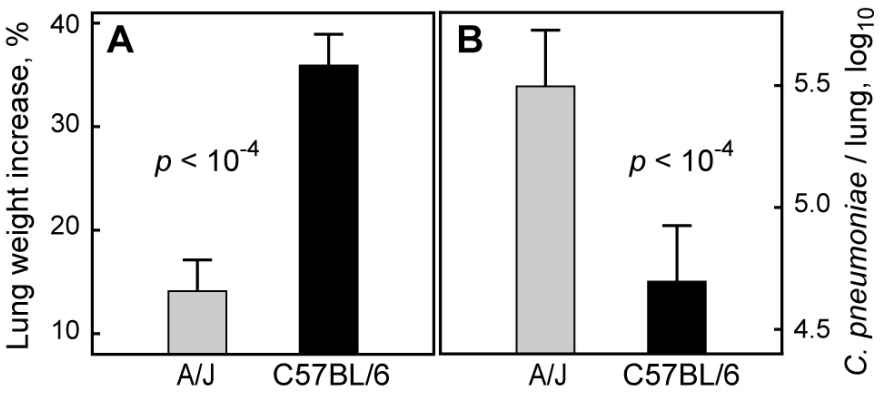

Figure 1. The fundamental conundrum: prioritize minimizing disease or eliminating *C. pneumoniae*. Female A/J or C57BL/6 mice received a pre-challenge mock inoculum (naïve) or a low-dose *C. pneumoniae* inoculum ($5x10^6$ EB; immune), were fed a diet containing low (14%) or high (24%) protein and low antioxidant (3.56 g vitamin C + 0.85 g vitamin E acetate per kg diet) or high antioxidant (6.42 g vitamin C + 1.57 g vitamin E acetate per kg diet) concentrations, intranasally challenged 4 weeks later with $1x10^8$ *C. pneumoniae*, and sacrificed during early disease (3 days post inoculation, pi) or peak disease (10 days pi). Results are shown for all A/J mice (n = 160) and C57BL/6 (n = 160) mice as **A,** average percentage of lung weight increase ± 95% confidence interval and **B,** average $\log_{10}$ *C. pneumoniae* / lung ± 95% confidence interval. Grey bars denote A/J mice and black bars C57BL/6 mice. A/J mice had an average 14.1 % lung weight increase that was highly significantly lower than the 35.9 % lung weight increase of C57BL/6 mice (Tukey HSD test, A). The ratio A/J to C57BL/6 mice was reversed for the *C. pneumoniae* lung burden with $10^{5.5}$ copies of *C. pneumoniae* /lung in A/J mice that were highly significantly higher than $10^{4.7}$ copies in C57BL/6 mice (B).

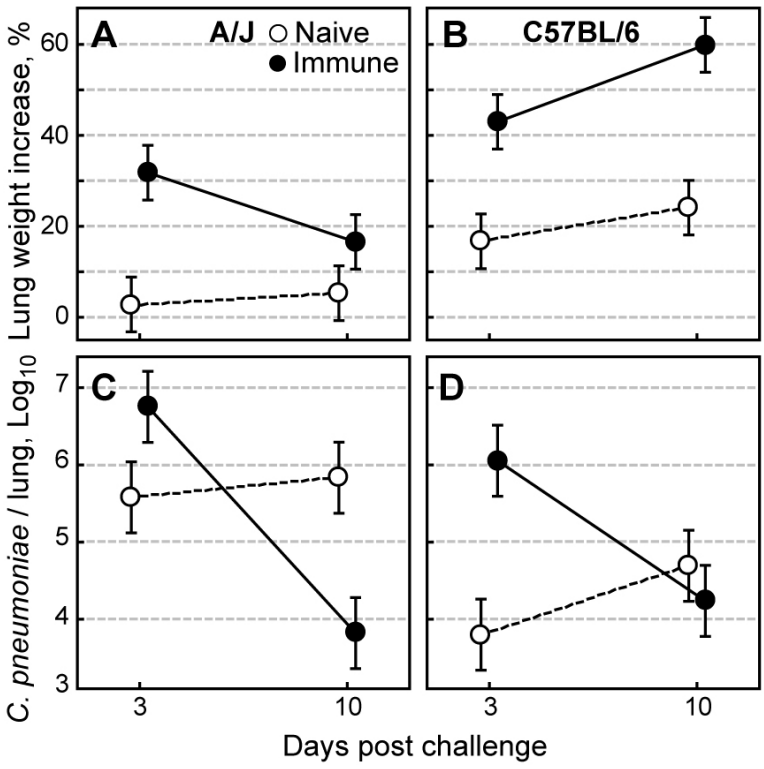

Figure 2. Influence of mouse strain, immune status and time after challenge inoculation on disease (lung weight increase) and *C. pneumoniae* lung burden. Data represent means per treatment group (n = 40) ± 95% confidence interval. Open circles (○) denote naive mice and closed circles (●) immune mice. Both immune A/J and C57BL/6 mice had significantly higher lung weight increase than naïve mice on day 3 and day 10 ($p \leq 10^{-4}$, Tukey HSD test; A, B). Between day 3 to day 10, the lung weight decreased significantly in immune A/J mice ($p = 10^{-4}$) and increased significantly in immune C57BL/6 mice ($p = 0.023$). The *C. pneumoniae* lung burden declined highly significantly between day 3 and day 10 in immune mice of both strains ($p \leq 10^{-4}$, C, D) and increased in naïve C57BL/6 mice ($p = 0.05$, D).

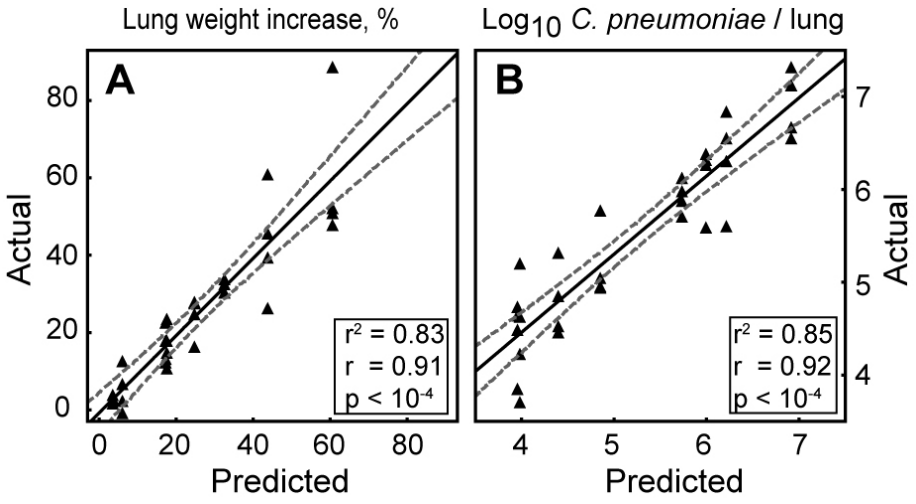

Figure 3. **Prediction of lung weight increase and *C. pneumoniae* lung burden in a 7-parameter full factorial PLS model.** Disease and *C. pneumoniae* lung burden outcomes of the means of all experimental groups (n = 32 groups of 10 mice each) were modeled by PLS analysis using the 3 dominant binomial variables (mouse strain, immune status, time post inoculation) and their full factorial combinations (mouse strain x immune status, mouse strain x time post inoculation, immune status x time post inoculation, and mouse strain x immune status x time post inoculation). This 7-parameter PLS model highly significantly predicted **A**, lung weight increase (± 95% CI) and **B**, *C. pneumoniae* lung burden (± 95% CI) with high accuracy. Regression lines with the use of individual animals (n = 320) instead of group means were identical, but the fit to the data was different (lung weight increase: $r^2 = 0.47$, r = 0.69, $p \leq 10^{-4}$; *C. pneumoniae* lung burden: $r^2 = 0.34$, r = 0.58, $p \leq 10^{-4}$).

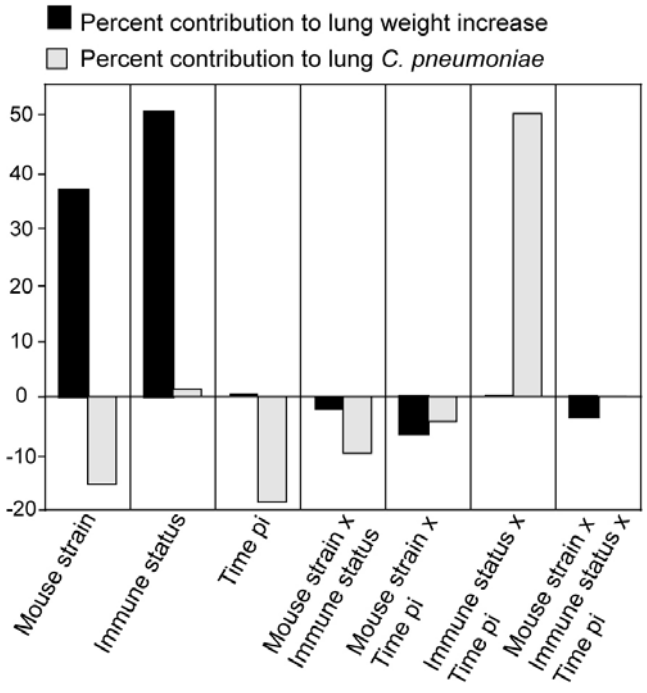

Figure 4. Relative contributions to lung weight increase and lung *C. pneumoniae* load of each parameter in the 7-parameter PLS model. Relative contributions of the 3 main variables (mouse strain, immune status, and time pi) and their full factorial combinations on lung weight increase and lung *C. pneumoniae* load outcomes in the 7-parameter PLS model were calculated from the factor scores. Black bars denote the contribution to lung weight increase, and grey bars to lung *C. pneumoniae* load. Lung weight increase was almost exclusively dependent on mouse strain and immune status, while *C. pneumoniae* lung load was dominantly influenced by the interaction of immune status with time pi, followed by time pi, mouse strain, and the interaction of mouse strain with immune status. The variable mouse strain has opposite influence on disease and *C. pneumoniae* lung load, while other variables such as immune status, or the interactions of main variables predominantly influence either disease or *C. pneumoniae* lung load.

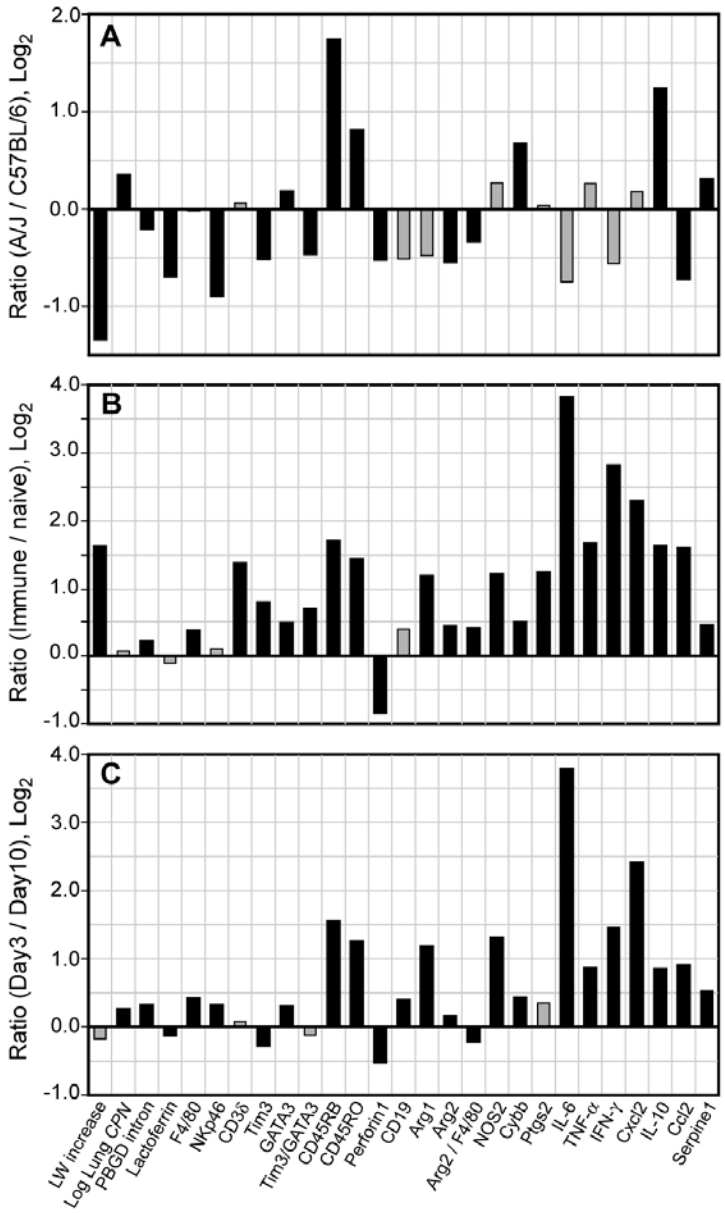

Figure 5. Contribution of mouse strain, immune status and time post inoculation on 27 outcome parameters in *C. pneumoniae* lung infection. Results are shown as log_2-transformed values of the means of **A**, all A/J mice (n = 160) over C57BL/6 mice (n = 160), **B**, naïve mice (n = 160) over immune mice (n = 160), and **C**, day-3 sacrificed mice (n = 160) over day-10 sacrificed mice (n = 160). Grey bars denote no significant

differences, and black bars denote significant differences for a parameter ($p < 0.05$, Turkey HSD test). C57BL/6 mice had higher transcript levels for most cellular markers with exception of T cell maturation markers CD45RB and CD45RO that were expressed in A/ J mice at significantly higher levels. Immune mice showed significantly higher transcript levels for most cytokines, inflammatory modulators, and cellular markers. The exception was the CD8 T cell marker perforin1**,** which was significantly higher in naïve mice. Mice sacrificed on day 3 pi had significantly higher levels of most parameters than those sacrificed on day 10. Significantly higher expression levels on day 10 were observed only for the parameters lactoferrin, Tim3, perforin1, and Arg2/F4/80.

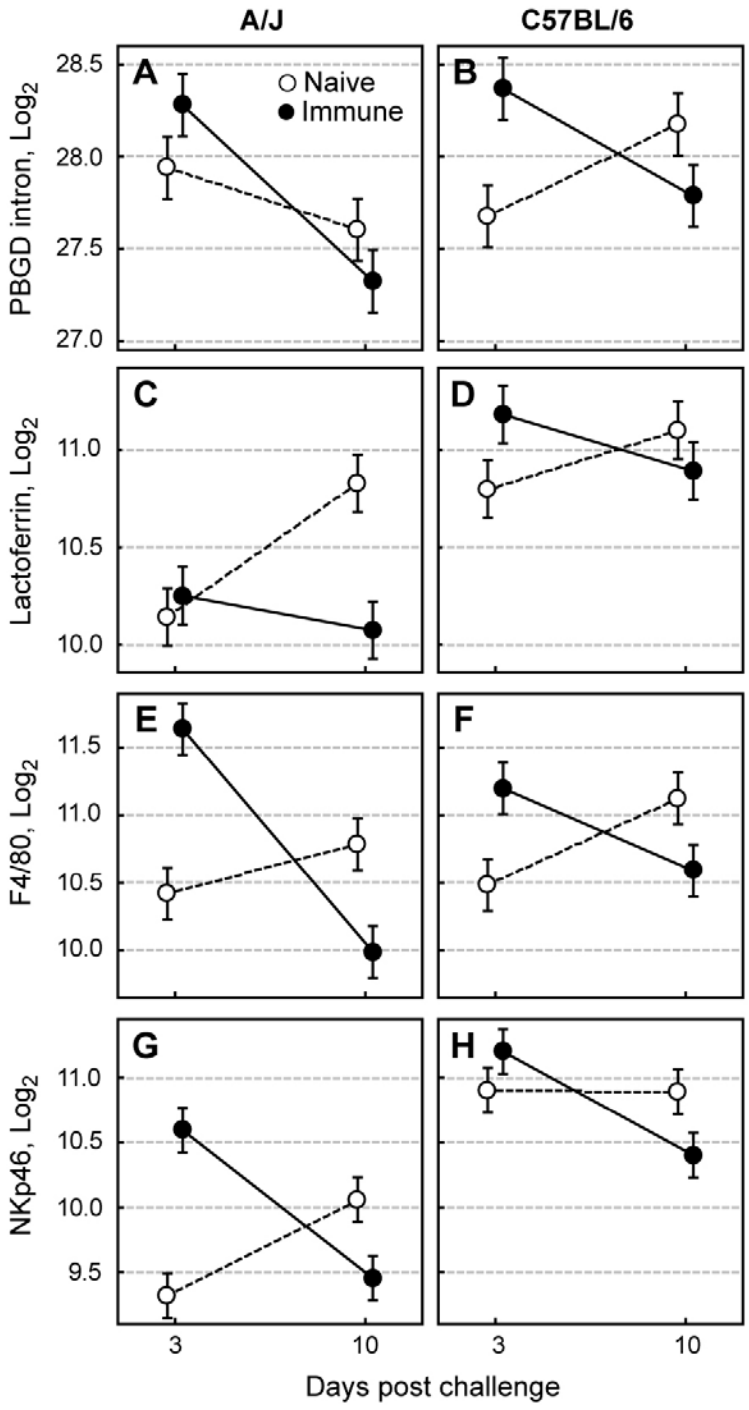

Figure 6. Influence of mouse strain, immune status and day post inoculation on total lung cell numbers (PBGD intron), and lung transcript levels of lactoferrin,

F4/80, and NKp46. Results are shown as $\log_2$-transformed values ± 95% confidence interval of the day-3 and day-10 means of naïve and immune animals for both A/J and C57BL/6 mice. Each data point represents 40 mice, comprising 4 groups of 10 mice fed one of the 4 diets. Open circles (o) denote naive mice, and closed circles (●) immune mice. In general, naïve mice of both strains had significantly lower levels of these four parameters on day 3 pi than on day 10 pi, while immune mice showed the opposite trend with significantly lower levels on day 10 pi than on day 3 pi (**A**-**H**). Significant differences typically can be deduced from the relative position of the error bars of the 95% CI: in 8-way post-hoc Tukey HSD comparisons of group means of a parameter, non-overlapping error bars indicate significantly different means, e.g., the day-10 means of the $\log_2$ PBGD intron of naïve and immune C57BL/6 mice are significantly different ($p = 0.03$).

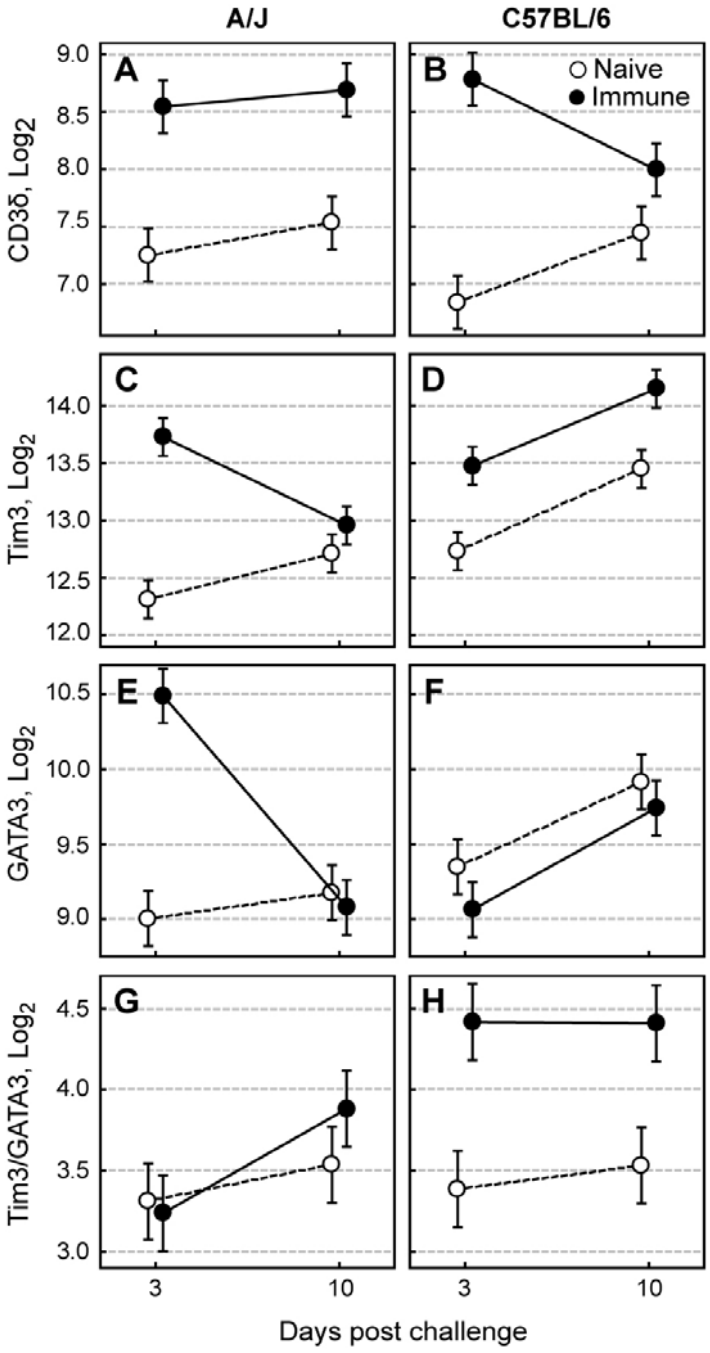

Figure 7. Influence of mouse strain, immune status and day post inoculation on lung transcript levels of CD3δ, Tim3, GATA3, and ratio Tim3/GATA3. In general, naïve mice had significantly lower transcript levels of CD3δ, Tim3, and GATA3 than

immune mice of both strains, particularly in A/J mice on day 3 pi (**A-F**). Interestingly, transcript levels of Tim3 and GATA3 decreased highly significantly in immune A/J mice ($p < 10^{-4}$), and increased highly significantly in immune C57BL/6 mice ($p < 10^{-4}$; **C-F**), which resulted in significantly higher ratios of Tim3/GATA3 or a stronger Th1 shift in immune C57BL/6 mice than in immune A/J mice (**G, H**).

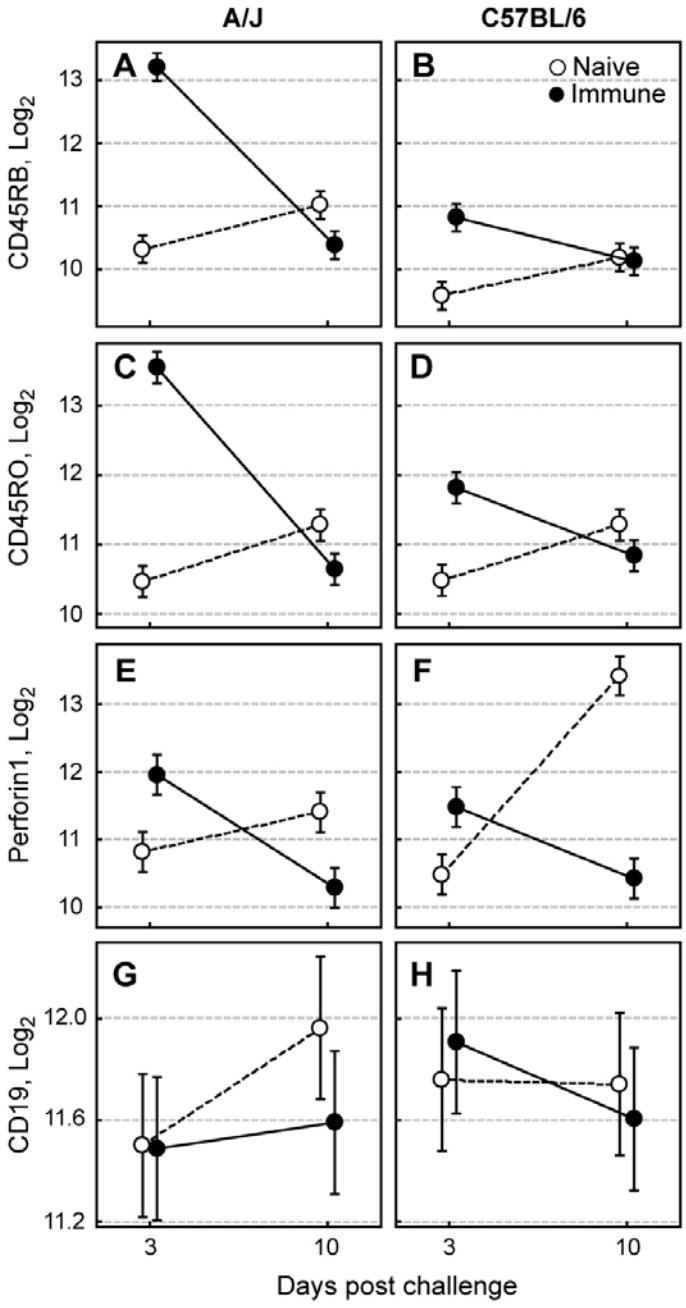

Figure 8. Influence of mouse strain, immune status and day post inoculation on lung transcript levels of CD45RB, CD45RO, Perforin1, and CD19. Transcript levels of CD45RO, CD45RB and perforin1 decreased in immune mice and increased in naive

mice of both strains. In general, on day 3 pi immune mice had significantly higher transcript levels than naïve mice, and on day 10 naïve mice had significantly higher transcript levels than immune mice, indicating a significant interaction between immune status and time pi (**A-F**). Transcript levels of CD19 with higher variance did not change significantly for mouse strains, immune status and day pi (**G, H**).

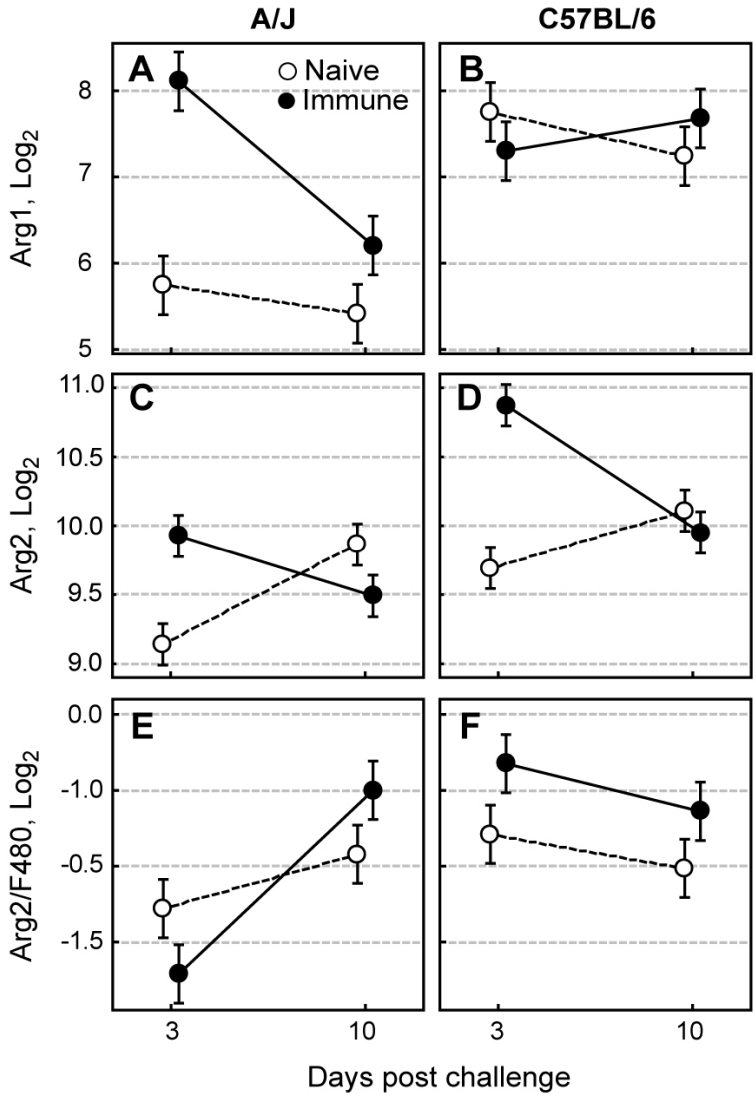

Figure 9. Influence of mouse strain, immune status and day post inoculation on lung transcript levels of Arg1 and Arg2, and ratio of Arg2/F480. Arg1 transcript levels decreased in A/J immune mice between day 3 and day 10 and increased in immune C57BL/6 mice (**A**, **B**). Trends for Arg2 transcript were similar in A/J and C57BL/6 mice, with significant increases between day 3 and 10 in naïve mice, and decreases in immune mice. However, overall expression of Arg2 was significantly higher in C57BL/6 mice (**C**, **D**). The ratio of Arg2/F480 increased significantly in naive A/J mice (p = 0.0007)

and immune A/J mice ($p = 10^{-4}$) from day 3 to day 10, and decreased significantly in naïve C57BL/6 mice ($p = 0.030$) and immune C57BL/6 mice ($p = 0.037$) from day 3 to day 10 (**E**, **F**).

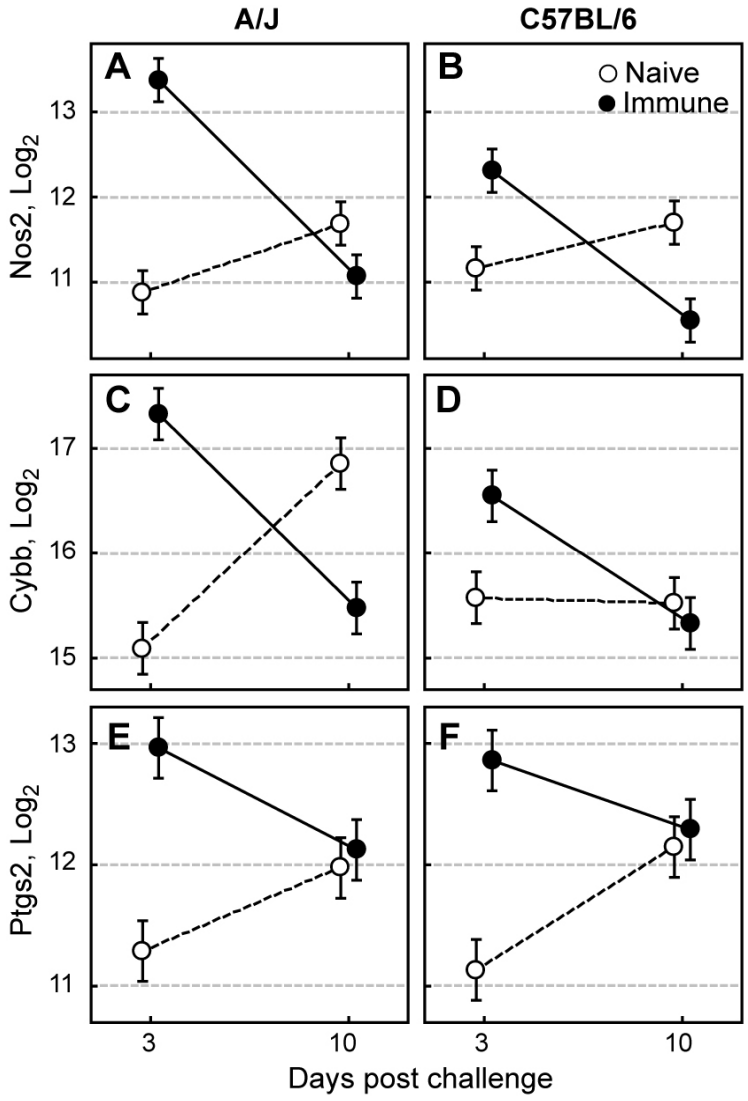

Figure 10. Influence of mouse strain, immune status and day post inoculation on lung transcript levels of inflammatory effectors Nos2, Cybb and Ptgs2. Transcript levels of Nos2, Cybb and Ptgs2 showed similar trends in both A/J and C57BL/6 mice. Transcript levels increased significantly in naïve mice and decreased significantly in immune mice (**A-F**). In general, immune A/J and C57BL/6 mice had significantly higher transcript levels on day 3 pi and lower transcript levels on day 10 pi.

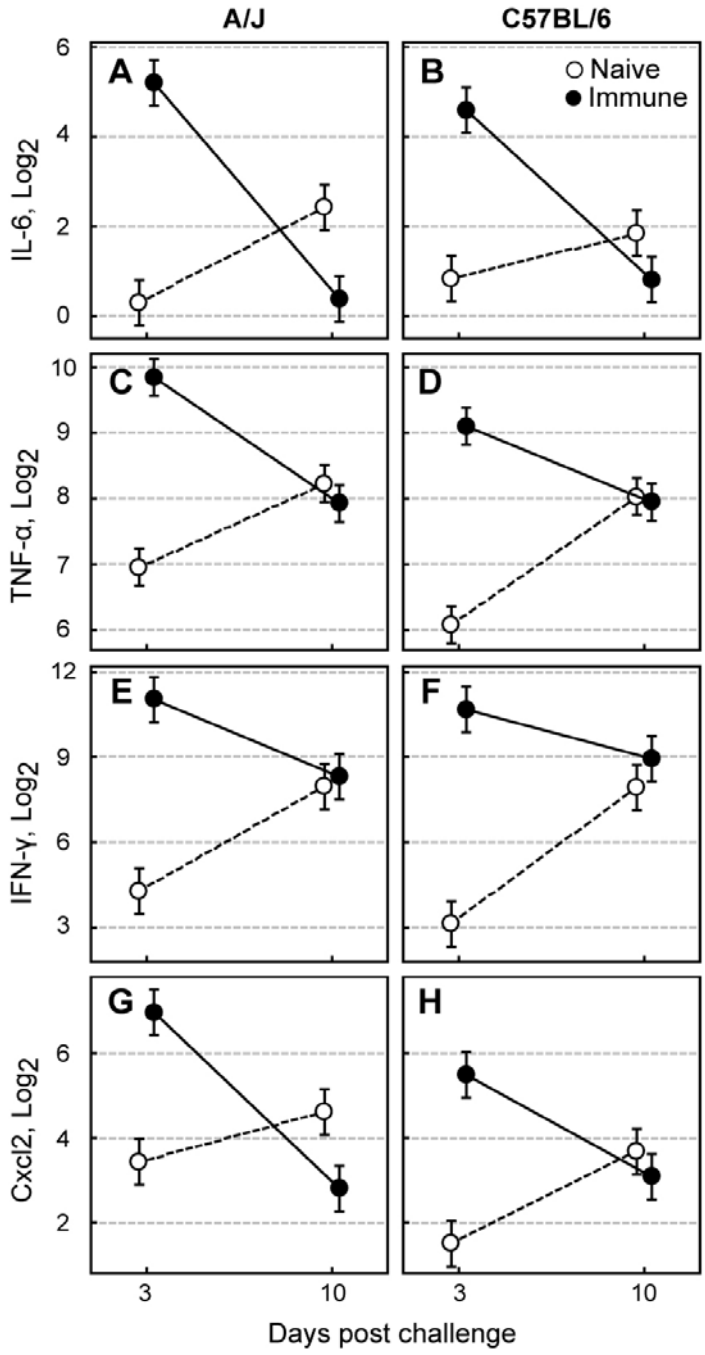

Figure 11. Influence of mouse strain, immune status and day post inoculation on lung transcript levels of Th1-associated cytokines IL-6, TNF-α, IFN-γ, and Cxcl2. Transcripts of IL-6, TNF-α, IFN-γ, and Cxcl2 in both strains declined significantly in

immune mice and increased significantly in naïve mice from day 3 to day 10 (**A**-**H**). On day 3 pi, immune mice of both strains had significantly higher transcript levels than naïve mice.

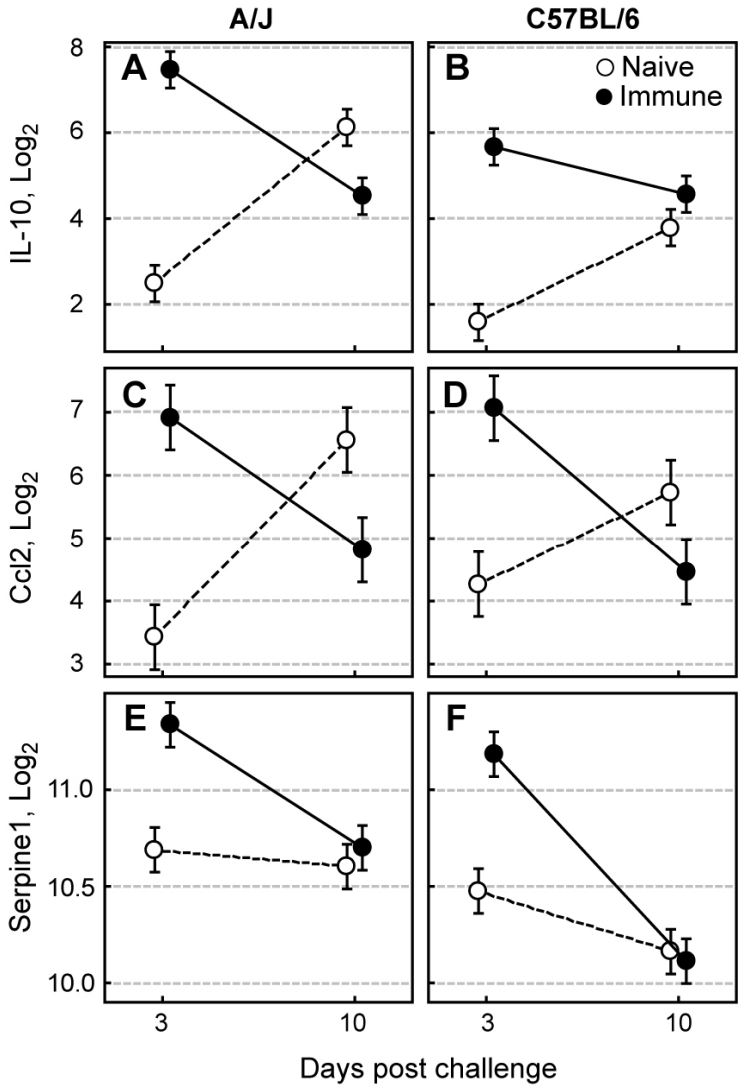

Figure 12. Influence of mouse strain, immune status and day post inoculation on lung transcript levels of Th2-associated cytokines IL-10 and Ccl2, and acute-phase protein Serpine1. Transcript levels of IL-10 and Ccl2 declined significantly from day 3 to day 10 in immune mice, and increased significantly from day 3 to day 10 in naïve mice in both strains (**A**-**D**). Serpine1 transcripts decreased in both naïve and immune mice between day 3 and day 10, but the decline was stronger in immune mice (**E**, **F**).

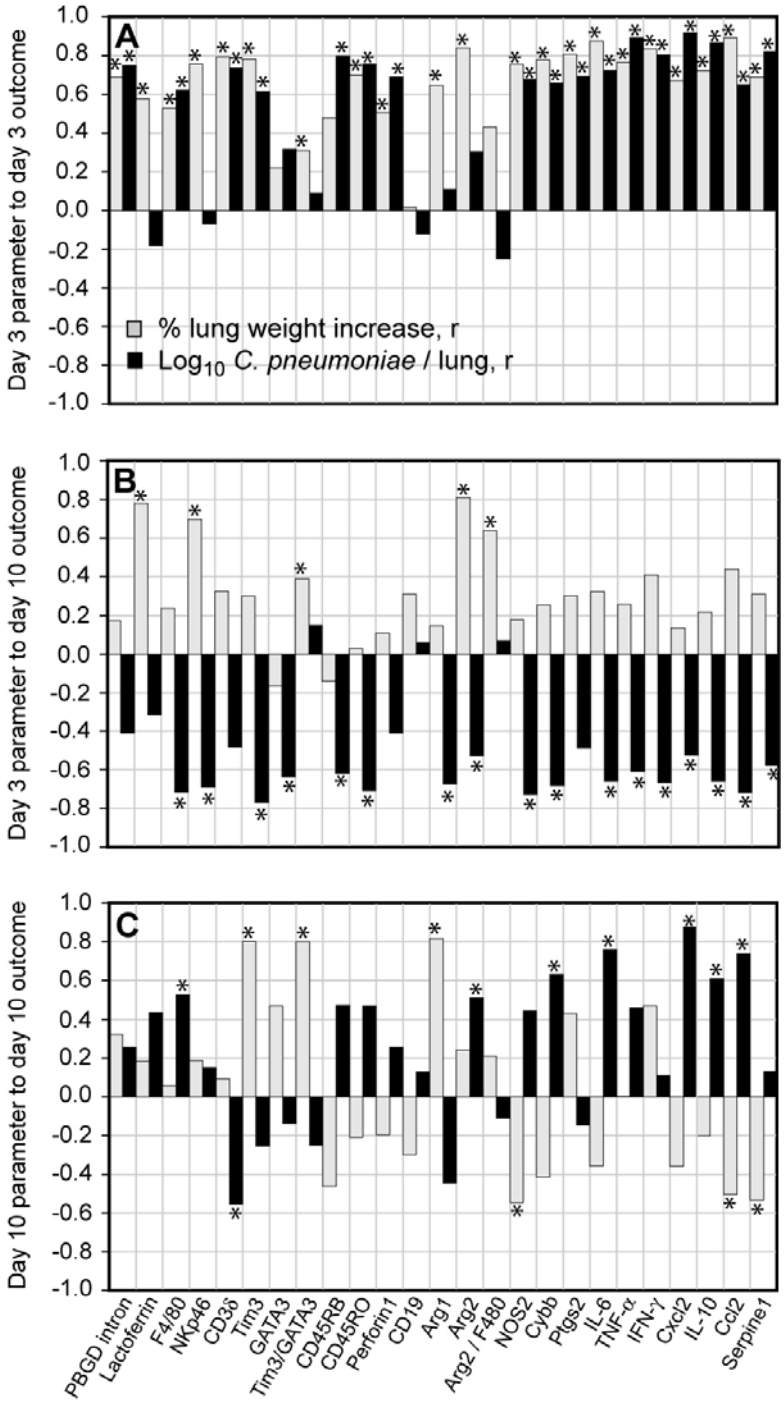

Figure 13. Correlations between day-3 or day-10 transcript concentrations and main outcomes of *C. pneumoniae* challenge inoculation (lung disease and *C.*

***pneumoniae* load).** Correlation coefficients (r) between lung weight increase or *C. pneumoniae* lung load and 25 transcript or gene copy (PBGD intron) parameters were calculated for **A**, day-3 parameters and day-3 outcomes (n = 160), and **C**, the day-10 parameters and day-10 outcomes (n = 160). **B**, correlations between day-3 parameters and day-10 outcomes were calculated from the means of corresponding day-3 and day-10 groups (n = 16). Grey bars indicate the correlation to lung weight increase, and black bars to $\log_{10}$ *C. pneumoniae* lung load. Asterisks denote significant correlations ($p < 0.05$). Day-3 parameters typically significantly correlated positively to both day-3 disease (lung weight increase) and day-3 *C. pneumoniae* lung load (**A**). Correlation of the late, day-10 parameters to day-10 outcomes was highly variable, but a significant correlation to both outcomes was observed only for transcripts of the cytokine Ccl2 (**C**). High levels of this transcript were significantly associated with low disease but high *C. pneumoniae* lung load. High levels of most day-3 transcripts correlated with high day-10 disease, but only lactoferrin, NKp46, Tim3/GATA3, Arg2, and Arg2/F4/80 did so significantly (**B**). High levels of most day-3 transcripts correlated significantly with low day-10 *C. pneumoniae* lung load. Interestingly, high NKp46 and Arg2 lung transcripts on day 3 after *C. pneumoniae* inoculation significantly correlated with later high disease on day 10, but also significantly with low day-10 *C. pneumoniae* lung load.

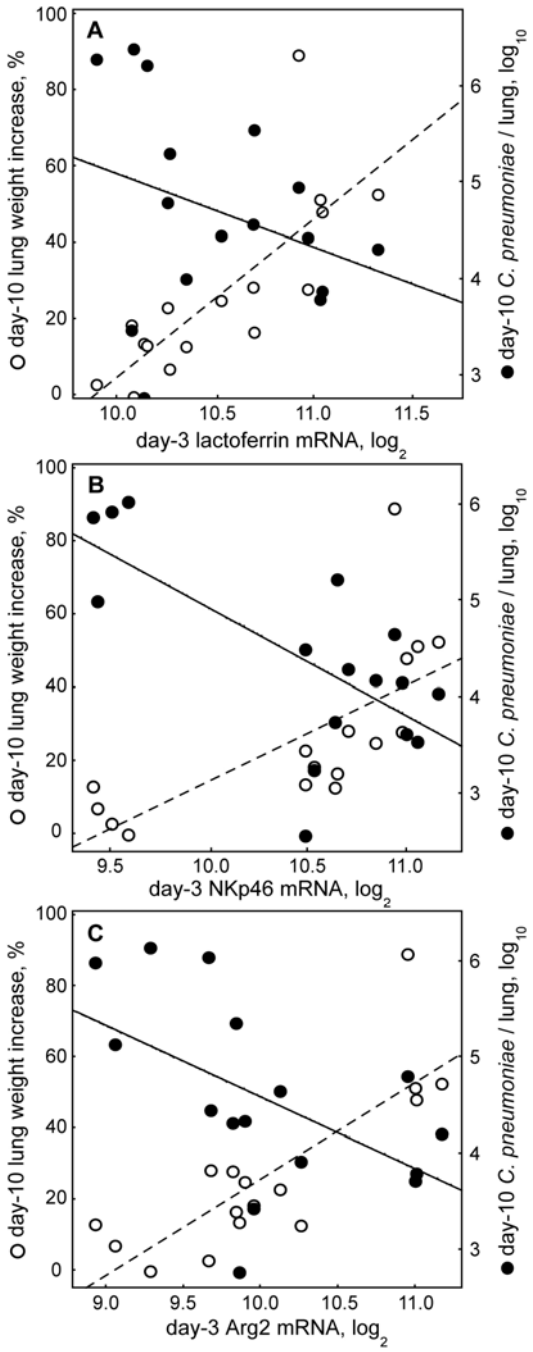

Figure 14. Day-10 disease and *C. pneumoniae* lung loads are inversely correlated to day-3 lactoferrin, Arginase 2, and NKp46 mRNAs. Open circles (o) and broken regression lines denote day-10 lung weight increase, and closed circles (●) and regression

lines day-10 $\log_{10}$ *C. pneumoniae* lung load. Day-3 transcripts of positively predicted day-10 lung weight increase, and negatively predicted day-10 $\log_{10}$ *C. pneumoniae* / lung: **A**, Lactoferrin: lung weight increase: $r^2 = 0.61$; $r = 0.78$, $p = 0.0004$; $\log_{10}$ *C. pneumoniae*: $r^2 = 0.10$; $r = -0.32$, $p = 0.23$; **B**, NKp46: lung weight increase: $r^2 = 0.49$; $r = 0.70$, $p = 0.003$; $\log_{10}$ *C. pneumoniae*: $r^2 = 0.48$; $r = -0.69$, $p = 0.003$; and **C**, Arg2: lung weight increase: $r^2 = 0.66$; $r = 0.81$, $p = 10^{-4}$; $\log_{10}$ *C. pneumoniae*: $r^2 = 0.28$; $r = -0.53$, $p = 0.035$.

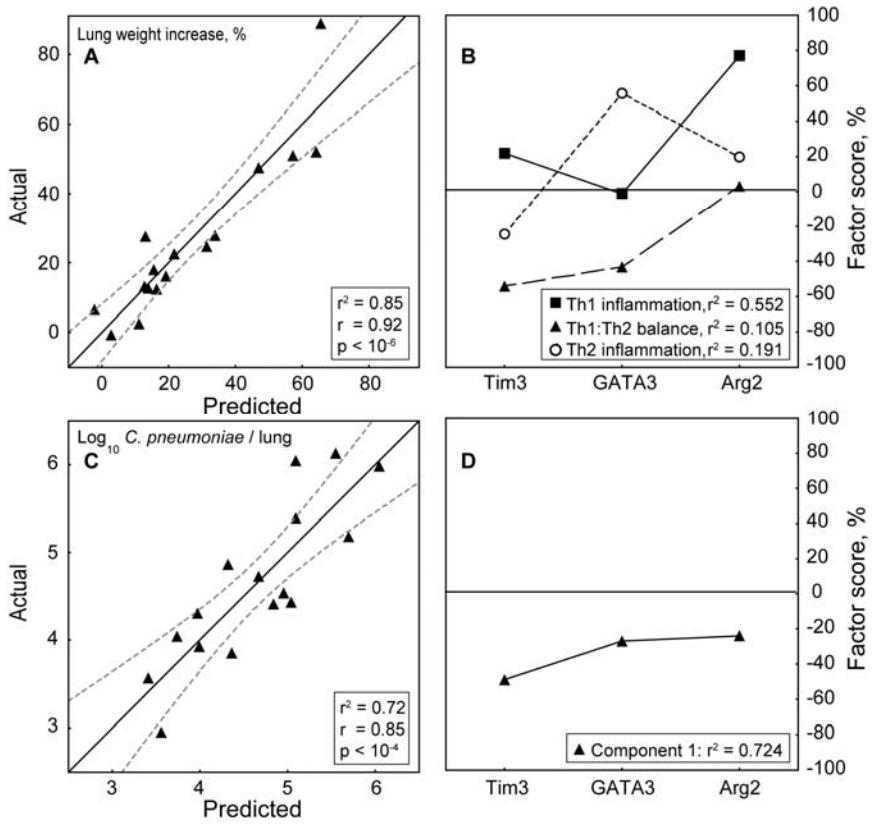

Figure 15. PLS models for modeling day 10 lung weight increase and *C. pneumoniae* load using lung levels of 3 day-3 transcripts. Disease and *C. pneumoniae* lung burden outcomes of the means of the day-10 experimental groups (n = 16 groups of 10 mice) were modeled using combinations of day-3 transcript means (n = 16 groups of 10 mice). **A**, initially, a simple, 3 transcript parameter (Tim3, GATA3, Arg2) best-fit model for lung weight increase was established by forward stepwise multiple regression. The same set of day-3 transcripts was also applied to model day-10 *C. pneumoniae* load ($r^2 = 0.74$). Both models were corroborated by use of mean data subsets of the even and odd cases. These models yielded regression equations similar to the full model, but with lower explanatory power (lung weight increase: $r^2 = 0.75$, 0.72 [even, odd], r = 0.87,

0.85; $p < 10^{-4}$; $\log_{10}$ *C. pneumoniae* lung load: $r^2 = 0.69, 0.52$ [even, odd], $r = 0.83, 0.72$; $p < 0.002$) **B**, the interaction of the transcripts to produce potential latent variables (components) with biological meaning was examined by PLS analysis. For lung weight increase, this analysis produced three components that each significantly influenced the overall model. Relative contribution of the three transcripts to each component is shown by the absolute fractional factor score, and the effect on lung weight by a positive or negative value. Based on the contribution of the transcripts, these components were termed Th1 inflammation, Th1:Th2 balance, and Th2 inflammation. **C**, the set of transcripts that resulted in a best fit model for day-10 disease was also used to model day-10 *C. pneumoniae* lung load in order to visualize the effects of the day-3 transcript on both day-10 disease and *C. pneumoniae* lung load outcomes. PLS analysis with these day-3 transcripts of the day-10 *C. pneumoniae* load revealed an $r^2 = 0.72$ for component 1, and r^2 values of 0.01 for components 2 and 3. Because of the minimal contribution, components 2 and 3 were not used in PLS modeling. **D**, fractional factor scores and their influence on *C. pneumoniae* load of the single component day-10 *C. pneumoniae* lung load model.

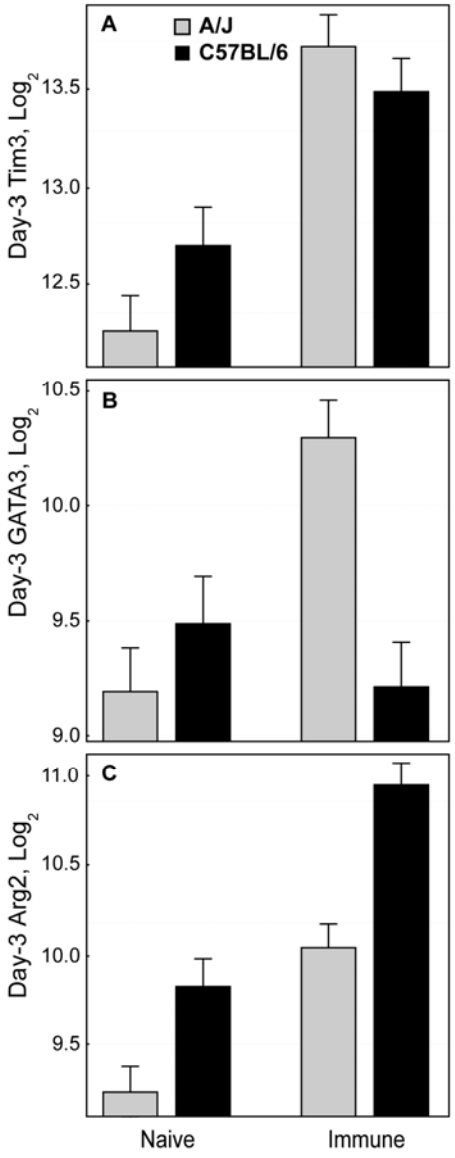

Figure 16. Day-3 lung concentrations of Tim3, GATA3, and Arg2 transcripts influenced by mouse strain and immune status. Day-3 concentrations of the 3 transcripts used for best fit modeling of day-10 lung weight increase are shown as log_2-transformed values ± 95% confidence interval of the means of naïve and immune A/J and C57BL/6 mice. Each data point represents 40 mice, comprising 4 groups of 10 mice fed one of the 4 diets. Grey bars denote A/J mice, and black bars C57BL/6 mice. Naïve A/J

mice had significantly lower levels of Tim 3, GATA3, and Arg2 transcripts than immune A/J mice (A, B, C; $p \leq 10^{-4}$). In C57BL/6 mice, transcript levels of Tim3 and Arg2 were significantly higher in immune mice (A, C; $p \leq 10^{-4}$), while GATA3 levels did not differ significantly between naïve and immune C57BL/6 mice (B). Naive C57BL/6 mice had significantly higher levels of Tim 3 and Arg2 transcripts than naïve A/J mice (A, C; $p \leq 0.003$). Immune C57BL/6 mice had significantly higher transcripts of Arg2 than naïve C57BL/6 mice (C; $p = 0.003$), and most importantly, immune C57BL/6 mice had highly significantly lower GATA3 transcript concentrations than immune A/J mice (B; $p < 10^{-4}$).

REFERENCES

1. **Balin, B. J., H. C. Gerard, E. J. Arking, D. M. Appelt, P. J. Branigan, J. T. Abrams, J. A. Whittum-Hudson, and A. P. Hudson.** 1998. Identification and localization of *Chlamydia pneumoniae* in the Alzheimer's brain. Med. Microbiol. Immunol. **187:**23-42.

2. **Beaumont, C., C. Porcher, C. Picat, Y. Nordmann, and B. Grandchamp.** 1989. The mouse porphobilinogen deaminase gene. Structural organization, sequence, and transcriptional analysis. J. Biol. Chem. **264**:14829-31484.

3. **Bjorgvinsdottir, H., L. Zhen, and M. C. Dinauer.** 1996. Cloning of murine gp91phox cDNA and functional expression in a human X-linked chronic granulomatous disease cell line. Blood. **87**:2005-2010.

4. **Boring, L., J. Gosling, F. S. Monteclaro, A. J. Lusis, C. L. Tsou, and I. F. Charo.** 1996. Molecular cloning and functional expression of murine JE (monocyte chemoattractant protein 1) and murine macrophage inflammatory protein 1 alpha receptors: evidence for two closely linked C-C chemokine receptors on chromosome 9. J. Biol. Chem. **271**:7551-7558.

5. **Bot, A., K. A. Smith, and M. von Herrath. 2004.** Molecular and cellular control of T1/T2 immunity at the interface between antimicrobial defense and immune pathology. DNA Cell Biol. **6:**341-350

6. **Botha, T., and B. Ryffel.** 2003. Reactivation of latent tuberculosis infection in TNF-deficient mice. J. Immunol. **171:**3110-3118.

7. **Bowen, R. A., P. Spears, J. Storz, and G. E. Seidel. Jr.** 1978. Mechanisms of infertility in genital tract infections due to *Chlamydia psittaci* transmitted through contaminated semen. J. Infect. Dis. **138:**95-98.

8. **Butler, N. S., M. M. Monick, T. O. Yarovinsky, L. S. Powers, and G. W. Hunninghake.** 2002. Altered IL-4 mRNA stability correlates with Th1 and Th2 bias and susceptibility to hypersensitivity pneumonitis in two inbred strains of mice. J. Immunol. **169**:3700-3709.

9. **Byrne, M. A., M. J. Turner, M. Griffiths, D. Taylor-Robinson, and W. P. Soutter.** 1991. Evidence that patients presenting with dyskaryotic cervical smears should be screened for genital-tract infections other than human papillomavirus infection. Eur. J. Obstet. Gynecol. Reprod. Biol. **41:**129-133.

10. **Chamseddine, A. H., and F. J. Miller. Jr.** 2003. Gp91phox contributes to NADPH oxidase activity in aortic fibroblasts but not smooth muscle cells. Am. J. Physiol. Heart Circ. Physiol. **285**:H2284-2289.

11. **Darville, T., C. W. Jr. Andrews, K. K. Laffoon, W. Shymasani, L. R. Kishen, and R. G. Rank.** 1997. Mouse strain-dependent variation in the course and outcome of chlamydial genital tract infection is associated with differences in host response. Infect. Immun. **65:**3065-3073.

12. **Dave, V. P., Z. Cao, C. Browne, B. Alarcon, G. Fernandez-Miguel, J. Lafaille, A. Hera, S. Tonegawa, and D. J. Kappes.** 1997. CD3d deficiency arrests development of the αβ but γδ T cell lineage. EMBO J. **16**:360-1370.

13. **de la Maza, L. M., S. Pal, A. Khamesipour, and E. M. Peterson.** 1994. Intravaginal inoculation of mice with the *Chlamydia trachomatis* mouse pneumonitis biovar results in infertility. Infect. Immun. **62:**2094-2097.

14. **De, A. K., K. M. Kodys, J. Pellegrini, B. Yeh, R. K. Furse, P. Bankey, and C. L. Miller-Graziano.** 2000. Induction of global anergy rather than inhibitory Th2 lymphokines mediates posttrauma T cell immunodepression. Clin. Immunol. **96:**52-66.

15. **DeGraves, F. J., D. Gao, H. R. Hehnen, T. Schlapp, and B. Kaltenboeck.** 2003. Quantitative detection of *Chlamydia psittaci* and *C. pecorum* by high-sensitivity real-time PCR reveals high prevalence of vaginal infection in cattle. J. Clin. Microbiol. **41:**1726-1729.

16. **Ejuma, K. L., I. M. Carvajal, P. A. Kritek., R. M. Baron, Y. H. Chen, J. Vom Saal, B. D. Levy., S. F. Yet, and M. A. Perrella.** 2003. Cyclooxygenase-2-deficient mice are resistant to endotoxin-induced inflammation and death. FASEB. J. **17**:1325-7.

17. **Elsen, P., K. Georgopoulos, B-A. Shepley, S. Orkin, and C. Terhorst.** 1986. Exon/Intron organization of the genes coding for the δ chains of the human and murine T-cell receptor/T3 complex. Proc. Natl. Acad. Sci. USA. **83**:2944-2948.

18. **Faist, E., C. Schinkel, and S. Zimmer.** 1996. Update on the mechanisms of immune suppression of injury and immune modulation. World J. Surg. **20:**454-459.

19. **Fransen, L., R. Muller, A. Marmenout, J. Tavernier, J. van der Heyden, E. Kawashima, A. Chollet, R. Tizard, H. van Heuverswyn, and A van der Vliet.** 1985. Molecular cloning of mouse tumor necrosis factor cDNA and its eukaryotic expression. Nucleic Acid Res. **13**:4417-4429.

20. **Gardby, E. and N. Y. Lycke.** 2000. CD19-deficient mice exhibit poor responsive ness to oral immunization despite evidence of unaltered total IgA levels, germinal centers and IgA-isotype switching in Peyer's patches. Eur. J. Immunol. **30**:1861-1871.

21. **Gardby, E., X. J. Chen, and N. Y. Lycke.** 2001. Impaired CD40-signalling in CD19 deficient mice selectively affects Th2-dependent isotype switching. Scand. J. Immunol. **53**:13-23.

22. **Gerard, H. C., K. L. Wildt, J. A. Whittum-Hudson, Z. Lai, J. Ager, and A. P. Hudson.** 2005. The load of *Chlamydia pneumoniae* in the Alzheimer's brain varies with APOE genotype. Microb. Pathog. **39:**19-26.

23. **Gray, P. W., and D. V. Goeddel.** 1983. Cloning and expression of murine immune interferon cDNA. Proc. Natl. Acad. Sci. USA. **80**:5842-5846.

24. **Hawkins, R. A., R. G. Rank, and K. A. Kelly.** 2002. A *Chlamydia trachomatis*-specific Th2 clone does not provide protection against a genital infection and displays reduced trafficking to the infected genital mucosa. Infect. Immun. **70:**5132-5139.

25. **Hermiston, M. L., Z. Xu, and A. Weiss.** 2003. CD45: A critical regulator of signaling thresholds in immune cells. Annu. Rev. Immunol. **21**:107-37.

26. **Hodges, R. J., R. G. Jenkins, C. P. Wheeler-Jones, D. M. Copeman, S. E. Bottoms, G. J. Bellingan, C. B. Nanthakumar, G. J. Laurent, S. L. Hart, M. L. Foster, and R. J McAnulty.** 2004. Severity of lung injury in cyclooxygenase-2-deficient mice is dependent on reduced prostaglandin E(2) production. Am. J. Pathol. **165**:1663-1676.

27. **Hodges, R. J., R. G. Jenkins, C. P. Wheeler-Jones, D. M. Copeman, S. E. Bottoms, G. J. Bellingan, C. B. Nanthakumar, G. J. Laurent, S. L. Hart, M. L. Foster, and R. J McAnulty.** 2004. Severity of lung injury in cyclooxygenase-2-deficient mice is dependent on reduced prostaglandin E(2) production. Am. J. Pathol. **165**:1663-1676.

28. **Hoskuldson, A.** 1988. Pls regression methods. J. Chemometrics. **2:**211-228.

29. **Huang, J. F. J. DeGraves, S. D. Lenz, G. Dongya, P. Feng, D. Li, T. Schlapp, and B. Kaltenboeck.** 2002. The quantity of nitric oxide released by macrophages regulates *Chlamydia*-induced disease. Proc. Natl. Acad. Sci. USA. **99:**3914-3919.

30. **Huang, J., F. J. DeGraves, D. Gao, P. Feng, T. Schlapp, and B. Kaltenboeck.** 2001. Quantitative detection of *Chlamydia* spp. by fluorescent PCRs in the LightCycler. BioTechniques **30:**151-157.

31. **Jendro, M. C., F. Fingerle, T. Deutsch, A. Liese, L. Kohler, J. G. Kuiper, E. Raum, M. Martin, and H. Zeidler.** 2004. *Chlamydia trachomatis*-infected macrophages induce apoptosis of activated T cells by secretion of tumor necrosis factor-α. Med. Microbiol. Immunol. **193**:45-52.

32. **Kappes, D. J., D. M. P. Lawrence, M. M. Vaughn, V. P. Dave, A. R. Belman, and G. F. Rall.** 2000. Protection of CD3 δ knockout mice from lymphocytic chrio-meningitis virus-induced immunopathology: Implications for viral neuro-invasion. Virol. **269**:248-256.

33. **Kaukoranta-Tolvanen, S. E., A. L. Laurila, P. Saikku, M. Leinonen, and K. Laitinen.** 1995. Experimental *Chlamydia pneumoniae* infection in mice: effect of reinfection and passive immunization. Microb. Pathog. **18:**279-88.

34. **Kelly, K. A., and R. G. Rank.** 1997. Identification of homing receptors that mediate the recruitment of CD4 T cells to the genital tract following intravaginal infection with *Chlamydia trachomatis*. Infect. Immun. **65:**5198-5208.

35. **Khademi, M., Z. Illes, A. W. Gielen, M. Marta, N. Takazawa, C. Baecher-Allan, L. Brundin, J. Hannerz, C. Martin, R. A. Harris, D. A. Hafler, V. K. Kuchroo, T. Olsson, F. Piehl, and E. Wallstrom.** 2004. T cell Ig- and mucin-domain-containing molecule-s (TIM-3) and TIM-1 molecules are differentially expressed on human Th1 and Th2 cells and in cerebrospinal fluid-derived mononuclear cells in multiple sclerosis. J. Immunol. **172**:7169-7176.

36. **Kim, J. M., C. I. Brannan, N. G. Copeland, N. A. Jenkins, T. A. Khan, and K. W. Moore.** 1992. Structure of the mouse IL-10 gene and chromosomal localization of the mouse and human genes. J. Immunol. **148**:3618-3623.

37. **Ko, L. J., M. Yamamoto, M. W. Leonard, K. M. George, P. Ting, and J. D. Engel.** 1991. Murine and human T-lymphocyte GATA-3 factors mediate transcription through a *cis*-regulatory element within the human T-cell receptor δ gene enhancer. Mol. Cell. Biol. **11**:2778-2784.

38. **Landers, D. V., K. Erlich, M. Sung, and J. Schachter.** 1991. Role of L3T4-bearing T-cell populations in experimental murine chlamydial salpingitis. Infect. Immun. **59:**3774-3777.

39. **Li, D., A. Vaglenov, T. Kim, C. Wang, D. Gao, and B. Kaltenboeck.** 2005. High-yield culture and purification of *Chlamydiaceae* bacteria. J. Microbiol. Meth. **61:**17-24.

40. **Lin, H. H., L. J. Stubbs., and M. L. Mucenski.** 1997. Identification and characteri-zation of a seven transmembrane hormone receptor using differential display. Genomics. **41**:301-308.

41. **Lyons, C. R., G. J. Orloff, and J. M. Cunningham.** 1992. Molecular cloning and functional expression of an inducible nitric oxide synthase from a murine macrophage cell line. J. Biol. Chem. **267**:6370-6374.

42. **McLoughlin, R. M., J. Witowski, R. L. Robson, T. S. Wilkinson, S. M. Hurst, A. S. Williams, J. D. Willams, S. Rose-John, S. A. Jones, and N. Topley** 2003. Interplay between IFN-γ and IL-6 signaling governs neutrophil trafficking and apoptosis during acute inflammation. J. Clin. Invest.112:598-607.

43. **Mitchell, W. M., and C. W. Stratton.** 2005. *Chlamydia pneumoniae* and acute coronary syndrome. N. Engl. J. Med. **353:**525-528.

44. **Monney, L., C. A. Sabatos, J. L. Gaglia, A. Ryu, H. Waldner, T. Chernova, S. Manning, E. A. Greenfield, A. J. Coyle, R. A. Sobel, G. J. Freeman, and V. K. Kuchroo.** 2002. Th-1 specific cell surface protein Tim-3 regulates macrophage activation and severity of an autoimmune disease. Nature. **415**:536-540.

45. **Mori, M., and T. Gotoh.** 2004. Arginine metabolic enzymes, nitric oxide and infection. J. Nutr. **134**:2820S-2825S.

46. **Murray, P. J., and R. A. Young.** 1999. Increased antimycobacterial immunity in interleukin-10-deficient mice. Infect. Immun. **67**:3087-3095.

47. **Nawijin, M. C., R. Ferreira, G. M. Dingjan, O. Kahre, D. Drabek, A. Karis, F. Grosveld, and R. W. Hendriks.** 2001. Enforced expression of GATA-3 during T cell development inhibits maturation of CD8 single-positive cells and induces thymic lymphoma in transgenic mice. J. Immunol. **167**:715-723.

48. **Noma, Y., P. Sideras, T. Naito, S. Bergstedt-Lindquist, C. Azuma, E. Severinson, T. Tanabe, T. Kinashi, F. Matsuda, and Y. Yaoita.** 1986. Cloning of cDNA encoding the murine IgG1 induction factor by a novel strategy using SP6 promoter. Nature **319**:640-646.

49. **O'Banion, M. K., V. D. Winn, and D. A. Young.** 1992. cDNA cloning and functional activity of a glucocorticoid-regulated inflammatory cyclooxygenase. Proc. Natl. Acad. Sci. USA. **89**:4888-4892.

50. **Ohnishi, S., S. Maeda, S. Nishiguchi, T. Arao, and K. Shimada.** 1988. Structure of the mouse C-reactive protein gene. Biochem. Biophys. Res. Commun. **156**:814-822.

51. **Okamoto, T., K. Gohil, E. I. Finkelstein, P. Bove, T. Akaike, and A. van der Vliet.** 2004. Multiple contributing roles for NOS2 in LPS-induced acute airway inflammation in mice. Am. J. Physiol. Lung Cell. Mol. Physiol. **286**:198-209.

52. **Pai, S-Y., M. L. Truitt, and I-C. Ho.** 2004. GATA-3 deficiency abrogates the development and maintenance of T helper type 2 cells. Proc. Natl. Acad. Sci. USA. **101**:1993-1998.

53. **Perry, L. L., K. Feilzer, and H. D. Caldwell.** 1997. Immunity to *Chlamydia trachomatis* is mediated by T helper 1 cells through IFN-gamma-dependent and -independent pathways. J. Immunol. **158:**3344-3352.

54. **Pessino, A., S. Sivori, C. Bottino, A. Malaspina, L. Morelli, L. Moretta, R. Biassoni, and A. Moretta.** 1998. Molecular cloning of NKp46: A novel member of the immunoglobulin superfamily involved in triggering of natural cytotoxicity. J. Exp. Med. **188**:953-960.

55. **Podack, E. R., H. Hengartner, and M. G. Lichtenheld.** 1991. A Central role of perforin in cytolysis? Annu. Rev. Immunol. **9**:129-157.

56. **Ramsey, K. H., and R. G. Rank.** 1991. Resolution of chlamydial genital infection with antigen-specific T-lymphocyte lines. Infect. Immun. **59:**925-931.

57. **Ramsey, K. H., L. S. Soderberg, and R. G. Rank.** 1988. Resolution of chlamydial genital infection in B-cell-deficient mice and immunity to reinfection. Infect. Immun. **56:**1320-1325.

58. **Rebecca, J. H., R. Gisli Jenkins, Caroline P.D. Wheeler-Jones, D. M. Copeman, S. E. Bottoms, G. J. Bellingan, C. B. Nanthak-umar, G. J. Laurent, S. L. Hart, M. L. Foster, and R. J. McAnulty.** 2004. Severity of lung injury in Cyclooxygenase-2-deficient mice is dependent on reduced prostaglandin E_2 production. Am. J. Pathol. **165**:1663-1676.

59. **Rogan, M. P., C. C. Taggart, C. M. Greene, P. G. Murphy, S. J. O'Neill, and N. G. McElvaney.** 2004. Loss of microbicidal activity and increased formation of biofilm due to decreased lactoferrin activity in patients with cystic fibrosis. J. Infect. Dis. **190**:1245-1253.

60. **Rothfuchs, A. G., M. R. Kreuger, H. Wigzell, and M. E. Rottenberg.** 2004. Macrophages, $CD4^+$ or $CD8^+$ cells are each sufficient for protection against *Chlamydia pneumoniae* infection through their ability to secrete IFN-gamma. J. Immunol. **172:**2407-2015.

61. **Rutledge, L. G. B., J. Fiorillo, C. Ernst, I. Grewal, R. Flavell, R. Gladue, and B. Rollins.** 1997. In vivo properties of monocyte chemoattractant protein-1. J. Leukocyte Biol. **62**:577-580.

62. **Saga, Y., J. S. Lee, C. Sariya, and E. A. Boyse.** 1990. Regulation of alternative splicing in the generation of isoforms of the mouse Ly-5 (CD45) glycoprotein. Proc. Natl. Acad. Sci. USA. **87**:3728-3732.

63. **Sato, S., D. A. Steeber, and T. F. Tedder.** 1995. The CD19 signal transduction molecule is a response regulator of B-lymphocyte differentiation. Proc. Natl. Acad. Sci. USA. **92**:11558-11562.

64. **Schaller, E., A. J. Macfarlane, R. A. Rupec, S. Gordon, A. J. Mcknight, and K. Pfeffer.** 2002. Inactivation of the F4/80 glycoprotein in the mouse germ line. Mol. Cell. Biol. **22**:8035-8043.

65. **Shi, O., D. Kepka-Lenhart, S. M. Morris, W. E. O'Brien.** 1998. Structure of the murine arginase II gene. Mammal. Genome. **9**:822-824.

66. **Shirsat, N. V., S. Bittenbender, B. L.Kreider, and G. Rovera.** 1992. Structure of the murine lactotransferrin gene is similar to the structure of the other transferring-endocing genes and shares a putative regulatory region with the murine myelo-peroxidase gene. Gene **110**:229-234.

67. **Sivori, S., D. Pende, C. Bottino, E. Marcenaro, A. Pessino, R. Biassoni, L. Moretta, and A. Moretta.** 1999. NKp46 is the major triggering receptor involved in the natural cytotoxicity of fresh or cultured human NK cells. Correlation between surface density of NKp46 and natural cytotoxicity against autologous, allogeneic or xenogeneic target cells. Eur. J. Immunol. **29**:1656-1666.

68. **Szabol, S. J., B. M. Sullivan1, S. L. Peng, and L. H. Glimcher.** 2003. Molecular mechanisms regulating Th1 immune response. Annu. Rev. Immunol. **21:**713–758.

69. **Takiguchi, M., Y. Haraguchi, and M. Mori.** 1988. Human liver-type arginase gene: structure of the gene and analysis of the promoter region. Nucleic Acids Res. **26**:8789-8892.

70. **Taylor, H. R., S. L. Johnson, R. A. Prendergast, J. Schachter, C. R. Dawson, and A. M. Silverstein.** 1982. An animal model of trachoma II. The importance of repeated reinfection. Invest. Ophthalmol. Vis. Sci. **23:**507-515.

71. **Tekamp-Olson, P., C. Gallegos, D. Bauer, J. McClain, B. Sherry, M. Fabre, S. van Deventer, and A. Cerami.** 1990. Cloning and characterization of cDNAs for murine macrophage inflammatory protein 2 and its human homologues. J. Exp. Med. **172**:911-919.

72. **Trapani, J. A., B. S. Kwon, C. A. Kozak, C. Chintamaneni, J. D-E. Young, and B. Dupont.** 1990. Genomic organization of the mouse pore-forming protein (perforin) gene and localization to chromosome 10, Similarities to and differences from C9. J. Exp. Med. **171**:545-557.

73. **Tuffrey, M., C. Woods, and D. Taylor-Robinson.** 1991. The effect of a single oral dose of azithromycin on chlamydial salpingitis in mice. J. Antimicrob. Chemother. **28:**741-746.

74. **Van Snick, J., S. Cayphas, J. P. Szikora, J. C. Renauld, E. van Roost, T. Boon, and R. J. Simpson.** 1988. cDNA cloning of murine interleukin-HP1: homology with human interleukin 6. Eur. J. Immunol. **18**:3618-3623.

75. **Vankayalapati, R., B. Wizel, S. E. Weis, H. Safi, D. L. Lakey, O. Mandelboim, B. Samten, A. Porgador, and P. F. Barnes.** 2002. The NKp46 receptor contributes to NK cell lysis of mononuclear phagocytes infected with an intracellular bacterium. J. Immunol. **168**:3451-3457.

76. **Veillard, N. R., S. Steffens, F. Burger, G. Pelli, and F. Mach.** 2004. Differential expression patterns of proinflammatory and antiinflammatory mediators during atherogenesis in mice. Arterioscler. Thromb. Vasc. Biol. **24**:2339-2344.

77. **Wang, C., D. Gao, A. Vaglenov, and B. Kaltenboeck.** 2004. One-step duplex reverse transcription PCRs simultaneously quantify analyte and housekeeping gene mRNAs. Biotechniques **36:**508-519.

78. **White, D. W., A. MacNeil., D. H. Busch, I. M. Pilip, E. G. Pamer, and J. T. Harty.** 1999. Perforin-deficient $CD8^{+}$T cells: *In vivo* priming and antigen-specific immunity against *Listeria monocytogenes*. J. Immunol. **162**:980-988.

79. **Xu, F., J. A. Schillinger, L. E. Markowitz, M. R. Sternberg, M. R. Aubin, and M. E. St Louis.** 2000. Repeat *Chiamydia trachomatis* infection in women: analysis through a surveillance case registry in Washington State, 1993-1998. Am. J. Epidemiol. **152:**1164-1170.

80. **Yamamoto, K., K. Takeshita, T. Shimokawa, H. Yi, K. Isobe, D. J. Loskutoff, and H. Saito.** 2002. Plasminogen activator inhibitor-1 is a major stress-regulated gene: implications for stress-induced thrombosis in aged individuals. Proc. Natl. Acad. Sci. USA. **99**:890-895.

81. **Yamashita, M., M. Ukai Tadenuma, T. Miyamoto, K. Sugaya, H. Hosokawa, A. Hasegawa M. Kimura, M. Taniguchi, J. DeGregori, and T. Nakayama.** 2004. Essential role of GATA3 for the maintenance of type 2 helper T (Th2) cytokine production and chromatin remodeling at the Th2 cytokine gene loci. J. Biol. Chem. **279:**26983-26990.

82. **Yang X.** 2001. Distinct function of Th1 and Th2 type delayed type hypersensitivity: protective and pathological reactions to chlamydial infection. Microsc. Res. Tech. **53:**273-277.

83. **Yang, X., and R. C. Brunham.** 1998. Gene knockout B cell-deficient mice demonstrate that B cells play an important role in the initiation of T cell responses to *Chlamydia trachomatis* (Mouse Pneumonitis) lung infection. J. Immunol. **161**:1439-1446.

84. **Yang, Z. P., C. C. Kuo, and J. T. Grayston.** 1993. A mouse model of *Chlamydia pneumoniae* strain TWAR pneumonitis. Infect. Immun. **61:**2037-2040.

85. **Zheng, W., and R. A. Flavell.** 1997. The transcription factor GATA-3 is necessary and sufficient for Th2 cytokine gene expression in CD4 T cells. Cell. **89**:587-596.

86. **Zhong. G., and R. C. Brunham.** 1992. Antibody responses to the chlamydial heat shock proteins hsp60 and hsp70 are H-2 linked. Infect. Immun. **60:**3143-3149.

87. **Zhou, L., H. M. Smith, T. J. Waldschmidt, R. Schwarting, J. Daley, and T. F. Tedder.** 1994. Tissue-specific expression of the human CD19 gene in transgenic mice inhibits antigen-independent B-lymphocyte development. Mol. Cell. Biol. **14**:3338-3894.

88. **Zhu, J., B. Min, J. Hu-Li, C. J. Watson, A. Grinberg, Q. Wang, N. Killeen, J. F. Urban Jr., L. Guo, and W. E. Paul.** 2004. Conditional deletion of Gata3 shows its essential function in Th1-Th2 responses. Nature Immunol. **5:**1157-1165.

CHAPTER 4. Overall Conclusions

Reverse transcription PCR is a sensitive and powerful tool for detecting and quantifying RNA. In its standard implementation, separate reactions are performed for amplification of a reference mRNA (housekeeping gene mRNA) and of a target mRNA (analyte mRNA). Such separate reactions render quantitative real-time RT-PCR inherently inaccurate and cumbersome. In this study, we established a one-step duplex RT-PCR method on the LightCycler® platform, allowing simultaneous RT and real-time PCR amplification of two mRNAs of any analyte and reference gene in a single-tube reaction. This single-step duplex RT-PCR reliably and accurately determined 10-10,000 copies of each target over a 100,000-fold range of target copy ratios. This method was critical for accurate and high-throughput quantitative analysis of transcription patterns in a multivariate mouse *C. pneumoniae* challenge experiment.

In the second part of this study, multivariate regulation of disease and chlamydial burden was examined in a *C. pneumoniae* mouse lung challenge model. Specifically, the simultaneous influence on disease as measured by lung weight increase and on *C. pneumoniae* lung load was analyzed. Binomial variables were host (inbred mouse strain: A/J vs. C57BL/6), its anti-*C. pneumoniae* immune status (naïve vs. immunized by low-dose *C. pneumoniae* infection 4 weeks prior to challenge), the time of sacrificing after inoculation (3 days vs. 10 days), and the full factorial combinations of these variables. In addition, the influence of transcription of 25 genes on the disease and bacterial load

outcomes was evaluated. Data indicated that A/J mice prioritized minimizing disease at the cost of inefficient pathogen elimination, while C57BL/6 mice prioritized elimination of *C. pneumoniae* at the cost of high disease. Therefore, the host genetic makeup was the decisive factor that determined if the infection resulted in severe or marginal disease. Disease was always more severe in animals that had established immunity against *C. pneumoniae* as compared to animals that had not been previously exposed to the bacteria. Immune animals reduced *C. pneumoniae* bacteria in the lung by about 100- to 1000-fold between 3 and 10 days after inoculation while naïve animals did not achieve net reduction of the bacteria during this time. Thus, the adaptive immune response accomplishes the indispensable requirement of eliminating the bacteria from the infected host but also enhances disease in a time-dependent and host-restricted fashion. The corollary of this observation is that host regulation of the early response to the *C. pneumoniae* inoculum is the key disease determinant.

Transcript lung levels on day 3 were used to model the day-10 peak disease and *C. pneumoniae* load outcomes. A simple best-fit model used day-3 Tim3, GATA3, and Arg2 transcript concentrations to predict day-10 lung weight increase and *C. pneumoniae* lung load with $r^2 = 0.85$ and 0.72, respectively. This model indicated that host-dependent levels of early Th1 and Th2 responses, and their ratio, highly significantly predicted the late disease and *C. pneumoniae* lung load. Transcript levels of the Th2-specific transcription factor GATA3 were critical in *C. pneumoniae* disease regulation. They were high in immune A/J mice that developed virtually no late disease, while they were low in immune C57BL/6 mice that developed high disease. Thus, regulation of Th1 vs. Th2 immunity determines the outcome of murine *C. pneumoniae* lung infection.